Neural cell adhesion molecule-associated polysialic acid regulates synaptic plasticity by balancing the signaling through NR2A- and NR2B-containing NMDA receptors in the mouse (*Mus musculus* L., 1758)

Dissertation

zur Erlangung des Doktorgrades des Departments Biologie der Fakultät für Mathematik, Informatik und Naturwissenschaften an der Universität Hamburg
vorgelegt von Gaga Kochlamazashvili

Hamburg, 2008

Genehmigt vom Department Biologie
der Fakultät für Mathematik, Informatik und Naturwissenschaften
an der Universität Hamburg
auf Antrag von Frau Professor Dr. M. SCHACHNER
Weiterer Gutachter der Dissertation:
Professor Dr. K. WIESE
Tag der Disputation: 27. Juni 2008

Hamburg, den 13. Juni 2008

Professor Dr. Jörg Ganzhorn
Leiter des Departments Biologie

Table of contents

I. Abstract

Recognition molecules are not only implicated in cell interactions during nervous system development, but they are also recognized as important mediators of synaptic plasticity in the adult (Schachner, 1997). Among these molecules is the neural cell adhesion molecule NCAM (Lüthi et al., 1994; Muller et al., 1996) and its associated α-2,8 polysialic acid (PSA) (Becker et al., 1996; Muller et al., 1996). Abnormalities in PSA and NCAM expression are associated with schizophrenia in humans (Barbeau et al., 1995) and result in deficits in hippocampal synaptic plasticity and contextual fear conditioning in mice. Mice with a constitutive ablation of the NCAM gene show impaired long-term potentiation (LTP) at CA3-CA1 synapses (Muller et al., 1996, 2000), mossy fiber-CA3 synapses (Cremer et al., 1998) and perforant path-dentate gyrus synapses (Stoenica et al., 2006). Enzymatic removal of NCAM-associated PSA and genetic ablation of polysialyltransferase ST8SiaIV – required for polysialylation of NCAM in adult hippocampus – leads to impairment of LTP and long-term depression (LTD) in CA1 (Becker et al., 1996; Muller et al., 1996; Eckhardt et al., 2000). Application of recombinant polysialylated NCAM (PSA-NCAM) or PSA to acute slices of NCAM-deficient mice restores normal CA1 LTP (Senkov et al., 2006). Since application of non-polysialylated NCAM is not effective in restoring normal LTP, the combined data indicate that PSA is both necessary and sufficient for normal induction of CA1 LTP.

Other recent experiments revealed that PSA suppresses activation of NR2B-containing NMDA receptors by low concentrations of glutamate (Hammond et al., 2006), suggesting that PSA may restrain activity of these receptors extrasynaptically. It is noteworthy in this respect that (i) the synaptic pool of NMDA receptors activates the extracellular signal-regulated kinases (ERK), whereas the extrasynaptic pool triggers a signaling pathway that results in the inactivation of ERK (Ivanov et al., 2006); (ii) NR2B-containing NMDA receptors may signal via the Ras-guanine nucleotide-releasing factor 1 (Ras-GRF1) to the Rac effector p38 MAP kinase, which promotes synaptic depression in an age-dependent manner (Li et al., 2006).

My study examined NR2A- and NR2B-mediated transmission in the CA1 region of NCAM deficient hippocampal slices using isolation of NMDA receptor-mediated fEPSPs and imaging of NR2B-dependent Ca^{2+} transients activated via local uncaging of glutamate in aspiny domain of dendritic tree. My results demonstrate that a deficit in NCAM increases transmission via NR2B-containing receptors in expense of NR2A-containing ones. Accordingly, the deficits in LTP in NCAM/PSA deficient hippocampal slices are

rescued by treatments either increasing activity of NR2A-containing NMDA receptors (D-cycloserine) or suppressing activity of extrasynaptic NR2B-containing NMDA receptors (Ro 25-6981 and glutamate scavenger). Deficits in LTD in NCAM deficient mice can also be rescued by an agonist of NR2A-containing NMDA receptors, whereas antagonists to either NR2A- or NR2B-containing NMDA receptors block LTD in both genotypes, supporting the view that signaling via both subtypes of NMDA receptors is required for induction of LTD. Analysis of mechanisms downstream of extrasynaptic NR2B revealed hyperactivity of p38 MAPK in NCAM deficient mice. Furthermore, ablation of Ras-GRF1 or inhibition of hyperactive p38 MAPK in NCAM deficient mice could restore impaired LTP in PSA/NCAM deficient slices. In agreement with rather late role of Ras-GRF1 in LTP (Li et al., 2006), the deficit in LTP in NCAM-deficient mice is age-dependent: normal LTP is found in 2.5-week-old mice, whereas LTP is impaired in 2.5-month-old mice and impairment becomes even more prominent in 12- and 24-month-old mutants. Also, impaired LTP in aged NCAM deficient mice can not be fully rescued by treatments that are fully effective in 2.5-month-old mice. Thus, we conclude that 1) PSA carried by NCAM restrains the NR2B - Ras-GRF1 - p38 pathway and regulates synaptic plasticity by setting a proper balance in signaling through extrasynaptic NR2B- and synaptic NR2A-containing NMDA receptors and 2) a deficit in NCAM has most dramatic consequences for synaptic plasticity in aged brains.

The significance of these results is underscored by numerous previous findings that expression of NCAM and PSA is dysregulated under neuropathological conditions, such as schizophrenia. Furthermore, NCAM is considered to be one of the most prominent candidate genes for cognitive abnormalities in schizophrenia. Thus, the fact that several distinct pharmacological treatments can fully restore deficits in synaptoc plasticity in NCAM or PSA deficient animals are interesting not only from a basic science point of view, but may have also important practical ramifications. These findings may eventually foster therapeutic strategies for compensation of schizophrenia-related genetic defects in functions of cell adhesion molecules.

II. Zusammenfassung

Zellerkennungsmoleküle sind nicht nur wichtig für Zellinteraktionen während der ontogenetischen Entwicklung des Nervensystems, sondern sie sind auch in synaptische Plastizität im erwachsenen Zustand impliziert (Schachner, 1997). Zu diesen Zellerkennungsmolekülen gehören auch das Zelladhäsionsmolekül NCAM (Lüthi et al., 1994; Muller et al., 1996) und die mit NCAM assoziierte α2,8 Polysialinsäure (PSA) (Becker et al., 1996; Muller et al., 1996). Abnormalitäten in der Expression von NCAM und PSA sind beim Menschen mit dem Krankheitsbild der Schizophrenie assoziiert (Barbeau et al., 1995) und resultieren in Reduktion der hippocampalen synaptischen Plastizität und Furcht-Konditionierung bei Mäusen. Mutanten in der Maus mit einer konstitutiven Defizienz des NCAM-Gens zeigen eine reduzierte Langzeitpotenzierung (LTP) an der CA3-CA1 Synapse (Muller et al., 1996, 2000), an der Moosfaser CA3-Synapse (Cremer et al., 1998) und an der Synapse, die vom perforanten Pfad und dem Gyrus dentatus gebildet wird (Stoenica et al., 2006). Enzymatischer Verdau des NCAM-assoziierten PSA und genetisch induzierte Defizienz der Polysialyltransferase ST8SiaIV – die für die Polysialylierung von NCAM im erwachsenen Hippocampus notwendig ist – führen zur Reduktion von LTP und von Langzeitdepression (LTD) in der CA1-Region des Hippocampus (Becker et al., 1996; Muller et al., 1996; Eckhardt et al., 2000). Zugabe von rekombinanten polysialylierten NCAM (PSA) oder PSA zu frischen Schnitten von NCAM-defizienten Mäusen normalisiert LTP in der CA1-Region (Senkov et al, 2006). Da die Zugabe von unpolysialylierten NCAM, die LTP nicht normalisiert, können wir daraus ableiten, dass PSA sowohl notwendig als auch ausreichend für die Induktion normaler LTP in der CA1-Region ist.

Andere Experimente haben gezeigt, dass PSA die Aktivierung von NR2B-enthaltenden NMDA-Rezeptoren bei niederen Konzentrationen von Glutamat hemmen (Hammond et al., 2006). Diese Ergebnisse machen wahrscheinlich, dass PSA die Aktivität dieser Rezeptoren extrasynaptisch inhibiert. Es ist in dieser Hinsicht interessant, dass der synaptische Pool von NMDA-Rezeptoren die „extracellular signal-regulated“ Kinasen (ERK) aktivieren, während der extrasynaptische Pool den Signaltransduktionsmechanismus aktiviert, der eine Inaktivierung der ERK-Kinasen programmiert (Ivanov et al., 2006); i. e. NR2B-enthaltende NMDA-Rezeptoren signalisieren wahrscheinlich über den „Ras-guanine nucleotide-releasing factor 1“ (GRF1) zu der „Rac effector p38 MAP“ Kinase, die die synaptische Depression in einer altersabhängigen Weise fördert (Li et al., 2006).

ZUSAMMENFASSUNG

In meiner Doktorarbeit habe ich die synaptische Transmission untersucht, die durch die NMDA-Rezeptoren NR2A und NR2B in der CA1-Region in hippocampalen Schnitten von NCAM-defizienten Mäusen untersucht. Die NMDA Rezeptor-vermittelten fEPSPs wurden isoliert und durch Darstellung der NR2B-abhängigen Calcium-Transienten über die lokale Freisetzung von Glutamat im dendritischen Baum von nicht-dornigen Synapsen erzeugt. Meine Beobachtungen zeigen, dass ein Defizit in NCAM die Transmission über NR2B-enthaltende Rezeptoren vermittelt, und zwar auf Kosten der NR2A-abhängigen Rezeptoren. Es war daher zu erwarten, dass die reduzierte LTP in NCAM-PSA-defizienten hippocampalen Schnitten durch Behandlung mit D-Cycloserin vermittelt werden und dass die Aktivitäten der NR2A-enthaltenden NMDA-Rezeptoren erhöht oder die Aktivität der extrasynaptischen NR2B-enthaltenden NMDA-Rezeptoren unterdrückt (durch die spezifischen Inhibitoren Ro 25-6981 und Glutamat-Scavenger). Defizite in der LTD von NCAM-defizienten Mäusen können auch durch den Agonisten von NR2A-enthaltenden NMDA-Rezeptoren neutralisiert werden. Antagonisten für NR2A oder NR2B-enthaltende NMDA-Rezeptoren führten zu einer Blockierung von LTD in beiden Genotypen. Diese Ergebnisse unterstützen die Ansicht, dass die Signaltransduktion durch beide Subtypen der NMDA-Rezeptoren für die Induktion von LTD verantwortlich ist. Analyse der Mechanismen, die der Aktivierung von extrasynaptischen NR2B-Rezeptoren folgt, zeigte, dass in NCAM-defizienten Mäusen die p38 MAPK-Aktivität erhöht ist. Auch konnte ich zeigen, dass Inhibition von Ras-GRF1 oder Inhibition der hyperaktiven p38 MAPK in NCAM defizienten Mäusen die reduzierte LTP in PSA/NCAM-defizienten Schnitten normalisiert. Da die in der Signaltransduktion späte Aktivität von Ras-GRF1 in der LTP belegt ist (Li et al., 2006), ist die Defizienz in der LTP in NCAM-defizienten Mäusen abhängig vom Alter der Tiere: Eine normale LTP wird in 2.5 Wochen alten Mäusen gefunden, während eine reduzierte LTP in 2.5 Monate alten Mäusen gefunden wurde. In 12 und 24 Monate alten Mutanten wird diese Reduktion noch prominenter. Ich konnte weiterhin zeigen, dass reduzierte LTP in älteren NCAM-defizienten Mäusen nicht voll normalisiert werden kann durch Behandlungen, die in 2.5 Monate alten Mäusen wirken. So können wir folgern, dass NCAM-assoziiertes PSA dem NR2B – Ras-GRFI – p38 MAPK Signaltransduktionsmechanismus reduziert und synaptische Plastizität reguliert wird durch ein ausgewogenes Gleichgewicht in der Signaltransduktion durch extrasynaptische NR2B und synaptische NR2A enthaltende NMDA-Rezeptoren, und 2. dass ein Defizit in NCAM so dramatische Konsequenzen für synaptische Plastizität in gealterten Gehirnen darstellt.

ZUSAMMENFASSUNG

Die Signifikanz dieser Resultate wird durch viele Untersuchungen unterstrichen, die zeigen, dass die Expression des NCAM-Proteins und von PSA unter neuropathologischen Bedingungen abnormal ist. Zu diesen neuropathologischen Bedingungen gehört auch die Schizophrenie. Außerdem konnten genetische Untersuchungen zeigen, dass NCAM eines der prominenten Kandidaten-Gene für die kognitiven Abnormalitäten in der Schizophrenie ist. Die Tatsache, dass verschiedene pharmakologische Einwirkungen die Defizite in der synaptischen Plastizität in NCAM- oder PSA-defizienten Mäusen normalisiert, ist besonders interessant nicht nur aus grundlagenwissenschaftlicher Sicht, sondern auch von einer therapeutischen Warte aus.

III. Abbreviations

ACSF	Artificial cerebrospinal fluid
AMPA	α-amino-3-hydroxy-5-methyl-4-isoxazoleproprionic acid
AMPAR	AMPA-receptor
ANOVA	Analysis of Variances
APV	2-D,L-aminophosphonovaleric acid;
ATP	Adenosine triphosphate
BDNF	Brain derived neurotrophic factor
BSA	Bovine serum albumin
FGF	Fibroblast growth factor
CamKII	Ca^{2+}/calmodulin kinase II
CAMs	Cell adhesion molecules
CNQX	6-cyano-7-nitroquinoxaline-2,3-dione
CNS	Central nervous system
CSPG	Chondroitin Sulfate Proteoglycans
dACSF	Dissection artificial cerebrospinal fluid
DCS	D-cycloserine
ECM	Extracellular matrix
EDTA	Ethylenediaminetetraacetic acid
EndoN	Endo-neuraminidase N
EndoNF	Endo-neuraminidase NF
EndoNF-	Mutated endo-neuraminidase NF
EPSP	Excitatory postsynaptic potential
ERK	Extracellular signal-related protein kinase
FAK	Focal adhesion kinase
fEPSP	Field excitatory post synaptic potential
FGF	Fibroblast growth factor
FGFR	Fibroblast growth factor receptor
Fluo4	Fluorescent calcium indicator
FN-III	Fibronectin type three domain
GABA	Gamma amino butyric acid
GAPDH	Glyceraldehyde-3-phosphate dehydrogenase
GEF	Guanine nucleotide exchange factor
GluR	Glutamate receptor
GPI	Glycosylphospatidylinositol
GPT	Glutamic-pyruvic transaminase
HEPES	4-(2-hydroxyethyl)-1-piperazineethanesulfonic acid
HFS	High frequency stimulation
HNK-1	3'sulfated glucuronic acid
Ig	Immunoglobulin
iGluRs	Ionotropic Glutamate Receptors
LFS	Low frequency stimulation
LTD	Long term depression

ABBREVIATIONS

LTP	Long term potentiation
MAP	Mitogen-activated protein
MAPK	Mitogen activated protein kinase
mGluR	Metabotrophic Glutamate receptor
NCAM	Neural cell adhesion molecule
PSA-NCAM	Neural cell adhesion molecule bearing polysialic acid
NBQX	6-nitro-7-sulphamoylbenzo[f]quinoxaline-2,3-dione
NMDA	N-methyl-D-aspartate
NMDAR	N-methyl-D-aspartate receptor
NR2	NMDAR subtype
NVP-AAMO77	(4-bromo-phenyl)-ethylamino]-(2,3-dioxo-1,2,3,4-tetrahydroquinoxalin-5-yl)-methyl]-phosphonic acid
PBS	Phosphate buffered saline
PKA	Protein kinase A
PKC	Protein kinase C
PPD	Paired pulse depression
PPF	Paired pulse facilitation
PSA	Polysialic acid
PSD	Postsynaptic density
PST	Polysialic acid transferase
PTP	Post tetanic potentiation
p38	Isoform of mitogen-activated protein kinase
Ras-GRF	Ras-guanin nucleotide-releasing factor
RNA	Ribonucleic acid
Ro 25	(R-(R*,S*)-a-(4-hydroxyphenyl)-b-methyl-4-(phenylmethyl)-1-piperidine propanol
SEM	Standard error of mean
STD	Short term depression
STP	Short term potentiation
STX	Sialyltransferase X
TBS	Theta burst stimulation
TM	Transmembrane domain

IV. Review of the literature

1. Preface

The great challenge of neural science in recent years is to elucidate the mechanisms which enable learning and memory. In order to understand how the brain integrates and stores information, it is highly important to study the molecular mechanisms of neuronal signaling and synaptic plasticity in the structures involved in these processes. Another challenge is to elucidate the mechanisms that might underlie mental illnesses and use this knowledge to develop new approaches for treatment of these illnesses. Recent studies show that cell adhesion molecules, expressed on the cell surface, are actively involved in signal transduction and plastic changes of the brain. Thus, targeting of signaling mediated by cell adhesion molecules can be one of the promising direction for new clinical approaches in psychiatry and neurology.

2. The hippocampal formation

The hippocampal formation is one of the most widely studied structures of the brain; it is of interest to all neuroscientific disciplines. This interest is supported from one side by relatively simple organization of its principal cell layers coupled with the highly organized laminar distribution of many of its inputs, which has encouraged its use as a model system for modern neurobiology. From the other side, the hippocampus is attractive due to its specific function and highly specific role in learning and memory.

The hippocampus is believed to play essential role in long-term memory formation. This hypothesis is supported by the evidence that damage to the hippocampus usually causes deficit in transforming new memories to the long term memory - anterograde amnesia, and normally also affects access to memories prior to the damage - retrograde amnesia. Although the retrograde effect normally extends some years prior to the brain damage, in some cases older memories remain (Scoville and Milner, 1957). This sparing of older memories led to the idea that consolidation over time involves the transfer of memories out of the hippocampus to the other parts of the brain. Damage to the hippocampus does not affect some aspects of memory, such as the ability to learn new skills, suggesting that such abilities depend on different brain regions.

The hippocampal formation is a group of structures organized from many millions of neurons into a network, making up the limbic system. It includes the hippocampus, dentate gyrus, subiculum, presubiculum, parasubiculum, and entorhinal cortex. The hippocampus itself is subdivided into three subregions called CA3, CA2, and CA1. The main justification

for including these regions under the term hippocampal formation is that they are linked, one to the next, by largely unidirectional intrahippocampal circuits and highly distributed three-dimentional organization of intrinsic associational connections (Andersen et al., 1971).

Much of the neocortical inputs reach the hippocampal formation through entorhinal cortex, which is considered to be the first step in intrinsic hippocampal circuitry. Entorhinal cortex projects, to the dentate gyrus via the perforant path. The dentate granule cells project via their distinctive mossy fibers to the CA3 field of the hippocampus. CA3 neurons send there major input to the CA1 field via Schaffer collateral axons. The pyramidal cells of CA1 field on its own projects to the subiculum and entorhinal cortex. Furthermore, whereas the subiculum does project to the presubiculum and the parasubiculum, its more prominent cortical projection is directed to the entorhinal cortex. Through these connections both CA1 and the subiculum close the hippocampal processing loop that begins in the superficial layers of the entorhinal cortex and ends in its deep layers.

All connections between hippocampal formation structures mentioned above are unidirectional (with little exceptions), and makes hippocampal formation unique among other brain regions mostly connected to each other reciprocally. Furthermore hippocampus has widespread connections with other brain regions, but from practical point of view, a famous trisynaptic pathway within the hippocampus has been commonly used for experimental studies of synaptic plasticity (Figure 1). Other excitatory pathways are less well studied than synapses of trisynaptic circuit, for several reasons: First, the trisynaptic circuit and laminar organization is well preserved within the slice in transverse hippocampal slice preparation. Second, pharmacological agents applied to hippocampus could be rapidly washed in and out, allowing intracellular and patch-clamp recordings. Third, all of the components of the trisynaptic circuit display both long-term potentiation (LTP) and long-term depression (LTD). LTP and LTD are the two classic forms of stimulus-induced synaptic plasticity, implying respectively, a long-lasting increase and decrease of the synaptic efficacy. Thus, hippocampal structure provides the excellent model to study mechanisms of activity-induced synaptic changes, underlying memory formation. In the present study all experiments were performed on the synapses of the Schaffer collateral pathway, the most studied connection in the CNS.

2.1. The Schaffer collateral connections

The CA3 pyramidal cells send highly collateralized axons that distribute fibers both within the ipsilateral hippocampus to CA3, CA2, and CA1 and to the same fields in the contralateral hippocampus. CA3 to CA3 and CA3 to CA2 ipsilateral projections are called associational connections, whereas CA3 contralateral projections to CA3, CA2, and CA1 are called commissural projections. The CA3 projections to the ipsilateral CA1 field was first described in 1892 by Hungarian anatomist Karl Schaffer (who gave his name: Schaffer collaterals), are typically called the Schaffer collaterals. The CA3 pyramidal cells which are located close to dentate gyrus give rise to axons which project somewhat more heavily to distal portions of CA1, whereas CA3 projections from the cells located distally in CA3 terminate more heavily in CA1 closer to CA2. The truly thick Schaffer collaterals, those that Schaffer originally described, originate from proximal CA3 cells from *stratum oriens* and travels to the distal part of CA1, where it terminates in *stratum radiatum* and *stratum oriens* (Figure 1).

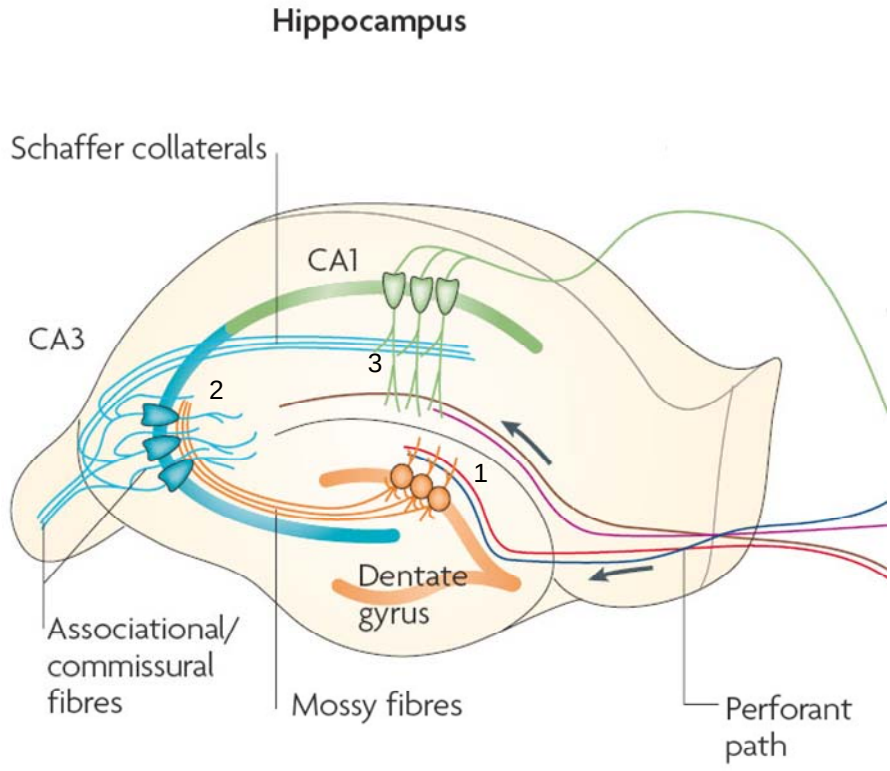

Figure 1. Basic anatomy of the hippocampus. *The diagram of the hippocampus is presented as a trisynaptic loop. The major input is carried by axons of the perforant path to the dentate gyrus (synapse one). Dentate granule cells project, through their axons (the mossy fibres), to the proximal apical dendrites of CA3 pyramidal cells (synapse two) which, in turn, project to CA1 pyramidal cells through Schaffer collaterals (synapse three) (Neves et al., 2008).*

2.2. The hippocampal neuroanatomy

One of the most fascinating features of the hippocampus is its neuroanatomy and especially its laminar organization. The hippocampal principal cells are aggregated in a single layer and form well-defined layered structure that consist from pyramidal cell layer, *striatum oriens*, *striatum lucidum*, *striatum radiatum* and *striatum lacunosum-moleculare*. In rodents, the pyramidal cell layer is about 5 cells thick and is divided in two major regions: a large cell region (CA3 and CA2) and smaller cell region (CA1). The relatively cell-free layer located deep to the pyramidal cell layer is called the *striatum oriens*. *Striatum oriens* consists from the basal dendrites of the pyramidal cells and several classes of interneurons. It is in this layer where CA3 to CA3 associational connections and the CA3 to CA1 Schaffer collateral connections are located. In the CA3 field, but not in CA2 and CA1, a narrow acellular zone, *the striatum lucidum*, is located just above the pyramidal cell layer and is occupied by the mossy fibers. The *striatum radiatum* is located superficial to *striatum lucidum* in CA3 and directly above the pyramidal cell layer in CA2 and CA1. The *striatum radiatum* contains apical dendrites of the pyramidal cells and it is in this layer where CA3 to CA3 associational connections and the CA3 to CA1 Schaffer collateral connections are located. The most superficial layer of the hippocampus is called the *striatum lacunosum-moleculare*. In this layer fibers from the entorhinal cortex terminate. The *striatum radiatum* and the *striatum lacunosum-moleculare* contain several classes of interneurons.

2.3. Neuronal organization of the CA1 region

The principal neuronal cell type of the CA1 region is the pyramidal cell. The CA1 pyramidal neurons are the most studied class of neurons in the brain, this is because of the relatively ease to register field potentials and perform intracellular recordings in this region. The cells from CA1 region are also more viable then cell from other regions of the hippocampus and brain; therefore it is generally easier to keep them alive and healthy in slice preparations. Pyramidal cells have basal dendrite trees that occupy the *striatum oriens* and an apical dendrite tree that occupy the *stratum radiatum* and the *striatum lacunosum-moleculare*. The CA1 pyramidal cells show remarkable homogeneity of their dendrite trees. Regardless of where pyramidal cell is located in the CA1, it has about the same total dendrite length and size of pyramidal cell bodies (Pyapali et al. 1998). The density of dendritic spines and synapses on CA1 pyramidal neurons is highest in the *striatum radiatum*, 54% of all excitatory synapses contact spines in the apical dendrites in the

stratum radiatum, 36% in the *stratum oriens*, but this percentage is lower in the *stratum lacunosum-moleculare*, where only 10% of all excitatory synapses contact spines.

In comparison to the pyramidal neurons which show high anatomical homogeneity in CA1 region, there is fairly heterogeneous group of interneurons that are scattered through all layers (Freund and Buzsaki 1996). Most types of interneurons are found in all the hippocampal subfields.

3. The synapse – target of plasticity

The synapse (the term was coined from Sir Charles Scott Sherrington, from the Greek "syn-" ("together") and "haptein" ("to clasp")), is specialized type of junctions through which the cells of the nervous system signal to each other and to non-neuronal cells such as those in muscles or glands.

In the modern understanding chemical synapse is specialized structural and functional unit that is composed of one or more adjacent synaptic specializations occurring at the interface between two neurons (the presynaptic and postsynaptic parts). Synapses serve several functions: 1) Information through one to the next neuron is passed via synapses. The signal (action potential) from the presynaptic specialization induces neurotransmitter release into the synaptic cleft (a narrow zone between presynaptic and postsynaptic parts), neurotransmitter diffuses across the synaptic cleft, and activates postsynaptic receptors. 2) Synapses play important role in integration of neuronal signal (the information is summated to the postsynaptic cell from excitatory and inhibitory inputs). 3) The efficacy of synaptic transmission is activity-dependent and highly modifiable and lasting modifications of synaptic efficacy are regarded as the biological substrate for learning and memory.

3.1. Ultrastructure of the synapse

Typical chemical synapse, such as those found at dendritic spines are mushroom-shaped projections from two cells towards each other. Such synapses are asymmetrical both in structure and how they operate. Only the so-called presynaptic neuron secretes the neurotransmitter, which binds to the receptors located on the postsynaptic cell. The pre- and postsynaptic sides are separated by synaptic cleft, a gap between them, which is about 20 nm wide. This cleft is narrower than other neuronal contacts (except for gap junctions and puncta adherentia) and appears relatively dense in both sides (presynaptic and postsynaptic density). Both sides of the membrane contains cell adhesion molecules, which are thought

to contribute to the formation, adhesion and stabilization of the synapse as well as they play important roles in signal transduction and plasticity of the synapses.

The presynaptic part of the synapse contains active zones, the parts of synapses where neurotransmitters are released. Active zones are identified by the presence of vesicles containing neurotransmitter molecules. These vesicles are relatively uniform in size and the morphological counterpart of the quanta that make up synaptic signals. Some of the vesicles are docked to the presynaptic membrane, and ready for to diffuse into the synaptic cleft, when action potential will reach presynaptic terminal. These processes are regulated by other components of presynaptic density necessary for exocytoses and proteins that interact with vesicular partners. The presynaptic density is also enriched with other molecules, as voltage-gated Ca^{2+} chanels, proteins involved in reuptake of neurotransmitter and regulation of synaptic transmission.

On the postsynaptic side of the synapse, there is also increased density of the membrane associated proteins, including several classes of glutamate receptors and diverse set of other signaling proteins and proteins for anchoring and trafficking of these receptors.

3.2. Glutamatergic synaptic transmission

Glutamate is the main excitatory neurotransmitter in the hippocampus as elsewhere in the brain. Synaptic transmission begins when the nervous impulse reaches the presynaptic axon, leading to depolarization of the presynaptic membrane. The voltage-gated Ca^{2+} channels open and result in Ca^{2+} ions flowing into the axon terminal, which initiates a sequence of events leading to neurotransmitter release into the synaptic cleft. After release from the presynaptic nerve terminals, glutamate crosses the synaptic cleft and activates three different types of ionotropic glutamate receptors, located on the postsynaptic side of the synapse: L-α-amino-3-hydroxy-5-methyl-4-isoxazolepropionic acid (AMPA), kainate and N-methyl-D-aspartate (NMDA) receptors, named according to the types of synthetic agonists that activate them in relatively selective fashion. The activation of receptors mediates the specific ion entry into the postsynapse and generates the response, an excitatory postsynaptic potential (EPSP).

Fast ionic inward current is generated by AMPA receptors contributing to the early peak of the EPSP. Kainate receptors play a relatively poorly understood role in synaptic transmission, they do not contribute to the fast EPSP appreciably. However, a low amplitude kainite receptor-mediated current can be detected in some neurons in response to high-frequency stimulation (Castillo et al., 1997; Cossart et al., 1998, 2002). The NMDA receptor (NMDAR) channels are blocked by Mg^{2+} at resting membrane potential and they

are relieved from Mg^{2+} block when the membrane is depolarized by stimulation (Mayer et al., 1984; Nowak et al., 1984). Thus, under physiological ionic conditions, both glutamate and depolarization of the membrane are necessary to open the NMDAR channel. Since NMDAR channel activate and deactivate relatively slowly compared to non-NMDAR channels, NMDARs contribute only to the late component of the EPSP. Another class of glutamate receptors is represented by metabotropic receptors, which are G-protein-coupled receptors acting on ion channels indirectly via a cascade of second messengers. Whereas glutamate always has an excitatory effect via ionotropic glutamate receptors (iGluRs), via metabotropic glutamate receptors (mGluRs) it can produce either facilitation or inhibition of synaptic transmission.

3.3. General structure of ionotropic glutamate receptors

All ionotropic glutamate receptors are ligand-gated ion channels, which are selectively permeable for cations, principally Na^+, K^+ and sometimes Ca^{2+} ions that mediate most of the excitatory neurotransmission in the hippocampus. The receptors are heteromeric assembles of four pore-forming subunits, with each distinct subunit encoded by its own gene. The molecular diversity of the subunits is further extended by alternative splicing of the primary transcripts and through posttranscriptional RNA editing (Figure 2).

All ionotropic glutamate receptor subunits share a common basic structure. According to current understanding, the ionotropic glutamate receptor subunits TMI, TMIII and TMIV are transmembrane domains. However, in contrast to other domains, the TMII domain, does not traverse membrane bilayer and forms a re-entrant loop (Figure 2), which determines the ion selectivity of the channel (it is permeable to monovalent and in some instances to divalent cations). The extracellular ligand-binding site is formed by N-terminus extracellular binding domain and by the extracellular loop between TMIII and TMIV. The intracellular C-terminus is the specialized site for interactions with intracellular partners of the receptors.

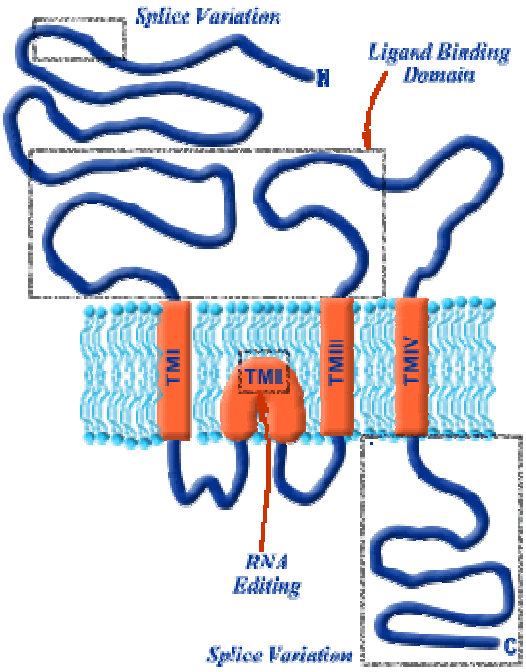

Figure 2. General structure of an ionotropic glutamate receptor subunit*. All ionotropic glutamate receptor subunits share a common basic structure and contain four hydrophobic regions within the central portion of the sequence (TMI – IV). Three of them TMI, TMIII and TMIV are transmembrane domains, but TMII which does not transverse the membrane bilayer, forms a pore-loop region. The receptors have the extracellular N-terminal domain and the intracellular C-terminal domain.*

3.4. Subunits and splice variants of AMPA receptors

AMPA receptors are heterotetramers composed of subunits GluR1-4, all of which are expressed in the CA1 region of the hippocampus. AMPA receptor current is induced via Na^+ influx across the membrane. AMPA receptors are also permeable for K^+ ions at depolarized potentials and depending on their subunit composition they are permeable for Ca^{2+} ions. AMPA receptor subunit distribution varies significantly among hippocampal cell types. Hippocampal pyramidal cells express mainly GluR1 and GluR2, whereas GluR3 is present at lower levels and GluR4 only in embryonic and early postnatal stages, whereas hippocampal interneurons express mainly GluR1 and GluR4 subunits. Among other subunits, GluR2 subunit plays the most critical role in determining ion channel properties: GluR2-containing channels have low Ca^{2+} permeability. This electrophysiological profile is determined by a single amino acid residue of the GluR2 TMII pore-loop segment (Figure 2). Whereas GluR1, 3 and 4 subunits contain glutamine in this position, the GluR2 subunit primary transcript undergoes selective RNA editing that changes the glutamine into an arginine (Seeburg et al., 1998). GluR1 subunits have been suggested to undergo a redistribution during activity-dependent synaptic plasticity (Carroll, Beattie et al. 1999; Shi

2001). It has been also reported that GluR2-GluR3 receptors constitutively recycle in the synapse, whereas the delivery of GluR1-GluR2 receptors is regulated in an activity-dependent manner (Passafaro, Piech et al. 2001).

All AMPA receptor subunits exist as two splice variants, *flip* and *flop*. The receptor primary transcripts undergo alternative splicing cassette of the extracellular loop between TMIII and TMIV. Although the change in the receptor subunits is small (only a few amino acids are changed), the effect can be quite dramatic, resulting in altered desensitisation kinetics: *flip* forms desensitize with slower kinetics compared to *flop* forms (Sommer et al., 1990). In addition to the *flip* and *flop* alternative splicing, the primary transcripts of AMPA receptors undergo an addition alternative splicing of C-terminal domain coding sequences. The AMPA receptor subunit C-terminal domains are grouped into ,,long'' (GluR1, GluR4) and ,,short'' (GluR2, GluR3) cytoplasmic tails.

3.5. The NMDA receptor

N-methyl-D-aspartate receptors are ionotropic ligand-gated voltage-dependent glutamate receptors, composed of assemblies of NMDAR subunits. NMDAR subunits are grouped into three sub-classes: NR1, NR2 and NR3 (Hollmann, 1999; Moriyoshi et al., 1991; Monyer et al., 1992,1994; Sugihara et al., 1992; Das et al., 1998). The NR1 subunit is encoded by a single gene but via posttranslational splicing exists as eight splice isoforms (Dingledine et al., 1999). In the CA1 region of the hippocampus NR1A subunit is predominated. In NMDAR heteromeric complexes NR1 subunits are the essential subunits (Forrest et al., 1994), responsible for anchoring of the receptor (in its absence, no functional NMDAR are formed) and co-agonist binding (Anson et al., 1998). The NR2 subunit which contains glutamate-binding site (Kuryatov et al., 1994) is presented by four members NR2 A-D. They are encoded by four different genes and are variably expressed in different regions of the brain and at different stages of development. The NR2 subunits differ in their physical and pharmacological properties and are main determinants of NMDAR function. The NR3 subunits (NR3A-B) do not appear to play an important role in the hippocampus. The NR3 subunit can assemble with NR1 and NR2 subunits, resulting in a receptor with diminished activity (Das et al., 1998), and NR3 subunits can assemble with NR1 alone to create a functional glycine-gated ion receptor (Chatterton et al., 2002).

To form a functional NMDAR complex, the NMDAR subunits must assemble to tetrameric complex with two NR1 subunits and two NR2 subunits or NR3 subunits (Behe et al., 1995; Sheng et al., 1994). Depending on the presence of the NR2 and NR3 subunits, the NMDAR can be subdivided into the NR2A subtype (tetramer of two NR1 and two NR2A),

NR2B subtype (two NR1 and two NR2B), and so on. The NMDA subunits can also form triheteromeric tetrameric complexes where two NR1 subunits are in complex with more then one type of the NR2 subunit NR2A/NR2B or NR2C/NR2D (Dunah et al., 1998; Luo et al., 1997), but it is still unknown to what extent these assemblies are expressed *in vivo*. In the mature hippocampus of the mice NMDAR are presented mostly by NR2A, NR2B and in some portion NR2A/NR2B subtypes. The NR2 subunits determine the electrophysiological and pharmacological profile of the channels, affecting its open time, conductance, and Mg^{2+} sensitivity. The NR2 subunits expression is regulated developmentally.

3.6. Developmental profile of NMDA receptor subunits and subtype distribution

Whereas NR1 is continuously and ubiquitously expressed in the CNS, the expression of the distinct NR2 subunits depends on the developmental stage and brain region (Monyer et al., 1994; Akazawa et al., 1994). The NR2A and NR2B subunits are the major and most widespread NR2 subunits, with NR2C largely restricted to the cerebellum and NR2D most heavily expressed early in development. The expression of NR2B subunit predominates early in development and then gradually decreases, whereas NR2A is weakly expressed shortly after birth but progressively increases its expression (Monyer et al., 1994; Sheng et al., 1994) and synaptic incorporation during postnatal development (Stocca and Vicini, 1998; Tovar and Westbrook, 1999). The NR2A/NR2B expression ratio increases during postnatal development, indicating that the NR2B-type NMDARs are more important at the early postnatal stage, whereas the NR2A receptor plays a major role at mature hippocampal synapses (Monyer et al., 1994). Although NR2A subunits are incorporated synaptically late in development, NR2B subunits are still highly persistent at extrasynaptic sites (Stocca and Vicini, 1998; Rumbaugh and Vicini, 1999; Tovar and Westbrook, 1999). Furthermore the distribution of NR2B receptors is reported to be asymmetrical between the left and right hippocampus and between the apical and basal dendrites of single neurons (Kawakami et al., 2003). The distinct expression and developmental profile of the NMDAR subunits explains differential involvement of NMDAR subunits into different types of NMDAR dependent synaptic plasticity.

3.7. Functional properties of NMDA receptors

The NMDARs are nonselective ion channels: Na^+ and Ca^{2+} ions move from extracellular compartments into the cell and K^+ out of the cell. The NMDARs are among the most tightly regulated neurotransmitter receptors. There are no fewer than six distinct

binding sites for endogenous ligands that influence the probability of ion-channel opening (Figure 3). These consist of two different agonist-recognition sites, one for glutamate and one for glycine, and a polyamine regulatory site, all of which promote receptor activation, and separate recognition sites for Mg^{2+}, Zn^{2+} and H^{+} that inhibit ion flux through agonist-bound receptors. NMDARs are highly permeable to Ca^{2+} ions, show slower activation kinetics plus longer open time and high affinity for glutamate.

In addition to glutamate (the NMDAR true agonist), a second-agonist binding site must be occupied to activate NMDAR (Kleckner and Dingledine, 1988). The strychnine-insensitive glycine binding site is located on NR1 subunit of NMDAR and is activated by extracellular glycine. The estimated concentration of extracellular glycine is expected to be enough to occupy most NMDAR binding site (Schell et al., 1995), but still the concentration extracellular glycine varies brain region specific manner and different NMDA subunits have different sensitivity. The ambient concentrations of glycine and D-serine are sufficient to saturate the glycine binding site of NR2B- but not NR2A-NMDARs due to a higher affinity of glycine and DCS binding to NR2B-NMDARs (Priestley et al., 1995). Unsaturated glycine binding site could serve as modulatory site for NMDARs (Billard and Rouaud, 2007).

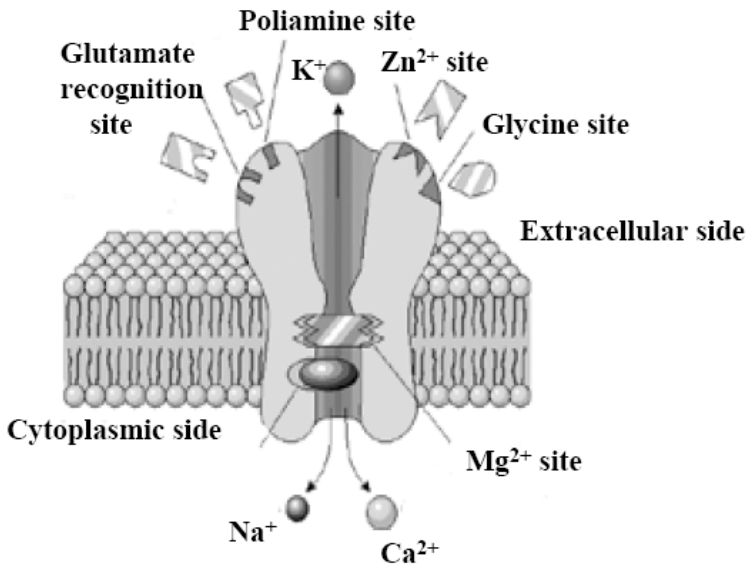

Figure 3. Schematic representation of the NMDA receptor complex. *The NMDAR complex possess a glutamate recognition site to which receptor agonists and competitive antagonists bind, as well as other binding sites for glycine, polyamines, Mg^{2+} and Zn^{2+}. Channel opening permits an influx of Na+ and Ca2+ ions, and an efflux of K+ ions (Scatton, 1993).*

In the presence of glutamate and glycine NMDAR may still unable to mediate ion flux, they are blocked with Mg^{2+} ions in a voltage-dependent manner. The activation of NMDAR is only possible when membrane potential is sufficiently depolarized to remove Mg^{2+} ion block. This unique feature gives NMDARs the ability to act as coincidence detectors when presynaptic activity (glutamate release) and postsynaptic activity (sufficient depolarization of postsynaptic membrane) are synchronized. Ca^{2+} influx occurs only if there is a simultaneous presynaptic glutamate release and postsynaptic depolarization. NMDAR activation has been shown to trigger further release of Ca^{2+} from intracellular stores (Emptage et al., 1999). Furthermore, when the presynaptic neuron fires repeatedly so that the EPSPs summate to depolarize the postsynaptic cell, the NMDAR gives rise to a much larger Ca^{2+} current. Calcium ions are actually ubiquitous secondary messengers the subsequent postsynaptic influx of Ca^{2+} transduce the activation of NMDAR into Ca^{2+} dependent intracellular signaling. These integrative and other properties of ion channel of NMDARs underlie the induction of NMDAR-dependent synaptic plasticity, which is believed to be molecular mechanism of learning and memory.

The NMDAR show high affinity for glutamate with very slow activation kinetics and can continue to mediate an ion flux for several hundreds of milliseconds. The slow kinetic is explained by an extremely slow receptor unbinding rate. Once glutamate has become bound to NMDARs, they remain bound for long time, during which time the ionophore can undergo repeated openings (Lester et al., 1990). These features of NMDARs give possibility for high amount of Ca^{2+} to enter into the cell for to switch on intracellular signaling cascade systems.

4. Synaptic plasticity

The term ”synaptic plasticity“ was introduced by the Polish physiologist Jerzy Konorski to describe the persistent, activity-driven changes in synaptic efficacy to be the basis of information storage in the brain (Konorski, 1948). Synaptic plasticity is the ability of a single synapse to respond to specific patterns of activation with long-lasting increases or decreases in synaptic efficacy. Synaptic efficacy is inherently stochastic process that can be modulated by patterns of activation in the presynaptic or postsynaptic neuron and by a wide range of neuromodulators acting pre-and postsynaptically. This phenomenon is seen almost in all excitatory synapses in the brain. Some of the activity-dependent changes in synaptic efficacy that occur in the Shaffer collateral synapse are such as paired-pulse facilitation (PPF), short-term potentiation (STP), long-term potentiation and long-term depression.

4.1. Paired-pulse facilitation

The aftereffects on synaptic transmission of a single stimulus can be tested by delivering a second stimulus at a variable time after the first. The variability of second stimulus compared to the first is synapse specific. When pairs of stimuli are delivered to CA1 the Schaffer collateral synapses the amplitude of the second response is facilitated at interstimulus intervals of less than 300 ms (Andersen, 1960). The facilitation of the second response compared to the first, taken as facilitation ratio, reflects the increase in the probability of transmitter release (Zucker and Regehr, 2002). The increase of neurotransmitter release during second response is achieved by the transient increase in the concentration of Ca^{2+} into the axon terminal by invading action potentials. The concentration of Ca^{2+} declines to the basal level over a few hundred milliseconds, but the Ca^{2+} influx at the time of the second stimulus adds to the residual Ca^{2+} concentration from the first, resulting in an enhanced Ca^{2+} concentration and mobilization of synaptic vesicles and to increased probability of release (Wu and Saggau, 1994).

4.2. Short-term potentiation

Short-term potentiation is the first phase of post-tetanic potentiation which occurs after repetitive stimulation of presynaptic terminals and lasts several minutes. It is characterized as rapidly declining phase mirrored by a decrease in paired-pulse facilitation. It was relatively difficult to investigate the molecular mechanism of STP because next phase of post-tetanic potentiation, LTP, develops gradually over approximately the same time-course that STP decays. The controversy that STP has presynaptic versus postsynaptic expression mechanism still remained. One scenario that STP could have postsynaptic basis was supported by the possibility that AMPA receptors can undergo relatively fast internalization from extrasynaptic site into the synaptic one. By studying STP in isolation using trains subthershold for LTP and by the fact that the concentration of Ca^{2+} in terminal buttons rises during STP, suggest that it is a presynaptic process (Wu and Saggau, 1994; Tang and Zucker, 1997; Gustafsson et al., 1989). Additional test for discrimination of presynaptic from postsynaptic mechanisms, based on the fact that reduction in PPF following the expression of STP is due to the increase of probability of release, suggested that STP has presynaptic nature (McNaughton, 1982).

4.3. Long-term potentiationot

In addition to above-mentioned short-term forms of synaptic plasticity, activity could also induce long-term changes in synaptic efficacy, which appear to be critical for the

development of appropriate neuronal circuits and for many forms of neuronal plasticity, including learning and memory. The aftereffects of a repetitive stimulus on synaptic transmission in the form of the long-term potentiation was first discovered in 1973 (Bliss and Gardner-Medwin, 1973; Bliss and Lomo, 1973). Bliss and Lomo delivered few seconds of high-frequency electrical stimulation to the perforant path in rabbit hippocampus, and revealed that synaptic transmission between the stimulated axons and the postsynaptic granule cells was increased. Electrical stimulation induced increase in the amplitude of field EPSP in many cases could persist for hours, and under certain conditions, even for days and weeks (Bliss and Gardner-Mewin, 1973). In addition to high frequency stimulations, other stimulation protocols have been widely used to evoke LTP in CA1 region. For instance, pairing a low frequency presynaptic stimulation with postsynaptic depolarization has been reported as an effective way to induce LTP which can last for several hours (Gustafsson and Wigström, 1986; Wigström and Gustafsson, 1986; Gustafsson et al., 1987; Liao et al., 1995; Chen et al., 1999). Theta burst stimulation has been considered as a more natural way to induce LTP due to the occurrence of theta electroencephalogram rhythm (about 5 Hz) in the normal brain (Larson et al., 1986; Staubli and Lynch, 1987).

The first evidence that NMDA receptors are required in LTP induction come from 1983, when it was found that NMDA receptor specific antagonist APV (Davies et al., 1981) blocked induction of LTP in CA1 region (Collingridge et al., 1983). Activation of NMDA receptors leads to the influx of Ca^{2+} through the NMDA channel (MacDermott et al., 1986; Jahr and Stevens, 1987, 1993), and a rise in Ca^{2+} within the dendritic spine is absolutely necessary trigger for LTP (Lynch et al., 1983). Whereas most types of LTP depend on the activation of NMDA receptors, some forms of LTP are NMDA receptor indepent (Lynch, 2004). A rise in Ca^{2+} lasting less than 2-3 s (Malenka et al., 1992) appears to be sufficient for LTP. Ca^{2+} acts as an important second messenger and plays an essential role in inducing synaptic plasticity (Collingridge et al., 1983; Lynch et al., 1983).

Many protein enzymes have been considered as the targets of increased intracellular Ca^{2+} and their activation is believed to trigger LTP. Among them, calcium/calmodulin-dependent protein kinase II (CaMKII) is well known to mediate LTP (Lisman 1994; Malenka and Nicoll 1999; Lisman et al., 2002). Activated CaMKII can undergo autophosphorylation and keep itself staying at active state (Lisman et al., 2002). It affects AMPA receptors in two ways. First it phosphorylates the AMPA receptors that are already present in the postsynaptic membrane, thereby increasing the conductance for ions such as Na^{+}. CaMKII also promotes the movement of AMPA receptors from intracellular stores to

the membrane, making more receptors available to be activated. As a result of a change in AMPA receptor composition and number, the response to a stimulus at a given strength will be stronger than it was before the NMDA receptors were activated. In this way, the synaptic efficacy is enhanced and this physiological change is thought to be one of the mechanisms underlying the expression of LTP.

There are also other enzymes, for example, activation of cAMP-dependent protein kinase (PKA) (Yasuda et al., 2003), protein kinase C (PKC) (Bliss and Collingridge, 1993; Malenka and Nicoll, 1999) and mitogen-activated protein kinase (MAPK) have been implicated in LTP (Sweatt 2004). The PKA may be especially important in late (>3 h) phases of LTP, and might be a link to activation of protein synthesis via the transcriptional factors activation (Abraham and Williams 2003; Lynch 2004). Synthesis of new proteins is considered to be important for the long-term maintenance of LTP as well as for the stabilization of memory processes (Huang and Kandel, 2005).

4.4. Long-term depression

Long-term depression (LTD) is a remarkable capacity of individual synapses to undergo persistent decrease of synaptic transmission which lasts at least several hours. Homosynaptic, *de novo* LTD was first induced in 1992 by LFS applied for a relatively long period of 10-15 minutes (Dudek and Bear, 1992). Both size and slope of field EPSPs were depressed for several hours. Protocols employed for inducing LTD vary among investigators, partly due to general differences in experimental design, including the use of different brain areas and animal ages. For instance, in presence of certain neuromodulators, LTD can be effectively induced by a reduced number of stimuli (Kirkwood et al., 1999; Scheiderer et al., 2004). In the adult rat, where LTD is not readily induced by low frequency stimulation, a protocol with paired pulses (1 Hz, 900 pulses) appears to be more optimal (Thiels et al., 1996; Kemp et al., 2000; Lee et al., 2003). LTD is also dependent on an increase in intracellular Ca^{2+}, and in many cases requires Ca^{2+} entry through NMDA receptors (Bear and Malenka 1994). It is commonly believed that a large increase in intracellular Ca^{2+} concentration within a short period causes LTP and a moderate elevation of Ca^{2+} with a longer duration leads to LTD. Small or modest rise of Ca^{2+} is thought to activate serine-threonine protein phosphatase (Mulkey et al., 1994) and cause the dephosphorylation of PKA and PKC substrates (Kameyama et al., 1998; Lee et al., 1998; van Dam et al., 2002). This process results in dephosphorylation of AMPA receptors, and removal from synaptic side, thus leading to LTD (Mulkey et al., 1994). So LTD could be

considered as counterpart of LTP, since the intracellular signaling of LTD often overlaps with LTP.

4.5 NR2A and NR2B-NMDA receptors are differentially involved in long-term potentiation and long-term depression

A growing body of evidence suggests that different NMDAR subunits are involved in different forms on NMDAR-dependent LTP and LTD. It has been shown that LTP is specifically related to NR2A-containing NMDARs in the hippocampus (Kohr et al., 2003; Li et al., 2006; Liu et al., 2004) and cortical regions of the brain (Massey et al., 2004), whereas, there may be a substantial contribution of NR2B-NMDARs in LTP (Kohr et al., 2003; Zhao et al., 2005). On the other hand, LTD in both hippocampus and cortex was shown in several studies to specifically rely on NR2B-containing NMDARs (Liu et al., 2004; Massey et al., 2004). Also, it has been reported that the erasure of LTP, referred to as „depotentiation", is due to the involvement of NR2A subunits (Massey et al., 2004). Even so, the idea of subtype specificity has been questioned, suggesting that the important thing for LTP is the degree and temporal character of the Ca^{2+} influx, not the actual subtype of receptor involved (Berberich et al., 2005). Beside the Ca^{2+} concentration dependence, differential distribution of NMDAR subunits plays pivotal role in governing synaptic plasticity to differential directions. NR2A-NMDARs are the predominant NMDARs at the postsynaptic density (Petralia et al., 2005) and substantial fraction of NR2B-NMDARs is located extrasynaptically in the adult hippocampus (reviewed by Kohr, 2006). Differential NMDAR distribution can induce differential modulation of extracellular signal-related protein kinase (ERK) MAP signaling cascade a downstream molecule of which is CaMKII (Zhu et al., 2002). The ERK signaling cascade is a key pathway that mediates the NMDAR-dependent synaptic plasticity. NMDARs induce a complex modification of ERK that includes activation and inactivation resulting in long-term potentiation and long-term depression of synaptic efficacy. Activation of synaptic NMDAR by specific agonists (Bading and Greenberg, 1991; Kurino et al., 1995) or via an increase of synaptic activity (Hardingham et al., 2001) results in strong ERK phosporylation and activates ERK cascade (Ivanov et al., 2006) however, application of high concentration of NMDA (which induces activation of both synaptic and extrasynaptic NMDARs) results in moderate activation of ERK signaling (Ivanov et al., 2006; Chandler et al., 2001; Kim et al., 2005), suggesting inhibitory role of extrasynaptic NMDARs on ERK signaling. A very important link between intracellular Ca^{2+} concentration and activation of signaling cascades responsible for synaptic plasticity was made by Li et al., 2006. The authors identified specific guanine

nucleotide factors Ras-GRF1 and Ras-GRF2 that couple calcium influx via NMDARs to activation of appropriate GTPases. Ras-GRF1 (Shou et al., 1992) and Ras-GRF2 (Fam et al., 1997) are activated by calcium via calcium/calmodulin binding to there N-terminal IQ motifs (Show et al., 1992; Farnworth et al., 1995; Fam et al., 1997). Both Ras-GRF1 and Ras-GRF2 contain two GEF domains, a C-terminal cell division cycle 25 (CD25) domain that activates the Ras/Erk signaling cascade (Shou et al., 1992; Fam et al., 1997) and a more N-terminal dbl homology (DH) domain that activates a Rac/p38 cascade (Fan et al., 1998; Innocenti et al., 1999; Kiyono et al., 1999; Buchsbaum et al., 2002). Analysis of mice deficient in either Ras-GRF1 or Ras-GRF2 revealed the critical role of the former in induction of LTD, whereas the latter was found to be important for LTP (Li et al., 2006).

4.6. Long-term potentiation and aging

Various factors can greatly influence the properties of LTP, such as induction protocol, synapse under investigation, phase of LTP and age of the animals. Changes in the molecular mechanisms of LTP are unlikely to change radically during normal aging: LTP induction, for example, still requires the activation of NMDA receptors (Barnes et al., 1996). However, during aging there are alterations in the LTP process that could contribute to a decline in cognitive function. At CA1 synapses, the primary deficit with aging seems to be a reduction in the magnitude of LTP, which may be explained by less activation of NMDA receptors (Deupree et al., 1991; Moore et al., 1993; Rosenzweig et al., 1997; Tombaugh et al., 2002). Thus, it appears that a major deficit in age-related changes in LTP is alterations in conditions affecting NMDA receptor function and its associated Ca^{2+} signaling. This is supported by the recent findings that facilitation of NMDA receptor function restores the level of LTP in aged rats to the level of young animals (Billard and Rouaud., 2007).

5. The immunoglobulin superfamily of cell adhesion molecules

Most cells are decorated with several types of proteins called cell adhesion molecules (CAMs), which allow their binding to other cells or to the extracellular matrix. These proteins are usually transmembrane receptors and are composed of three domains: an extracellular domain which interacts either with other CAMs of the same kind (homophilic binding) or with other CAMs or the extracellular matrix (heterophilic binding), a transmembrane domain and an intracellular domain that interacts with cytoskeleton. The importance of CAMs is not limited only for adhesion profile; beside cell adhesion function adhesion molecules are also capable of transmitting information from the extracellular

matrix to the cell. By means of signaling property CAMs can control nervous system development and maintenance. Important phenomena in which CAMs are involved include initial formation of the neural tube and the neural crest, cell growth, differentiation, migration, axonal outgrowth and guidance, target selection, synaptic stabilization and plasticity, myelination and nerve regeneration after injury (Gordon-Weeks and Fischer, 2000; Kater and Rehder, 1995).

There are several families of cell adhesion molecules. Among these are the immunoglobulin (Ig) superfamily cell adhesion molecules, integrins, cadherins, and selectins. The immunoglobulin superfamily include a large group of molecules which share homotypic structure by the presence of Ig-like domains that can be combined with other protein motifs in their extracellular domains (Brümmendorf and Rathjen, 1995; Crossin and Krushel, 2000). Often an array of Ig-like domains is coupled with fibronectin type III-like repeats. The amino acid sequence of fibronectin III-like repeats resembles to the FNIII repeats of fibronectin and therefore termed as FNIII-like repeats (Brümmendorf and Rathjen., 1995). An intracellular part of Ig CAM has more diverse structure and, it may contain a tyrosine kinase domain like in fibroblast grows factor receptor (FGF-R) or tyrosine phosphatase domain like in CRYPα1. The Ig superfamily is further divided into subfamilies of Ig CAM including different number of Ig-like domains and fibronectin III-like repeats. The best-studied members of this group are the neural cell adhesion molecules.

5.1. The neural cell adhesion molecule NCAM

The neural cell adhesion molecule NCAM is expressed by all neural cell types, where it promotes neuron-neuron and neuron-glia adhesion via homophilic and heterophilic interactions with other adhesion and extracellular matrix molecules. NCAM was the first Ig-like cell adhesion molecule to be isolated and characterized in the CNS (Brackenbury et al., 1977; Thiery et al., 1977; Cunningham et al., 1987). The extracellular part of NCAM contains five Ig-like domains and two fibronectin type III-like repeats (Figure 4). The NCAM gene, which is situated on chromosome 9 in mice (D'Eustacio et al., 1985) and on chromosome 11 in human (Nguyen et al., 1986), gives rise to several different isoforms by alternative splicing and posttranslational modifications of the primary transcript. Three major NCAM isoforms are known NCAM180, NCAM140 and NCAM120 named according to their approximate molecular weights (Cunningham et al., 1987). NCAM180 and NCAM140 are transmembrane molecules differing in the size of their intracellular domains whereas NCAM120 is linked to the membrane via a glycosylphosphatidylinositol (GPI) anchor (Figure 4) (Gennarini et al., 1984 a,b). Related molecules in other species are

the fasciclin II of *Drosophila melongaster* and the *Aplysia californica* cell adhesion molecule (apCAM), which both has 25 % homogenity with vertebrate NCAM.

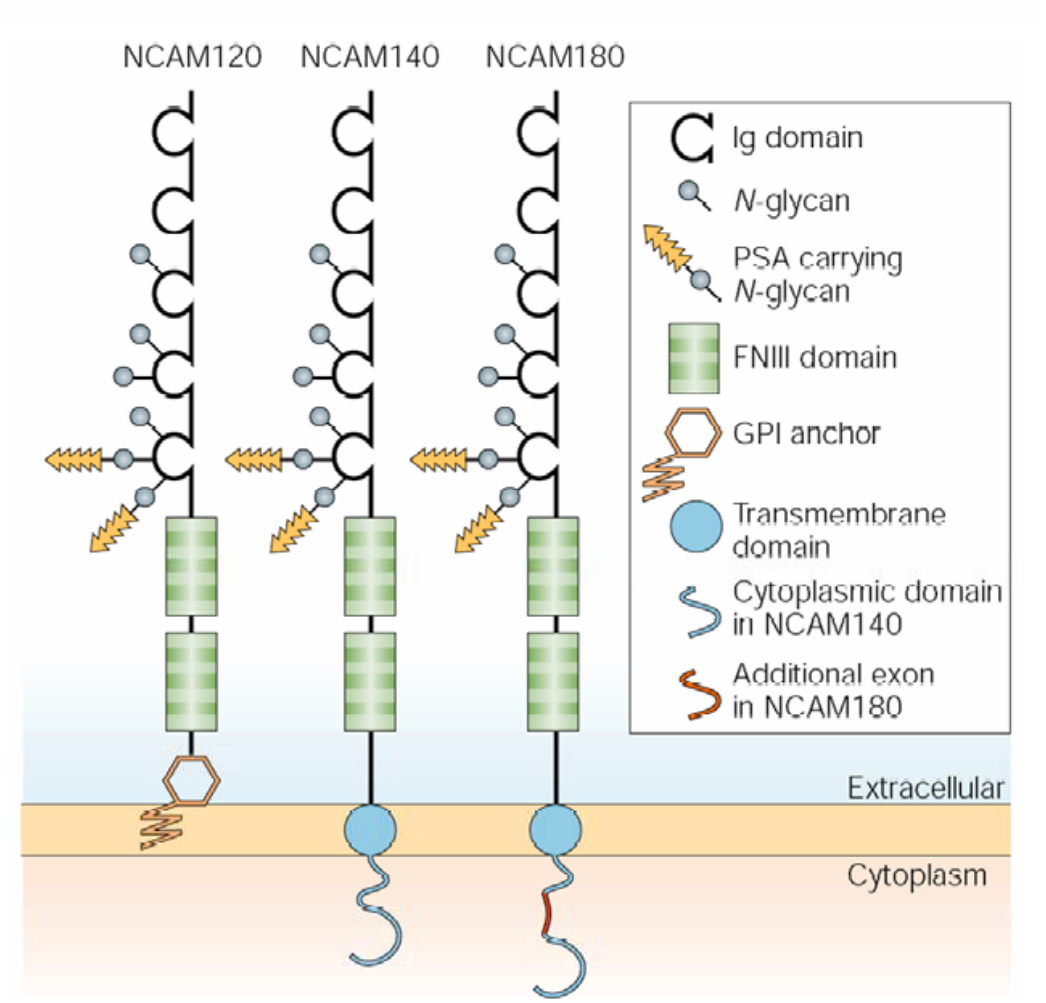

***Figure 4. Structure of three main isoforms of NCAM**. All three isoforms of the neural cell-adhesion molecule (NCAM) named according to their molecular weights. The glycosyl phosphatidylinositol (GPI)-anchored NCAM120 and the transmembrane NCAM140 and NCAM180 consist of five immunoglobulin (Ig)-like domains and two fibronectin type III repeats (FNIII). The cytoplasmic domains of NCAM140 and NCAM180 differ in length owing to the presence of an additional exon sequence in NCAM180 that results from alternative splicing. (Kleene and Schachner, 2004).*

In addition to the three main membrane isoforms of NCAM, there are several secreted forms; one (115 kDa) is produced by the expression of small so-called SEC-exon located between exons 12 and 13 (Bock et al., 1987; Gower et al., 1988), the others are produced by shedding of NCAM, an enzymatic removal of NCAM120 from the membrane by phosphatidylinositol specific phospholipase C (PI-PLC), or by proteolytic cleavage of the extracellular part of any of the three major isoforms (He et al., 1986).

In addition to different isoforms generated by alternative splicing and their soluble derivatives, NCAM is subject to post-translational modification by the addition varying

length of a highly negatively charged polysialic acid (PSA) (Figure 4). Interestingly, only vertebrate NCAM carries such a unique sugar like PSA, expression of which on NCAM can be extremely fast up- or down-regulated by synaptic activity and/or learning (Muller et al., 1996; Sandi et al., 2003; O'Connell et al., 1997).

As many neural cell adhesion molecules, NCAM also carries a carbohydrate epitope named HNK-1 (human natural killer cells) which contains sulfated glucuronic acid and is attached to NCAM by N-linked glycosylation through at least 5 different sites (Schachner and Martini, 1995; Wuhrer et al., 2003).

5.2. NCAM: expression, binding partners and signaling

The expression of alternatively spliced forms of NCAM, in terms of time and cell-type specificity, is differentially regulated and thus the isoforms are likely to play different roles in the organism (Jorgensen, 1995). Expression of NCAM starts very early during development, in *Xenopus*, for instance, first NCAM transcripts can be detected already 2 hours after neural induction (Balak et al., 1987)**.** Generally NCAM is very ubiquitously expressed. In hippocampus, for instance, all three isoforms are well visualized by monoclonal antibodies. Immunoassaying with polyclonal antibodies that recognizes all NCAM isoforms is intense in molecular layer of the dentate gyrus, *striatum lucidum*, CA3 and CA1 *striatum radiatum and striatum oriens,* but the *striatum lacunosum-moleculare* shows very little staining (Miller et al., 1993). It can be found on nearly all postmitotic neurons, on Schwann cells, oligodendrocytes, astrocytes and muscle cells (Moore and Walsh, 1986; Neugebauer et al., 1988; Seilheimer and Schachner, 1988). Some cell types or subcellular structures specifically express one of the three main isoforms. NCAM120 is predominantly expressed on glia rather than neurons (Goodman, 1996; Kiss et al., 2001). NCAM140 and NCAM180 seem to be expressed exclusively on neurons. NCAM140 is detectable on pre- and post-synaptic membranes, whereas NCAM180 accumulates in the postsynaptic densities of synapses of mature neurons (Persohn et al., 1989; Pollerberg et al., 1987; Schachner, 1997). NCAM180 long cytoplasmic tail interacts with the spectrin-actin cytoskeleton and thereby stabilizes synapse formation (Pollerberg et al., 1987; Persohn et al. 1989; Sytnyk et al., 2002).

Cell adhesion mediated by NCAM can occur by interaction between individual NCAM molecules (homophilic), located on opposite cells (*trans-interaction*) (Rutishauer et al., 1982). The homophilic *trans* NCAM-NCAM recognition involves antiparallel association of the five or two Ig domains. Additional evidence exists for another possibility of interaction between just the first Ig of one molecule domain and the second Ig domain of

the opposing molecule therefore NCAM can also *cis* interact homophilically (Crossin and Krushel, 2000). NCAM can also interact with some other cell adhesion molecules, for instance with L1 molecule of Ig superfamily (heterophilic *cis* interaction) (Kadmon et al., 1990a,b; Horstkorte et al., 1993). Interestingly, NCAM and L1 share several features very similar to each other including expression pattern and the binding partners like laminin, integrins, and the FGF receptor (Kadmon et al., 1990a,b; Walsh and Doherty, 1997 Williams et al., 1995). NCAM can bind to FGF receptor and can stimulate it directly. Application of either NCAM-F3II recombinant protein or a 15 amino acid-long mimicking peptide corresponding to the FGF receptor interaction site leads to phosphorylation of FGF receptor and followed by neurite outgrowth. NCAM may also interact with some components of the extracellular matrix (ECM); chondroitin sulfate proteoglycans (CSPG) and heparan sulfate proteoglycans (HSPGs), including agrin, neurocan and phosphacan (Cole et al., 1986; Burg et al., 1995; Grumet et al., 1993). For example, NCAM carries a short, 17 amino acid-long sequence in the IgII module which can bind to heparin, a glycosaminoglycan of ECM, and it occurs independently from homophilic NCAM-NCAM interactions (Cole et al., 1986, 1989).

NCAM has been demonstrated to participate in a number of direct or indirect interactions with many intracellular molecules. For example, in some studies NCAM180 can be anchored in the plasmatic membrane through intracellular interaction with a cytoskeletal linker-protein spectrin (Pollerberg et al., 1987) or all three isoforms of NCAM can immunoprecipitate spectrin (Leshchynska et al., 2003). Another study showed that NCAM180 and NCAM140 both can be associated with α- and β-tubulins and α-actinin, major components of the cytoskeleton (Büttner et al., 2003). It has been shown that NCAM can co-immunoprecipitate with several kinases, e.g., a member of the Src-family non-receptor tyrosine kinases, Fyn, and the focal adhesion kinase FAK, and GAP-43 (He and Meiri, 2002).

5.3. Polysialic acid: structure, synthesis and expression

Functions of NCAM is developmentally regulated by its glycosylation, particularly polysialylation has important impact on its functional properties. Attachment of long homopolymers of sialic acid residues, known as polysialic acid (PSA) (Rutishauser and Landmesser, 1996; Dityatev et al., 2004; Weinhold et al., 2005) reduces NCAM homophilic binding by attenuating cell-cell contacts (Bruses and Rutishauer, 2001). PSA is large linear highly negatively charged carbohydrate polymer, which can contain more than 100 alpha2,8-linked sialic acid residues (Figure 5). NCAM is predominant carrier of PSA

in the vertebrate CNS. The attachment of highly negatively charged PSA around the NCAM core protein results in a large hydratation sphere and modulates the function of the molecule. The polysialylated form of NCAM is thought to be involved in dynamic processes, such as cell migration, axonal growth, pathfinding and synaptic plasticity (Bruses and Rutishauer, 2001).

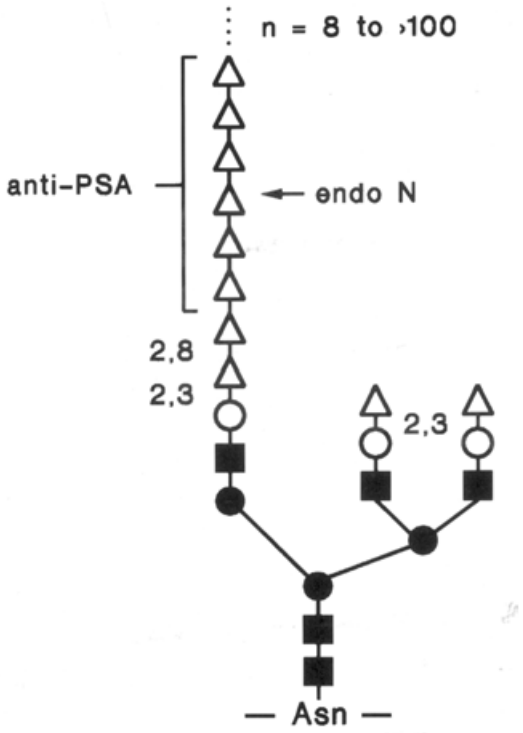

Figure 5. Structure of polysialic acid (PSA). *PSA is attached to NCAM via a typical N-linked core glycosylation. The unique structure of the α2,8-linked polymer allows for its specific recognition by monoclonal antibodies and by phage-derived endoneuraminidase (endo-N). Open triangles, sialic acid; open circles, galactose; closed squares, glucosamine; closed circles, mannose. (Rutishauser and Landmesser 1996).*

Addition of PSA to NCAM takes place in the trans-Golgi compartment as a regular step in the biosynthetic pathway of protein glycosylation in eukaryotes (Scheidegger et al., 1994). The polysialylation of NCAM occurs in all vertebrates but appears to be absent in invertebrates (Rutishauser, 1996; Rutishauser and Landmesser, 1996; Schachner, 1994). Polysialic acid can be attached to all three NCAM isoforms (including soluble ones), to their 5th Ig-domain (Nelson, et al., 1995; Finne et al., 1983). PSA is synthesized by two polysialyltransferases ST8SiaII/STX or ST8SiaIV/PST, which differ in their enzymatic activity and biological functions. STX and PST are highly homologous to each other and have 59% identity at the amino acid level (Eckhardt et al., 1995). Two enzymes are expressed in a tissue- and developmental- specific manner, resulting in markedly different

with respect to their spatial and temporal expression patterns (Kurosawa et al., 1997; Phillips et al., 1997; Hildebrandt et al., 1998; Ong et al., 1998). In mouse and rat, both PST and STX are expressed in early stages of development, reaching maximum level just before birth. In mouse, approximately 10 days after birth, STX is dramatically decreased while PST is just moderately decreased during development (Angata et al., 1998; Nakayama et al., 1998). These enzymes seem to be the regulators of PSA-NCAM synthesis and their activity is controlled at the mRNA and protein levels (Eckhardt et al., 1995). Whereas in the early development (in mice up to embryonic days 8 and 9) NCAM does not carry PSA, PSA-NCAM become predominant at later stages and reaches a maximum in the perinatal phase. However, postnataly the amount of PSA progressively declines, and only a minor fraction of NCAM remains in its polysialylated state (Rutishauser and Landmesser, 1996). In the adult brain, PSA-NCAM remains expressed in neuronal populations showing ongoing neurogenesis, cell migration, axonal outgrowth, and synaptic plasticity. Examples are the rostral migratory stream (Lois et al., 1996), the hippocampal formation (Seki and Arai, 1993), and the hypothalamic nuclei (Theodosis et al., 1991).

5.4. The role of PSA-NCAM in synaptic plasticity and learning

It is not any more arguable that NCAM and its associated PSA play an important mediator role of synaptic plasticity in the adult brain (Bukalo et al., 2004; Lüthi et al., 1994; Muller et al., 1996; Muller et al., 2000). Learning and synaptic plasticity *in vitro* and *in vivo* are altered in the CA1 and CA3 hippocampal subfields and in the dentate gyrus of mice deficient for NCAM (Cremer et al., 1998; Cremer et al., 1994; Muller et al., 1996; Senkov et al., 2006; Stoenica et al., 2006). In different types of synapses, synaptic plasticity is modulated by NCAM through either PSA-dependent or PSA-independent mechanisms. A possible link between NCAM and synaptic plasticity has been suggested by variety of experiments: Administration of anti-NCAM antibodies induces amnesia in rats (Doyle et al., 1992) and interferes with the consolidation of memory in chickens (Scholey et al., 1993). Injection of anti-NCAM antibodies into the CA1 region in rat inhibits subsequent LTP induction (Lüthi et al., 1994; Ronn et al., 1995). There were also several studies *in vivo* and *in vitro* also in which it has been shown that enzymatic removal of NCAM-associated PSA by endoneuraminidase N (Endo-N), an enzyme isolated from bacteriophages, which specifically recognizes the 3D-structure of sialic acid polymers and cleaves units of eight sugar residues (Finne and Mäkelä, 1985) leads to deficits in synaptic plasticity. For example, elimination of PSA by Endo-N injected via chronically implanted cannulas directly into the rat hippocampi led to a significant impairment in the formation of

spatial memory of rats in the Moris water maze (Becker et al., 1996). Also, Endo-N treatment completely prevented the induction of LTP and LTD in organotypic cultures made from the CA1 region of hippocampus, not affecting other cellular and synaptic parameters such as resting or action potentials (Muller et al., 1996). Also in hippocampal slices Endo-N treatment reduced LTP (Becker et al., 1996). Genetic ablation of polysialyltransferase PST (required for polysialylation of NCAM in the adult hippocampus) leads to learning defects and impairment of LTP and LTD in the CA1 region of the hippocampus, but not in mossy fiber – CA3 synapses or in perforant path synapses of the dentate gyrus (Becker et al., 1996; Eckhardt et al., 2000; Muller et al., 1996; Stoenica et al., 2006). Application of soluble polysialylated NCAM (PSA-NCAM) to acute slices of NCAM-deficient mice restores normal CA1 LTP and improves contextual fear memory (Senkov et al., 2006). Since application of non-polysialylated NCAM is not effective in restoring normal CA1 LTP, the combined data indicate that PSA is both necessary and sufficient for normal induction of CA1 LTP. Removal of PSA from NCAM by Endo-N also disrupted neuronal migration, axonal sprouting, branching and fasciculation (Durbec and Cremer, 2001; Yamamoto et al., 2000), and synaptogenesis (Dityatev et al., 2000, 2004). Interestingly, PSA reexpression after Endo-N treatment is Ca^{2+} dependent and can be modulated by neuronal impulse activity in cultures of cortical neurons (Kiss and Rougon, 1997) and at synapses in hippocampal organotypic cultures (Muller et al., 1996).

5.5. The role of PSA-NCAM in schizophrenia

A growing body of evidence has implicated NCAM as a susceptibility risk for neuropsychiatric disorders, including schizophrenia. Schizophrenia is a devastated disease that affects 1 % of the worlds population (Freedman R, 2003). Currently prevailing is the neurodevelopmental hypothesis of schizophrenia, which implicates altered neuronal development in disrupted neuronal connectivity and cognitive dysfunction (Muglia et al., 1999; Marenco and Weinberger, 2000). Alterations in NCAM may disrupt normal connectivity leading to cognitive dysfunction. NCAM 140 participates in several signaling pathways to activate axonal and dendritic growth and branching, while NCAM 180 interacts with cytoskeletal components and have prominent role in synaptic stability and memory formation (Hinkle and Maness, 2006; Maness and Schachner, 2007). NCAM was reported as compelling candidate gene in a meta-analysis of schizophrenia susceptibility loci (Lewis et al., 2003) and single nucleotide polymorphism are associated with cognitive impairment (Sullivan et al., 2007). PSA-NCAM levels are decreased in the hippocampus of

individuals with schizophrenia and the levels of soluble fragment of the extracellular domain of NCAM are increased in the cerebrospinal fluid (Barbeau et al., 1995). Soluble NCAM fragments (105-115 kDa) do not arise from alternative splicing as they were not recognized by antibodies raised against the secreted isoform (Vawter et al., 2001). Instead, they result from metalloprotease-mediated cleavage of NCAM by ADAM type proteases (Hinkle et al., 2006; Hubschmann et al., 2005; Kalus et al., 2006). At the neuronal level, abnormalities in both excitatory and GABAergic inhibitory neurons have been identified in individuals with schizophrenia (Lewis et al., 2005; Reynolds and Harte, 2007).

Studies in mouse models have advanced our understanding of the potential roles of NCAM in schizophrenia. Ventricular enlargement is the most reliable morphological feature in the schizophrenic brain (Gilmore et al., 1998) and often accompanied by cognitive impairments. Mice lacking only NCAM 180 display increased lateral ventricles, and also have deficits in learning (Wood et al., 1998). In contrast, mice lacking all isoforms of NCAM have abnormalities in the hippocampus and olfactory bulb, two regions affected in the disease, without ventricular enlargement (Stork et al., 2000; Chazal et al., 2000; Stork et al., 1999; Bukalo et al., 2004). Furthermore, NCAM deficient mice are more anxious and hypersensitive (Stork et al., 1999), show increased aggressive behavior of males toward an unfamiliar male intruding into their home cage, correlating with an increase in activation of limbic system areas when compared with their wild-type control littermates (Stork et al., 1997).

V. The aim of the study

Despite the fact that NCAM was the first isolated immunoglobulin superfamily cell adhesion molecule (Jorgensen and Bock, 1974; Thiery et al., 1977) and the interest in PSA and NCAM due to their links to schizophrenia (Barbeau et al., 1995) and synaptic plasticity (Becker et al., 1996; Muller et al., 1996), the mechanisms by which NCAM regulates synaptic plasticity in a PSA-dependent manner have so far remained elusive. Previous studies from our laboratory revealed that impaired LTP in NCAM-/- mice is rescued via elevating Ca^{2+} signaling and that impairment of LTP is not mediated by voltage-gated Ca^{2+} channels (Salmen, 2002). Also, it was found that PSA may prevent activation of NR2B-NMDARs at low concentrations of glutamate (Hammond et al., 2006). It is noteworthy in this respect that the synaptic pool of NMDAR (which can be either NR2A or NR2B) activates the extracellular signal-regulated kinases (ERK), whereas the extrasynaptic pool (NR2B) triggers a signaling pathway that results in the inactivation of ERK (Ivanov et al., 2006). These observations led us to a hypothesis that a dysbalance in NMDAR signaling can underlie impaired LTP in NCAM deficient mice. The aim of my study was to study synaptic transmission mediated by NR2A- and NR2B-containing NMDAR in NCAM or PSA deficient hippocampal slices and investigate how modulation of these two NMDAR subtypes may influence synaptic plasticity. More specific sub-aims of my study were:

1) To study basal synaptic properties of Schaffer collateral synapses in NCAM wild-type and NCAM-deficient mice;

2) To compare transmission mediated by NR2A- and NR2B-containing NMDA receptors at CA3-CA1 synapses in NCAM wild-type and NCAM-deficient mice;

3) To study the effects of NMDA receptor agonists and antagonists on LTP at CA3-CA1 synapses in NCAM wild-type and NCAM-deficient mice;

4) To study the effects of NMDA receptor agonists and antagonists on LTD at CA3-CA1 synapses in NCAM wild-type and NCAM-deficient mice;

5) To study the effects of NMDA receptor agonists and antagonists on LTP at CA3-CA1 synapses in hippocampal slices after enzymatic removal of PSA;

6) To study the effects of inhibitors of p38 MAPK and ablation of Ras-GRF1 on PSA-dependent inhibition of LTP at CA3-CA1 synapses;

7) To investigate LTP at CA3-CA1 synapses in NCAM wild-type and NCAM-deficient mice at different ages.

VI. Materials and methods

1. Animals

Constitutive NCAM deficient mice generated by Herald Cremer (Cremer et al., 1994), backcrossed for more than 8 generations on a C57BL6J background, were used in our experiments to investigate the role of NCAM in NMDAR-dependent synaptic plasticity. NCAM deficient mice showed total loss of all NCAM protein isoform immunoreactivity (Cremer et al., 1994), homozygous mutants are fertile and appear healthy, no gross morphological abnormalities were found in adult mutants even though they weight about 10% less than wild-type and heterozygous littermates. But in the nervous system subtle morphological changes were reported: overall brain weight was reduced by 10%, size of the olfactory bulb was reported to be reduced by 36%, which is due to a defect in migration of olfactory neuron precursors (Ono et al., 1994), and lamination of the CA3 mossy fiber projections was by 20% disrupted (Cremer et al., 1994, 1997). Although the size of the hippocampus was unaltered, the deficits in spatial learning were found using the Morris water maze paradigm (Cremer et al., 1994). Furthermore, long-term potentiation has been reported to be reduced in NCAM deficient mice in CA1 (Muller et al., 1996, 2000) and CA3 regions (Cremer et al., 1998), and in the dentate gyrus (Stoenica et al., 2006). NCAM deficient mice show increased aggressive behavior of males toward an unfamiliar male intruding into their home cage, correlating with an increase in activation of limbic system areas when compared with their wild-type control littermates (Stork et al., 1997). Furthermore, NCAM deficient mice are more anxious and hypersensitive to serotonin 1A receptor agonists (Stork et al., 1999), most likely because of increased cell surface expression of the downstream signaling target of NCAM and serotonin 1A receptor, namely the Kir3.1/2 inwardly rectifying K^+channels (Delling et al., 2002).

Constitutive NCAM deficient and their wild-type littermate mice of different ages (2.5-weeks, 2.5-moths, 1-year, and 2-years-old) of both sexes were studied in CA1 *in vitro*. In most experiments, 2.5-month-old animals were used to investigate the mechanisms of impaired LTP in NCAM deficient mice at the adult stage. Since the signaling mediated by NR2B receptors is different for young and adult mice, 2.5-week-old NCAM deficient mice were compared with age-matched wild-type controls. One and two years old mice were used to investigate the levels of LTP and the role of NCAM for synaptic plasticity in aged animals.

To investigate the role of Ras-GRF1 in PSA-dependent signaling, 3-month-old Ras-GRF1 deficient mice (Giese et al., 2001) inbred into C57BL/6J genetic background for at

least 6 generations were used. The Ras-GRF1-deficient mice were reported to be healthy and did not show any signs of neurological abnormalities (no ataxia, tremors, seizures, etc.). However, they had reduced body weight. At eight weeks of age the body weight of mutant males was reduced by approximately 23% in comparison to wild-type males. The body weight of eight-week-old mutant females was reduced by approximately 10% in comparison to female wild-type littermates. Light microscopy analysis of brain morphology did not detect any gross morphological deficits in the mutants (Giese et al., 2001). Ras-GRF1-deficient animals showed deficit in spatial learning when tested in the Morris water maze (Giese et al., 2001) and HFS induced LTP was also slightly lower but, TBS induced LTP did not show any impairment in CA1 region of the hippocampus (Li et al., 2006).

Six- to seven-week-old Sprague Dawley rats were used for two-photon Ca^{2+} imaging.

All efforts were made to minimize both the suffering and the number of animals used. All surgical procedures had been approved by the Committee on Animal Health and Care of the local governmental body. Animals were bred in the specific pathogen-free utility, reviewed and approved by an Institutional Animal Care and Use Committee in accordance to the German law of experimental animals.

2. Materials and chemicals

2.1. Materials for slice preparation

- Compressed CO_2 tank with regulator
- Transparent vessel to place a mouse
- Vibratome (VT 1200 from Leica, Nussloch, Germany)
- Razor blade (a new blade is used for every slice preparation)
- Acetone (all chemical are from Sigma, St. Louis, USA unless otherwise stated)
- Compressed gas mixture (95% O_2/5% CO_2) tank with regulator
- Aquarium air stone, tubing of an appropriate diameter to connect regulator and air stone
- Agar blocks (20% dissolved in water, approx. 1cm x 1 cm x 1cm)
- Agar solution (10% dissolved in water and kept at 60^{o}C in a water bath)
- Water bath (Inkubationsbad from GFL, Burgwedel, Germany)
- A chamber for incubation of brain slices
- Rapid (super) glue
- Small weighting spatula, scalpel, forceps, large scissors and a small sharp-nosed dissecting scissors
- Soft small paintbrush for transfer of slices

2.2. Materials for extracellular recordings of fEPSPs

- Glass microelectrode puller (DMZ Universal Puller, Zeitz, Munich, Germany)
- Glass microelectrods for extracellular recording (2 to 3 MΩ). The microelectrods are filled with artificial cerebrospinal fluid (ACSF)
- Upright microscope (BX50WI from Olympus, Hamburg, Germany)
- Two micromanipulators (LN Mini 25 from Luigs & Neumann, Ratingen, Germany)
- Stimulus isolator unit (A360, World Precision Instruments, USA)
- Amplifier (ECP9 from HEKA Lambrecht/Pfalz, Germany)
- Small pieces of nylon mesh (7x10 mm; made from insets NY80, Millipore, Billerica, USA) with a hole (2 mm in diameter) in the middle and two small metal loads to fix the mesh in the recording chamber
- Perfusion system consisting of a container of ACSF and polyethylene tubing that circulates ACSF through a peristaltic pump (Minipuls3 from ADInstruments GmbH, Spechbach, Germany) and the recording chamber
- Computer (IBM PC)
- Software for data acquisition and measurement of fEPSPs (Pulse from HEKA Lambrecht/Pfalz, Germany)

2.3. Chemicals

Abbreviate	**Full name**	**Function**	**Supplier**
DCS	D-Cycloserine synthetic	NMDAR agonist	Sigma
Ro 25	Ro 25-6981 hydrochloride	NR2B subunit antagonist	Sigma
NVP	NVP-AAMO77	NR2A subunit antagonist	Novartis Pharma
GPT	Glutamic-Pyruvic Transaminase	Glutamate scavenger	Sigma
APV	DL-APV	NMDAR antagonist	Sigma
NBQX	NBQX disodium salt	AMPA/Kainate antagonist	Tocris
PiTX	Picrotoxin	$GABA_A$ and glycine receptor antagonist	Tocris
SB 203580	SB 203580 powder	P38 MAPK antagonist	Sigma
PSA	Colominic acid sodium salt from E. coli	NR2B antagonist	Fluka
endoNF	Endoneuramidase NF	PSA-digesting enzyme	
NaCl	Sodium chloride	For ACSF	Roth
KCl	Potassium chloride	For ACSF	Merck
NaH_2PO_4	Sodium phosphate	For ACSF	Sigma

	monobasic monohydrate		
$NaHCO_3$	Sodium bicarbonate	For ACSF	Sigma
$MgCl_2$	Magnesium chloride hexahydrate	For ACSF	Sigma
$MgSO_4$	Magnesium sulfate	For dACSF	Merck
$CaCl_2$	Calcium chloride dihydrate	For ACSF	Sigma
Glucose	D-(+)-glucose anhydrous	For ACSF	Fluka
Sucrose	D(+)-saccharose	For dACSF	Fluka
Agarose	Agarose, for routine use	For agar blocks	Sigma
MNI-Glu	4-methoxy-7-nitroindolinylglutamate	Caged glutamate for optical stimulation	Tocris
CNQX	6-cyano-7-nitroquinoxaline-2,3-dione	AMPA/Kainate antagonist	Tocris
Fenobam	Fenobam	mGluR5 receptor antagonist	Tocris
TTX	Tetrodotoxin	Na+ channel blocker	Sigma
Co101244	Co 101244 hydrochloride	NR2B antagonist	Tocris
Na-pyruvate	Sodium Pyruvate	For experiments with glutamate scavenger	Sigma

2.4. Solutions

Dissection ACSF for CA1

2.5 mM KCl
1.25 mM NaH_2PO_4
24.0 mM $NaHCO_3$
1.5 mM $MgSO_4$
2.0 mM $CaCl_2$
2.5 mM Glucose
250 mM Sucrose

pH=7.35-7.4 with HCl Osmolarity 320

Recording ACSF for CA1 120 mM NaCl

2.5 mM KCl
1.25 mM NaH_2PO_4
24.0 mM $NaHCO_3$
1.5 mM Mg Cl_2
2.0 mM $CaCl_2$
27.5 mM Glucose

pH=7.35-7.4 with HCl Osmolarity 320

Mg^{2+}-free Solution

120 mM NaCl
2.5 mM KCl
1 mM NaH_2PO_4
26.2 mM $NaHCO_3$
2 mM $CaCl_2$
11 mM Glucose
2 mM Na-pyruvate
0.25 mM MNI-Glu

pH=7.35-7.4 with HCl Osmolarity 320

Intracellular solution

120 mM K-methanesulfonate
10 mM HEPES
4 mM $MgCl_2$
10 mM Na-phosphocreatine
0.4 mM NaGTP
4 mM Na_2ATP
0.1 mM Alexa 594
0.250 mM Fluo4

pH=7.35-7.4 with HCl Osmolarity 320

MATERIALS AND METHODS

Phosphate-buffer saline(PBS)	299 mM NaCl 5.0 mM KCl 10.0mM Na_2HPO_4 2.5 mM $NaH_2PO_4+H_2O$
Lysis buffer	10 mM Tris-HCl, pH 7.5 150 mM NaCl 1 mM EDTA 1 mM Na_3VO_4 1 mM PMSF 1 % NP-40 0.1 % SDS 1x complete™ EDTA-free protease inhibitor mixture
Sample buffer (2x)	125 mM Tris-HCl, pH 6.8 4 % SDS 20 % Glycerol 10 % β-mercaptoethanol 0.00625 % Bromphenol blue
Running buffer	25 mM Tris 192 mM Glycin 0.1 % (w/v) SDS
Stacking gel 5%	3.52 ml deionized water 0.625 ml of 1 M Tris-HCl, pH 6.8 0.05 ml of 10 % SDS 0.83 ml of 30 % Acrylamide-Bis 37:1 25 µl of 10 % APS 5 µl TEMED

Separating gel 12%	2.62 ml deionized water 4.65 ml of 1 M Tris-HCl, pH 8.8 0.125 ml of 10 % SDS 5.0 ml of 30 % Acrylamide-Bis 37:1 62.5 µl of 10 % APS 6.25 µl TEMED
Tris buffered saline (TBS)	10 mM Tris-HCl, pH 7.5 150 mM NaCl
Blocking buffer	5 % (w/v) fatty-free milk powder in 0.1% Tween-20 in TBS
Blotting buffer	25 mM Tris 192 mM Glycin 0.001 % (w/v) SDS
Stripping buffer	0.5 M NaCl 0.5 M acetic acid

3. Methods

3.1. Hippocampal slice preparation

A mouse was kept in a closed glass vessel into which CO_2 was slowly released via tubing until the mouse reached an anesthetic state, after that it was quickly decapitated using big scissors.

The skin and skull were cut with sharp-nose scissors and brain was quickly removed using a small spatula and placed into a Petri dish with ice-cold dissection ACSF (dACSF). Time was minimized required for this step to 1-1.5 min.

The cerebellum was dissected away and the brain was cut into two hemispheres by scalpel. One of hemispheres was placed to the vibratome chamber filled with ice-cold dissection buffer bubbled with 95%O_2, 5%CO_2 (to be sliced later on). The other half was

glued upright on the object mounting platform with the rapid glue next to the agar block, which was glued prior to the dissection of brain. For recordings in CA1, the cut surface was glued to the brain mounting platform. Thereafter 10 % agar was applied to embed the hemisphere and fill a gap between it and the block. The platform with the glued hemisphere was immediately placed in the vibratome chamber.

The attached cerebral hemisphere was then cut with a vibratome into slices. Blade was cleaned in acetone for several minutes and then washed in water. The blade was fixed in the blade holder to ensure positioning of the blade parallel to the tissue. The thickness of slices used in our experiments for all aged groups of animals was 350 μm-thicks.

The slices were separated from agar with the scalpel and transferred to the slice incubation chamber filled with ACSF and maintained at room temperature for 1.5-2 hours before the beginning of electrophysiological recordings.

A chamber for incubation of brain slices was made from a plastic vessel (10 cm in diameter and height) inside which a plastic cylinder (5 cm in diameter, 3 cm in height) was glued at the middle of the wall. The slices were placed at the bottom of the cylinder that was made of nylon stockings glued to the edges of the cylinder. The vessel was filled with ACSF to the top of cylinder. The aquarium stone was placed at the bottom of the vessel, outside of cylinder, and gas pressure was adjusted to saturate solution but not strong enough to make the slices move or float.

At the end of preparation, a 2-3-mm long piece of mouse tail was cut with scissors (cleaned with ethanol), placed into a 1.5 ml tube, labeled with a code of the animal and stored in a freezer for re-genotyping (particularly necessary in cases in which an unexplainable variability in results was observed).

3.2. Recordings of field excitatory postsynaptic potentials

A slice with a clearly visible hippocampus was transferred to the recording chamber using a paintbrush and spatula. The recording chamber with slice was continuously superfused at a rate of 3-5 ml/min with ACSF bubbled with 95%O_2 and 5%CO_2.

A mesh was put on the top of slice in such a way that a hole in the mesh was located above the hippocampus. The mesh was fixed by two small metal loads. Slices of good quality normally do not stick to the paintbrush and have clearly visible (light) layers of pyramidal and granule cells.

Recordings in CA3-CA1 synapses*:* Stimulating and recording electrodes were placed at the slice surface approximately 400 μm apart from each other in the *stratum radiatum,* approximately at the same distance from the *stratum pyramidale* of the CA1 region as

shown in (Figure 6A). Stimulation (50-70 μA, 0.2 ms) was applied to CA3 axons every 20 sec and the recording and stimulation electrodes were slowly advanced towards the slice until maximal amplitude of fEPSPs was attained.

After 10-15 minutes of stabile recordings to induce long-term potentiation the following experimental procedures were performed: stimulus-response curve was determined (Figure 7A), 10 minute baseline was recorded (Figure 7D), with the same stimulation strength a TBS stimulation protocol was applied (Figure 7C), short-term potentiation and long-term potentiation was recorded 1 hour after TBS protocol application to see stabile plastic changes (Figure 7D).

3.3. Calculation of stimulus-response curve

Field EPSPs were collected in response to stimulation pulses (0.2 ms, every 20 s) of increasing intensity (e.g., from 10 μA by step of 10 μA; Figure 7A) until a population spike (upward going inflection) appeared on the decaying phase of fEPSPs (Figure 7A). Typically, the amplitude of supramaximal fEPSPs (i.e. without population spike) was >1 mV and the amplitude of presynaptic volleys (Figure 6B) were several times smaller than that of fEPSPs.

3.4. Baseline recordings

Field EPSPs were elicited every 20 s for at least 10 min with the stimulation strength that provided fEPSPs with a slope of 50% of the subthreshold maximum. It is very important to obtain measurements of fEPSPs before induction of LTP to verify that the baseline is stable, i.e. there is no progressive increase or decrease in the amplitude/slope of responses during recording (Figure 7D). If systematic increase/decrease of fEPSPs was observed, the recording of baseline was continued until it reached a stable level. Thereafter, the stimulus-response curve was determined again to select a stimulation intensity that provides fEPSPs with a slope of 50% of the subthreshold maximum.

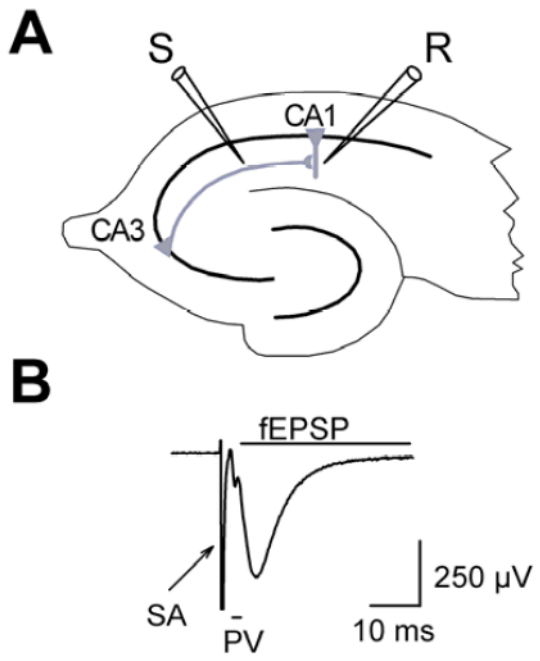

Figure 6. Scheme of the hippocampal slice. *(A) Location of stimulating and recording electrodes for registration of CA3-CA1 responses. (B) Examples of fEPSPs recorded in CA3-CA1 synapses. S, Stimulating electrode; R, recording electrode; SA, stimulus artefact; PV, presynaptic volleys; Horizontal bars indicate duration of fEPSP and PV (Bukalo and Dityatev, 2006).*

3.5. Induction of LTP by theta-burst stimulation

Four TBSs were applied every 20 s to induce LTP. Each TBS consisted of 10 bursts were delivered at 5 Hz, each burst consisted of 4 pulses (0.2 ms) delivered at 100 Hz. The stimulation strength was the same as for the baseline, i.e. set to elicit fEPSPs with amplitude of approximately 50% from the subthreshold maximum. Examples of fEPSP elicited by TBS and TBS-induced LTP in CA3 – CA1 synapses are shown in (Figure 7C, D). This protocol (4 x TBS) has been shown to reliably induce LTP in CA3-CA1 synapses. Induction of this form of LTP is dependent on activity of the NMDA receptor (Eckhardt et al., 2000).

Field EPSPs elicited by TBS normally (i.e., in healthy slices from wild-type mice) should not decline to the baseline during stimulation (Figure 7C). This slow component partially reflects depolarization of neuronal membrane due to summation of long-lasting synaptic responses mediated by NMDARs. However, depolarization of electrodes may also result in a similar pattern. Therefore, it is useful to collect (after the end of LTP recording) TBS-induced stimulus artifact by taking the stimulating electrode out of the slice. The artifact can be digitally subtracted from TBS-induced fEPSP, thus, providing “true” synaptic response.

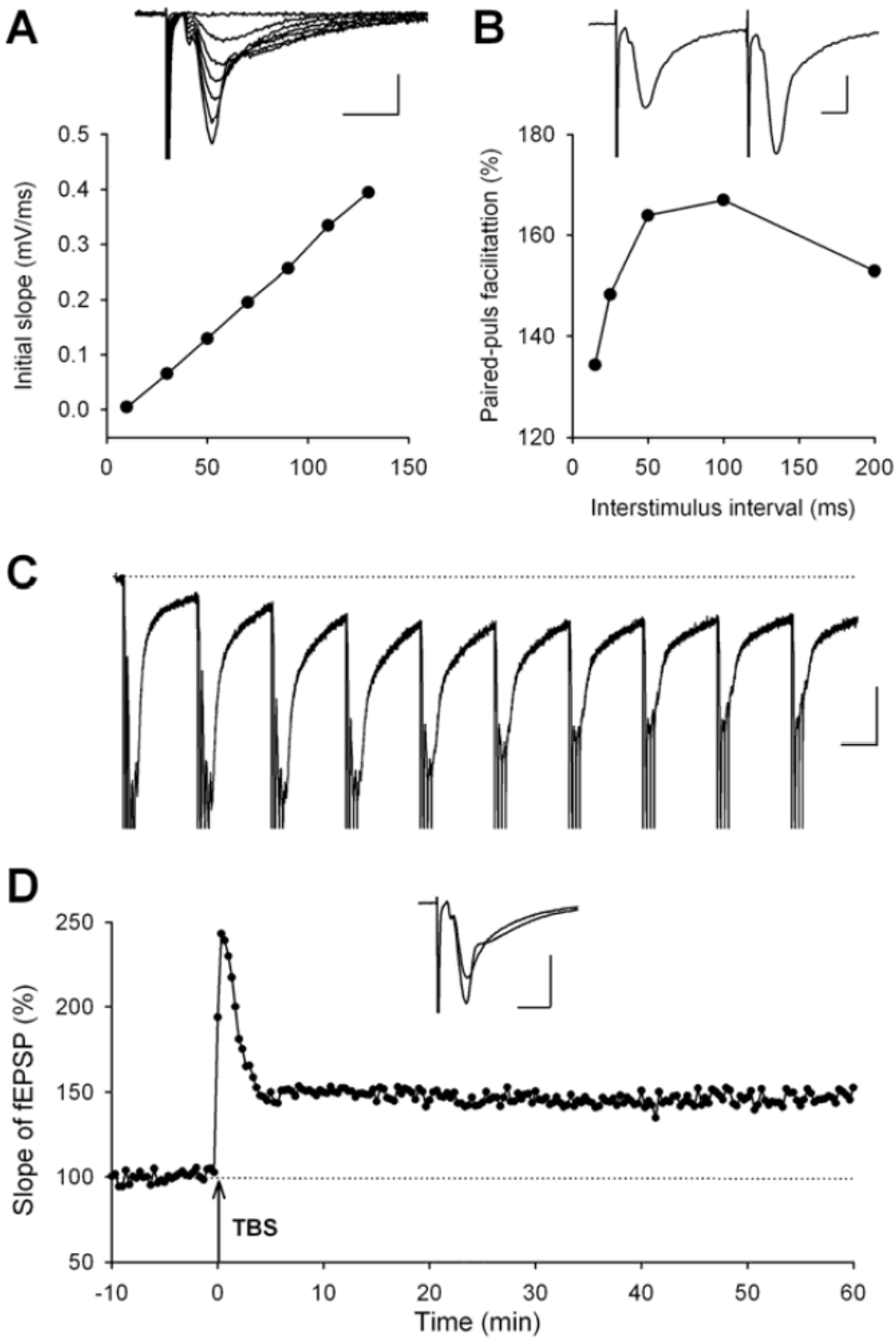

Figure 7. Basal synaptic transmission, paired-pulse facilitation, short- and long-term potentiation at CA3-CA1 synapses. *(A) The stimulus - response curve. Inset shows traces representing fEPSPs evoked with different stimulus strengths (from 10 μA by steps of 20 μA) in CA3-CA1 synapses. Bars, 10 ms and 0.5 mV. (B) Analysis of paired-pulse facilitation. A ratio between the slopes of fEPSPs evoked by the second and first pulses is plotted as a function of interstimulus interval. An example of recordings is given in the inset for the interval of 50 ms. Bars, 10 ms and 0.25 mV. (C) Response elicited by TBS. Bars, 100*

ms and 0.25 mV. (D) A profile of TBS-induced short- and long-term potentiation. Traces on the top provide fEPSPs (average of 30 sweeps) collected before and 50-60 min after TBS administration. The mean slope of fEPSPs recorded 0-10 min before TBS is taken as 100%. Bars, 10 ms and 0.5 mV (Bukalo and Dityatev, 2006),

3.6. Induction of LTD by low-frequency stimulation (LFS)

LTD was induced by two trains of LFS applied at 1 Hz for 10 min with a 10-min interval between them. Stimulation strength during baseline recordings and after induction of LTD was set to 30-40% of supramaximal fEPSPs. Stimulation strength was set to 60-70% when 1 Hz trains are delivered. The amplitudes of fEPSP were not less then 1 mV at this stimulation strength. This protocol has been shown to induce input-specific NMDAR-dependent LTD in CA3-CA1 synapses in adult rodents (Eckhardt et al., 2000; Kerr and Abraham, 1995). An example of low-frequency stimulation induced LTD is shown in Figure 8.

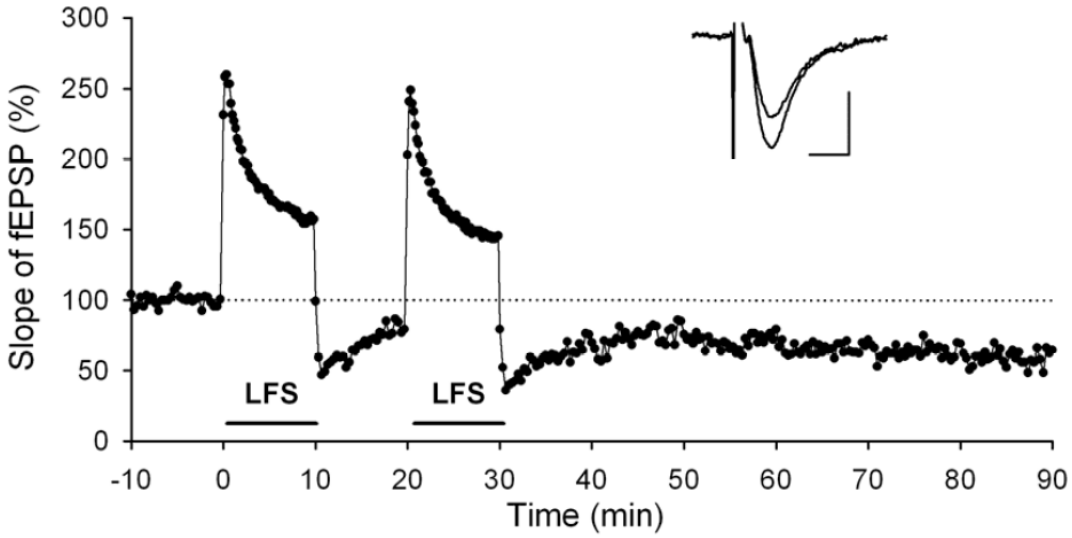

Figure 8. Long-term depression in CA3-CA1 synapses. *Two trains of low-frequency stimulation (LFS) of CA3 axons induce a persistent decrease in slopes of fEPSPs in CA3-CA1 synapses. The mean slope of fEPSPs recorded 0-10 min before LFS was taken as 100%. Horizontal bars indicate delivery of LFS. Inset shows fEPSPs recorded before and 60 min after LFS. Scale bars, 10 ms and 0.25 mV (Bukalo and Dityatev, 2006).*

3.7. Paired-pulse facilitation analysis at different interpulse intervals

Paired-pulse facilitation (PPF) was defined as A2/A1×100%, where A1 and A2 are the amplitudes of the fEPSPs evoked by the first and second pulse, respectively (with a 10, 20, 50, 100 and 200 ms inter-pulse interval). The ratio of the second pulse slope or amplitude compared to the first one (paired-pulse facilitation ratio) was analyzed at the following interpulse intervals: 10, 20, 50, 100, 200 ms. For comparison of PPF at different

interpulse intervals, the stimulation strength was set to 30 % of the subthreshold maximum to avoid contamination by populational spike. For small interpulse intervals (10-20 ms) overlap between the decaying phase of the first response, and the rising part of the second response usually has been observed. To avoid artifacts due to these superimposed traces, the first response was subtracted before the analysis of the second response, assuming linear addition of the two superimposing responses.

3.8. Measurements and calculation of parameters

It is important to compare fEPSPs before and after induction of LTP and LTD, as shown in Figures 7D, 8. If the conditions of recordings are stable (hence, the experiment is acceptable for analysis), the stimulus artifact and the amplitude of presynaptic volley should be identical before application of high-frequency stimulation and at the end of LTP and LTD recording.

It is important to select an appropriate time-window for slope measurements in such a way that it would be in the phase of linear changes in fEPSPs for all stimulation intensities used to estimate the stimulus-response curve, during baseline and after induction of LTP.

In addition to the plot of stimulus intensity - slope of fEPSP, analysis of relationship between the amplitude of presynaptic volleys and slope of fEPSP is often performed. It provides a measure of relationship between the number of activated axons (presynaptic volleys) and resulting fEPSPs. It is important to keep recording and stimulating electrode at the defined and sufficiently long distance, because the amplitude of presynaptic volleys depends on this distance and may partially reflect generation of action potentials in directly activated CA1 neurons.

The mean magnitude of fEPSPs recorded during the baseline (at least 10 min before TBS) is taken as 100 % and changes are expressed relative to this level (Figure 7D). The transient potentiation immediately following TBS (or STP, short-term potentiation) is measured as a maximal increase in the fEPSP slope during 2 min after LTP induction. The values of LTP are calculated as increase in the mean slopes of fEPSPs measured at 50-60 min after induction of LTP.

3.9. Recording of NMDA receptor-mediated responses

After stabile baseline recordings and stimulus-response curve evaluation, stimulation strength was set to elicit fEPSPs with the slopes of 60%. AMPAR-mediated fast component of fEPSP, which amplitude was taken as 100%, was blocked by perfusion with ACSF containing 0.25 Mg^{2+}, the AMPA/kainate receptor antagonist NBQX and the

$GABA_A$/glycine receptor antagonist picrotoxin (PiTX), leaving NMDAR-mediated component. After NMDAR-mediated response isolation, NR2A specific antagonist was applied to isolate NR2B mediated component and in some cases additionally colominic acid was applied. At the end of all experiments, NMDARs were blocked with potent NMDAR antagonist APV. The amplitudes of components left after APV application were subtracted for both genotypes.

3.10. Two-photon Ca^{2+} imaging

Rat slices were incubated for 2 hours prior recording and then transferred to the recording chamber and superfused using a custom micro-perfusion system with a total volume of 2 ml and a flow rate of 2-3 ml/min. During recordings the slices were superfused with carbogenated Mg^{2+}-free ACSF. AMPA and kainate receptors were blocked with 20μM CNQX (Tocris); mGluR5 were blocked with 5μM Fenobam (Tocris). Action potentials were blocked with 2μM tetrodotoxin. Whole-cell current clamp recordings were made from CA1 pyramidal cells at room temperature (23-24 °C), using the patch pipette filled with intracellular solution. Recordings were discarded if the baseline Fluo4 fluorescence had changed more than 25% or the membrane potential had hanged more than 5 mV during the course of the experiment. Uncaging of MNI-Glu was done for 20 ms at a single spot with a 405 nm Laser (vortex mode of Olympus FV1000 Laser Scanning Microscope) at aspiny parts of dendrites to elicit a NMDAR-mediated response. Ca^{2+}-dependent fluorescence of Fluo4 was measured before and after uncaging using two-photon line-scan imaging (excitation at 810 nm). Active or inactive forms of endoNF were applied to slices at a concentration of 576μg/ml via a big-mouth pipette with a diameter of the tip equal to 30 μm. In the series of experiments with the active form of endoNF, 2μg/ml colominic acid was sequentially added to the bath to inhibit responses potentiated by endoNF. At the end of each experiment, 10μM Co101244 (Tocris), as selective NR1/NR2B antagonist (Kohl and Dannhardt, 2001), was applied, which largely blocked the response. Data are presented as mean ± SEM.

3.11. Enzymatic treatment with endoneuraminidase

To remove PSA carbohydrate chain from NCAM backbone before LTP recordings, we incubated hippocampal slices for 2 hours at room temperature in 2 ml carbogen-bubbled ACSF supplemented by recombinantly produced active (truncated by 245 amino acids) form of endoNF (9.6 μg/ml) (Stummeyer et al., 2005). The slices incubated without any enzyme or with a mutated (two substituted amino acids) inactive form of endoNF (9.6

µg/ml) (Stummeyer et al., 2005) served as controls. Immediately after the treatment, slices were placed into the recording chamber and were continuously superfused with carbogen-bubbled ASCF not containing the enzyme.

3.12. Immunostaining for PSA

To verify removal of PSA by endoNF and no changes in expression of NCAM or PSA by inactive endoNF, all enzymatically treated slices were fixed overnight in 4% formaldehyde in phosphate buffer saline, cut in 30µm-thick subslices and transferred to PBS in 48-well plates. Sections were washed three times for 10 min in PBS containing 0.1% BSA. Freely floating slices were treated for 1 hour with blocking solution containing 2% BSA and 0.2% Triton X100 in PBS, followed by monoclonal mouse antibody 735 against PSA (Frosch et al., 1985; 1:300) and NCAM polyclonal antibody (Niethammer et al., 2002; 1:200) overnight at 4°C. Sections were then washed three times for 10 min in PBS containing 0.1% BSA. Secondary anti-mouse IgG antibodies coupled to Cy3 (Dianova) (1:200) and Cy5-conjugated anti-rabbit (1:200) antibodies were applied for 1 hour at room temperature. Finally, sections were rinsed three times for 10 min in PBS containing 0.1% BSA and mounted in Aqua-Poly/Mount (Polyscience). Images of stained sections were acquired by confocal laser scanning microscopy (LSM 510).

3.13. Preparation of hippocampal homogenate

Hippocampi were isolated from brains of adult NCAM-/- mice and control littermates for homogenization in ice-cold lysis buffer with a Dounce homogenizer (Weaton, Telfon pestle, 1ml). Crude protein extracts were obtained by clearing the lysates by centrifugation at 13,000g for 20 min at 4 ^{o}C. Proteins were subjected to SDS-PAGE.

3.14. SDS-polyacrylamide gel electrophoresis

Proteins were separated by use of discontinuous SDS-polyacrylamide gel electrophoresis (SDS-PAGE) using the Mini-Protean III system (BioRad, Munich, Germany). The SDS- polyacrylamide gel consists of a stacking gel (5% acrylamide) and a separating gel (12% acrylamide). After complete polymerization of the gel, the electrophoresis chamber was set up according to the manufacturer's protocol. Protein samples were heated at 95 ^{o}C for 5 min in SDS sample buffer, and then loaded to a gel. Constant voltage of 60V for 20 min and then 100V was applied to the gel until the bromphenol blue line migrated to its bottom. Then, gels were subjected to Western blot analysis.

3.15. Western blot analysis

Proteins were transferred from SDS-polyacrylamide gel onto a nitrocellulose membrane (Protran, Nitrocellulose BA 85, Schleicher & Schüll, Dassel, Germany) using a Mini Transblot apparatus (BioRad) as described in the manufacturer's protocol. The blotting "sandwich" was assembled according to the manufacturer's recommendations. Proteins were transferred electrophoretically in blotting buffer at constant voltage 80V for 150 min at 4 ^{o}C.

After electrophoretic transfer, the nitrocellulose membrane was removed from the blotting sandwich. The side of membrane presenting the proteins was placed right-side up in a glass jar. Then the membranes were washed once with TBS and blocked in 5% non-fat dry milk powder in 0.1% Tween-20 in Tris buffered saline, pH 7.5 (TBS) for 1 hr at RT. Afterwards, membranes were incubated in 5% BSA in TBS containing phospho-p38 or total p38 antibodies, phospho-p44/42 or total p44/42 antibodies (1:1000, Cell Signaling Technology) for overnight at 4^{o}C on a shaking platform. The primary antibody was removed and the membrane was washed 6 times with TBST (TBS+0.1% tween-20), 5 min each. The appropriate secondary antibody coupled with HRP (1:10,000, Dianova, Hamburg, Germany) was applied in milk solution for 1 hr at RT, followed by washing with TBST for 6 times, 5 min each. Membranes were stripped in stripping buffer for 30 min and reblotted with GAPDH antibody as a loading control.

Immunoreactivity was visualized by enhanced chemiluminescence detection system (ECL) or ECL with extended duration (Pierce Biotechnology, Rockford, IL, USA) for detection of weak signals. The membrane was covered with detection solution (1:1 mixture of solutions I and II) for 2 min, and placed between two plastic foils and exposed to X-ray film (Kodak Biomax-ML, Sigma-Aldrich, Steinheim, Germany) for various time periods followed by development and fixation of film. The bands intensities were densitometrically quantified using the image software TINA 2.09 (raytest Isotopenmessgeräte GmbH, Straubenhardt, Germany).

3.16. Statistical analysis

All values are reported as mean ± SEM (standard error of mean). Student's *t* test was used to assess statistical significance using Sigma Plot 9.0 (SPSS, Chicago, IL). Statistical significance of differences was accepted if $p<0.05$. Two-way ANOVA (Systat, 9) was used to compare paired-pulse facilitation and stimulus-response curves between genotypes.

VII. Results

1. Analysis of basal synaptic transmission, short-term and long-term synaptic plasticity in constitutive NCAM deficient and corresponding wild-type mice.

1.1. Analysis of basal synaptic transmission and paired-pulse facilitation in the CA1 region of NCAM-/- mice.

The basic property of synaptic transmission were studied using input-output (stimulus-response) curves to determine weather NCAM plays a role in modulation of basal synaptic transmission. We measured several parameters of fEPSP evoked by stimulation of Schaffer collaterals every 20 seconds with progressively increased stimulation strength (Figure 9A). The amplitude of presynaptic fiber volley, the initial slope of fEPSP and the amplitude of fEPSP were analyzed (Figure 9B,C,D). As shown on Figure 9, there was no statistically significant difference between two genotypes in maximal intensity of stimulation required to evoke the maximal responses of fEPSPs, which was 100.4±3.2 μA in NCAM+/+ and 100.8±4.1 μA in NCAM-/- mice, respectively. The maximal amplitude of presynaptic fiber volley (Figure 9B), was 0.35±0.01 mV in NCAM+/+ and 0.36±0.02 mV in NCAM-/- mice. The slope elicited by the maximal stimulation did not differ between genotypes as well (Figure 9C), being 0.85±0.04 mV/ms in NCAM+/+ and 0.85±0.03 mV/ms in NCAM-/- mice. The amplitude of fEPSPs elicited at maximal stimulus strength was 2.56±0.10 mV for NCAM+/+ mice and 2.42±0.08 mV for NCAM-/- mice. Statistical evaluation of data using ANOVA revealed that there was no statistically significant difference between genotypes either in terms of intensity of stimulation or amplitude of presynaptic fiber volley, amplitude of fEPSP and slope of fEPSP.

Paired-pulse facilitation as a measure of short-term plasticity was used to investigate the role of NCAM molecule on after-effects of a single stimulus by delivering a second stimulus at a variable time after the first. Representative traces elicited by paired stimulation at different (10, 20, 50, 100 and 200 ms) interpulse intervals in both genotypes (Figure 10A) show increased synaptic responses to the second stimulus as compared to the first. The maximal facilitation of the second response was seen at 50 ms interpulse interval, which were 193.2±4.4 % and 199.0±3.4 % for the slope and 175.7±2.8 % and 178.1±2.5 % for the amplitude in NCAM+/+ and NCAM-/- mice, respectively. Analyses of paired-pulse facilitation did not reveal any genetype-specific difference either for slope (Figure 10B) or for the amplitude of fEPSPs (Figure 10C), demonstrating normal level of presynaptic modulation in NCAM-/- mice.

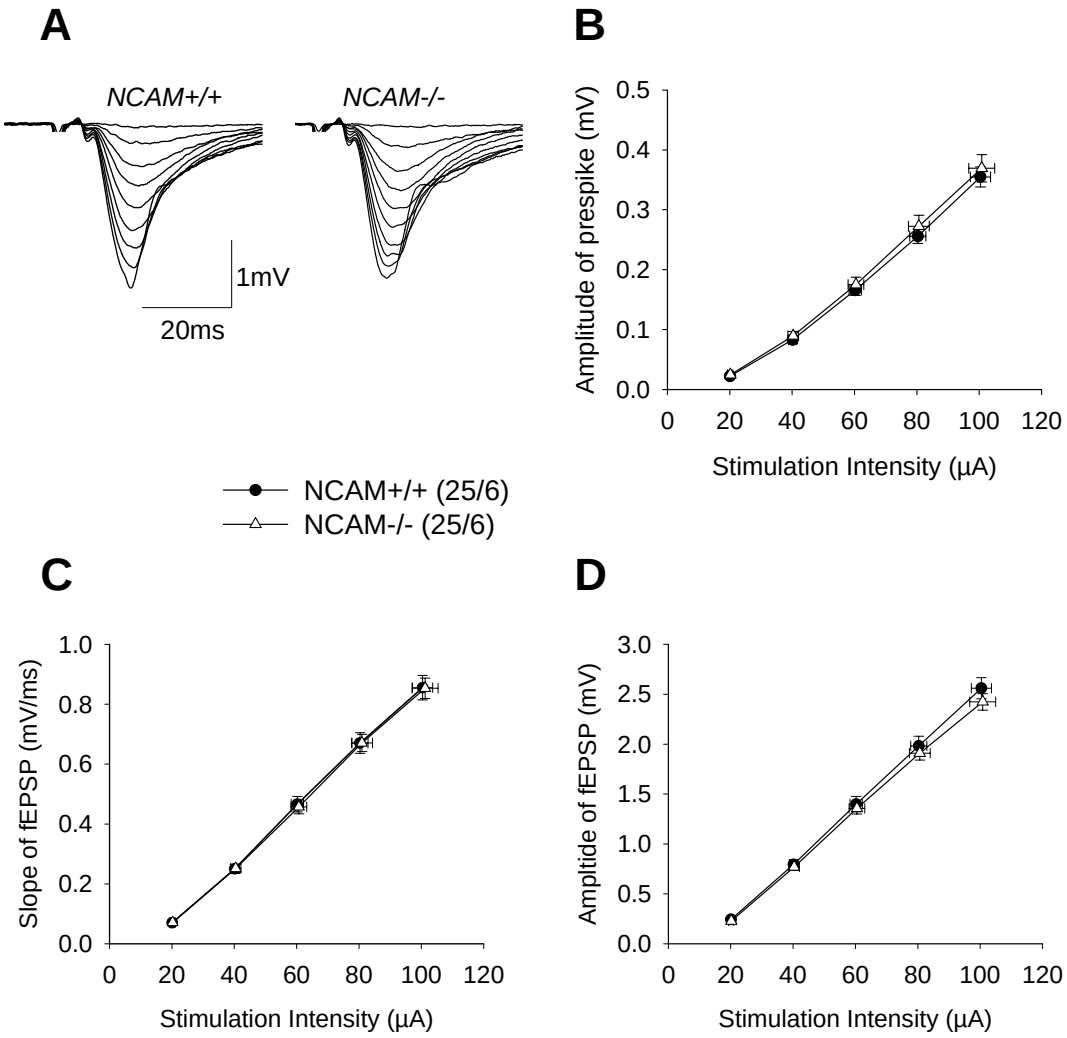

Figure 9. Basal synaptic transmission is not altered in CA1 in NCAM-/- mice. *(A) Traces representing fEPSPs evoked by stimulation with increasing intensity of stimulus strength (from 10 µA by step of 10 µA) in the CA1 region in slices from NCAM+/+ and NCAM-/- mice. (B) Stimulus strength-response curves for amplitude of presynaptic fiber volley. The stimuli with the same strength excited similar number of presynaptic fibers in both genotypes. Note that excitability is not altered in NCAM-/- mice. (C-D) Stimulus strength-response curves for the slope (C) and amplitude (D) of fEPSPs evoked by stimulation of Schaffer collaterals at different stimulus intensities. No genotype-specific difference in basal synaptic transmission was detected by measuring either slope (C) or amplitude (D) of fEPSPs. Data points represent the mean + SEM.*

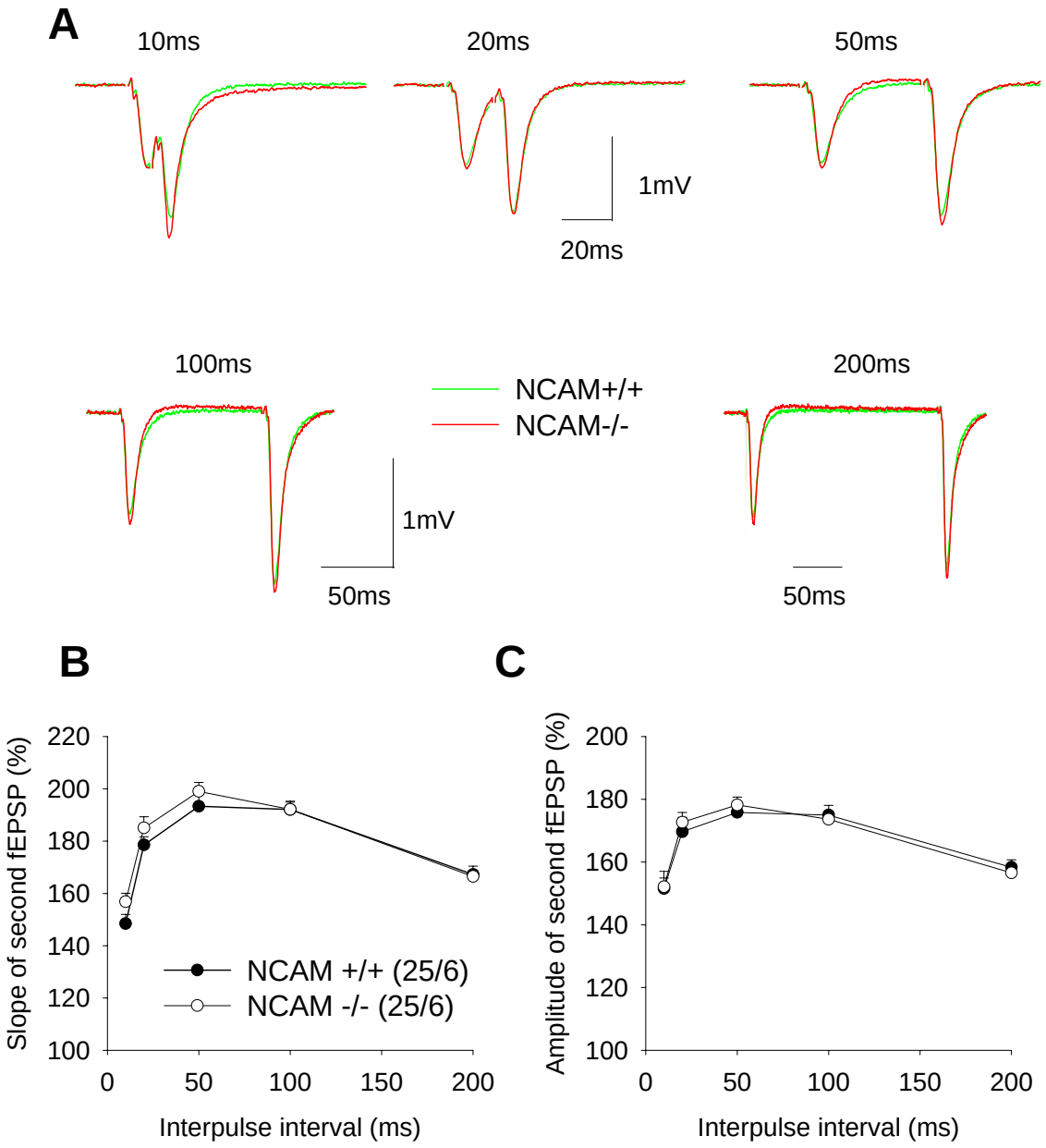

Figure 10. Paired-pulse facilitation (PPF) at different interpulse intervals is not altered in the CA1 region of the hippocampus in NCAM-/- mice. *(A) Representative traces illustrating paired-pulse facilitation at 10, 20, 50, 100 and 200 ms interpulse intervals recorded in slices from the CA1 region of NCAM+/+ (green) and NCAM-/- (red) mice. (B-C) Analysis of paired-pulse facilitation: the ratio between magnitutes of responses elicited by the second and first stimuli is plotted for various interpulse intervals (10, 20, 30, 50, 100 and 200 ms) for the slopes (B) and amplitudes (C) of fEPSPs. No genotype-specific difference in paired-pulse facilitation was detected by measuring either slope (B) or amplitude (C) of fEPSPs. Data points represent the mean + SEM*

1.2. Analyses of theta-burst stimulation-induced long-term potentiation in the CA1 region of constitutive NCAM-/- mice.

After we have not seen any deficit of basal synaptic transmission and paired-pulse facilitation in NCAM deficient mice, we tested TBS-induced short- and long-term synaptic plasticity in CA1 region. Application of four trains of TBS to the Schaffer collaterals induced reliable short- and long-term potentiation in all slices of 2.5-month-old wild-type animals (Figure 11). The mean level of STP measured as maximal potentiation during 1 min after TBS in slices from NCAM+/+ was 188.4±4.1% and the level of LTP measured 50-60 minutes after TBS was 144.3±1.7%. The level of STP in NCAM-/- mice was equal to 179.8±3.2% and was not significantly different from STP in NCAM+/+ mice, whereas the level of TBS-induced LTP was significantly reduced to 125.0±1.6% (Figure 11A,B,C), similar to the previously published data (Durbec and Cremer, 2001; Kiss and Muller, 2001; Kiss et al., 2001; Muller et al., 2000; Muller et al., 1996).

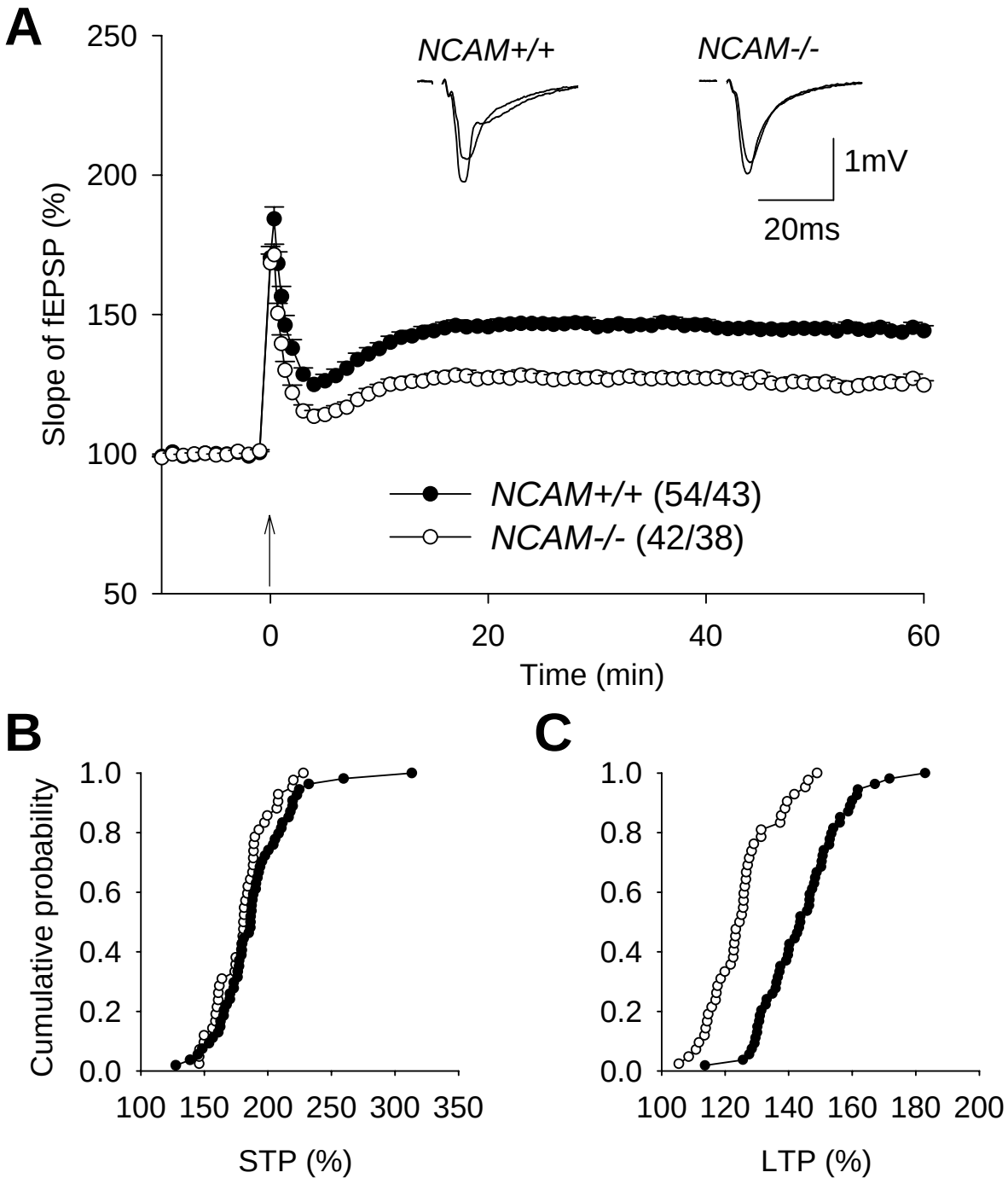

Figure 11. CA1 LTP induced by TBS is impaired in NCAM-/- mice. *(A) A profiles of TBS-induced short- and long-term potentiation shows impaired CA1 LTP in NCAM-/- mice, as compared to NCAM+/+ mice. Traces on the top provide fEPSPs (average of 30 sweeps) collected before and 50-60 min after TBS administration. The mean slope of fEPSPs recorded 10 min before TBS is taken as 100% and an arrow indicates delivery of TBS. Data represent mean + SEM, numbers of tested slices and mice are indicated in parentheses. (B-C) Cumulative plots representing levels of STP measured 1 min after TBS (B) and levels of LTP measured 50-60 min after TBS (C). Each symbol represents a single experiment. Cumulative probability at any given value x is the probability to observe potentiation less or equal to x. No significant difference between genotypes was found for STP, but LTP was significantly impaired in slices from NCAM-/- mice.*

2. Abnormal balance of synaptic transmission through NR2A- and NR2B-NMDA receptors in NCAM-deficient mice.

Next, we studied whether NMDAR-mediated signaling is altered in NCAM-/- mice. To perform long-term pharmacological analyses of NMDAR-mediated responses in slices from 2.5-month-old NCAM+/+ and NCAM-/- mice, we isolated NMDAR-mediated fEPSPs by perfusion with a low Mg^{2+}solution containing blockers of AMPA, kainate, $GABA_A$ and glycine receptors (Kullmann et al., 1996). Perfusion with this solution inhibited fast fEPSPs, uncovering slow fEPSPs (Figure 12A,B). The amplitude of these slow fEPSPs stabilized within one hour after application of low Mg^{2+} solution. At this time there was no difference between NCAM+/+ and NCAM-/- mice in amplitudes of slow fEPSPs (Figure 12A,C).

These fEPSPs were mediated predominantly by NMDARs because they were blocked by application of NMDAR antagonists NVP and APV (Figure 12A,B). The residual responses were about 1% of the amplitude of fEPSPs recorded before perfusion with low Mg^{2+} solution. The ratio between amplitudes of NMDA and AMPA receptor-mediated fEPSPs was not different between genotypes: 10.2±1.6% in NCAM-/- mice versus 9.7±0.6% in NCAM+/+ mice (Figure 12C). This result is similar to a previous analysis of NMDAR-mediated responses that did not reveal any abnormalities in PSA-deficient slices generated by treatment with endoneuraminidase N (Muller et al., 1996).

Since it is known that several subtypes of NMDARs with distinct properties are expressed in the hippocampus, in our next experiments we attempted to distinguish contributions of NR2B- versus NR2A-containing NMDARs in NCAM+/+ and NCAM-/- mice. We found that the inhibitor of NMDARs, NVP, inhibited NMDAR responses less effectively in NCAM-/- mice than in NCAM+/+ mice (Figure 12A). The concentration of NVP used inhibits approximately 80% of currents mediated by NR1/NR2A receptors and only about 20% of currents mediated by NR1/NR2B receptors (Bartlett et al., 2007). Thus, the NVP-insensitive component is predominantly mediated by NR2B-NMDAR under these conditions. The amplitude of this component was larger in NCAM-/- mice (35.7±3.4%) than in NCAM+/+ mice (22.3±1.0%) (Figure 12C).

To test if the difference between NCAM-/- and NCAM+/+ mice reflects a lack of inhibition of NR2B-NMDARs by PSA, we applied PSA to slices and found that it inhibited the NVP-insensitive NMDAR component more strongly in NCAM-/- than in NCAM+/+ mice (20.1±2.5% versus 12.0±1.7%, respectively) (Figure 13A,C). PSA predominantly inhibits NMDARs that are activated by micromolar concentrations of glutamate (Hammond

et al., 2006), similar to concentrations found in the extracellular space of normal and epileptic brains (Sherwin, 1999; Ueda et al., 2000). These concentrations are two orders of magnitude below those at the synaptic cleft after vesicular glutamate release, suggesting that the PSA-sensitive component in NCAM-/- mice reflects the activity of extrasynaptic NR2B-NMDARs. In NCAM+/+ mice this component is smaller due to inhibition of extrasynaptic NMDARs by endogenous PSA-NCAM. Another small NMDAR component (about 10% in both genotypes) that was not inhibited by NVP and PSA presumably represents a mixture of synaptic NR2B-NMDARs (resistant to PSA at high concentrations of glutamate) and NR2A-containing receptors (not inhibited at the used concentration of NVP) (Figure 13C). In summary, these observations suggest that despite of normal total NMDAR-mediated transmission in NCAM-/- mice, there is an imbalance in signaling between NR2B- and NR2A-NMDARs.

To investigate whether a deficit of PSA in hippocampal slices would increase NR2B-NMDAR-mediated transmission and Ca^{2+} influx in extrasynaptic sites, we performed recordings of Ca^{2+} transients in the aspiny part of CA1 apical dendrites (Figure 14A) before and after application of the PSA-digesting enzyme endoneuraminidase NF (endoNF) (Stummeyer et al., 2005). As a control, we used slices treated with an inactive mutated form of endoNF (Stummeyer et al., 2005). Ca^{2+} influx was elicited by local uncaging of glutamate and recorded using the Ca^{2+}-sensitive dye Fluo4 (Figure 14B,C). Treatment with endoNF increased the area of recorded Ca^{2+} signals to 209±31% of untreated slices (P=0.01, paired t-test). In line with findings that PSA suppresses opening of NR2B-NMDARs only at low micromolar glutamate concentrations (Hammond et al., 2006), the difference between Ca^{2+} transients recorded in control and endoNF treated cells was observed during the late phase, i.e. when concentrations of caged glutamate are low. PSA applied after endoNF treatment largely reversed the increase of the Ca^{2+} signal (137±9% of untreated slices; (Figure 14C,D). Further application of Co101244, a selective NR2B-NMDAR antagonist, reduced the Ca^{2+} signals to 23±6%, showing that they were predominantly mediated by NR2B-NMDARs (Figure 14C,D). Inactive endoNF, lacking its catalytic activity, did not significantly change the area of Ca^{2+} signals (113±8%), whereas further application of Co101244 reduced the responses to 19±5% (Figure 14C,D). These experiments directly visualize the acute upregulation of NR2B-NMDAR-mediated Ca2+ transients in CA1 pyramidal cells after removal of PSA.

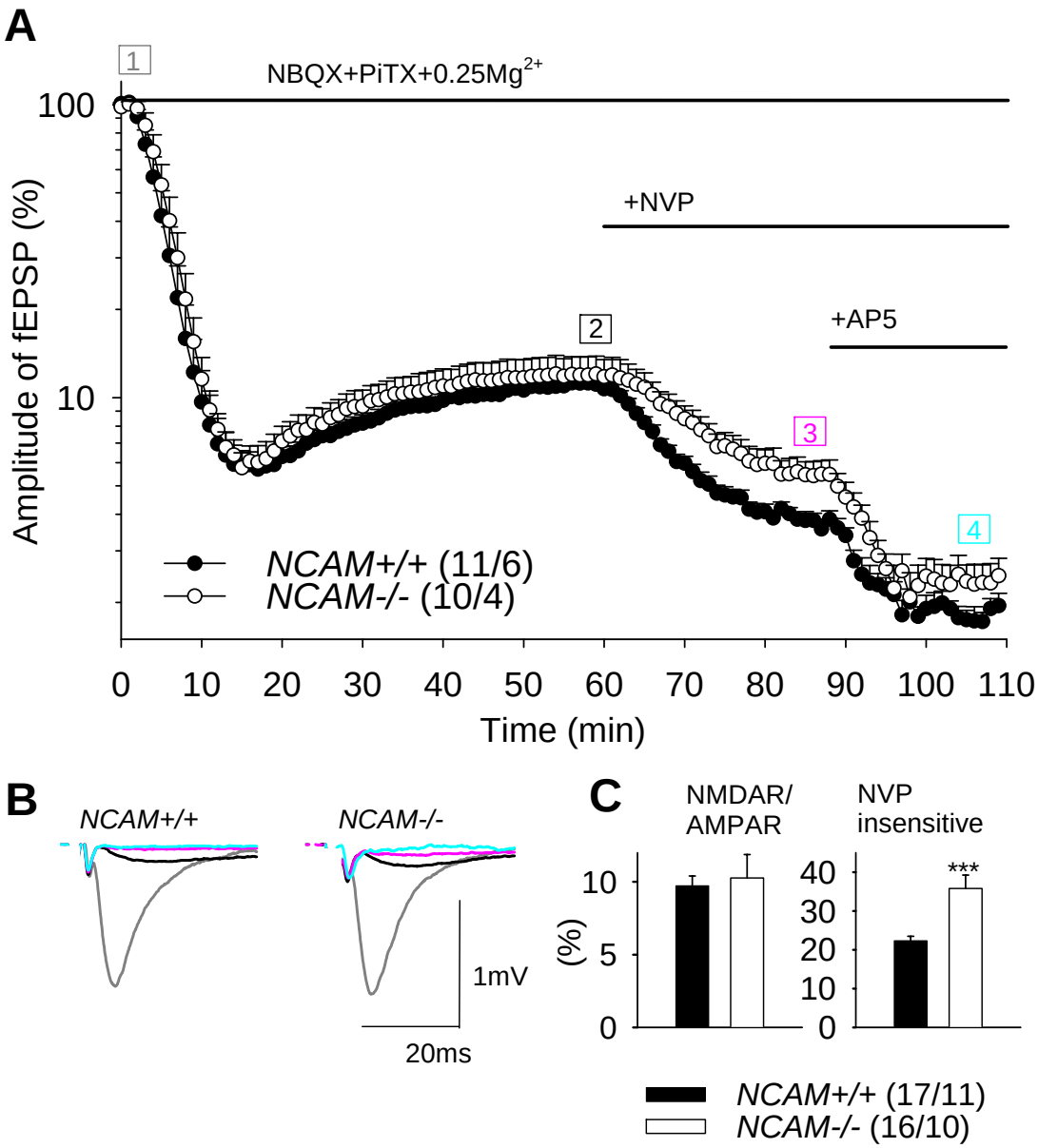

Figure 12. Increased responses mediated by NR2B-NMDA receptor in hippocampal slices of NCAM-/- mice. *(A) AMPA receptor-mediated fast component of fEPSP [1], the amplitude of which was taken as 100%, was blocked by perfusion with ACSF containing 0.25 Mg^{2+}, the AMPA/kainate receptor antagonist NBQX and the $GABA_A$/glycine receptor antagonist picrotoxin (PiTX), leaving NMDAR-mediated component [2]. Application of 0.25 μM NVP isolated fEPSPs mediated predominantly by NR2B-NMDARs [3], which could be blocked to 1-1.5% level by the NMDA receptor antagonist APV (50 μM) [4]. To present changes in high-amplitude AMPA receptor mediated fEPSPs and low amplitude NMDAR-mediated fEPSPs in one graph, a logarithmic Y-scale is used. (B) Representative traces corresponding to time intervals color-coded in (A). (C) Mean+SEM of the ratio between amplitudes of NMDA and AMPA receptor-mediated components, i.e. ([2]-[4])/[1], and of the amplitude of NVP-insensitive component, i.e. ([3]-[4])/([2]-[4]). The latter was significantly larger in NCAM-/- than in NCAM+/+ mice (***p<0.001, t-test). Numbers of tested slices and mice are indicated in parentheses.*

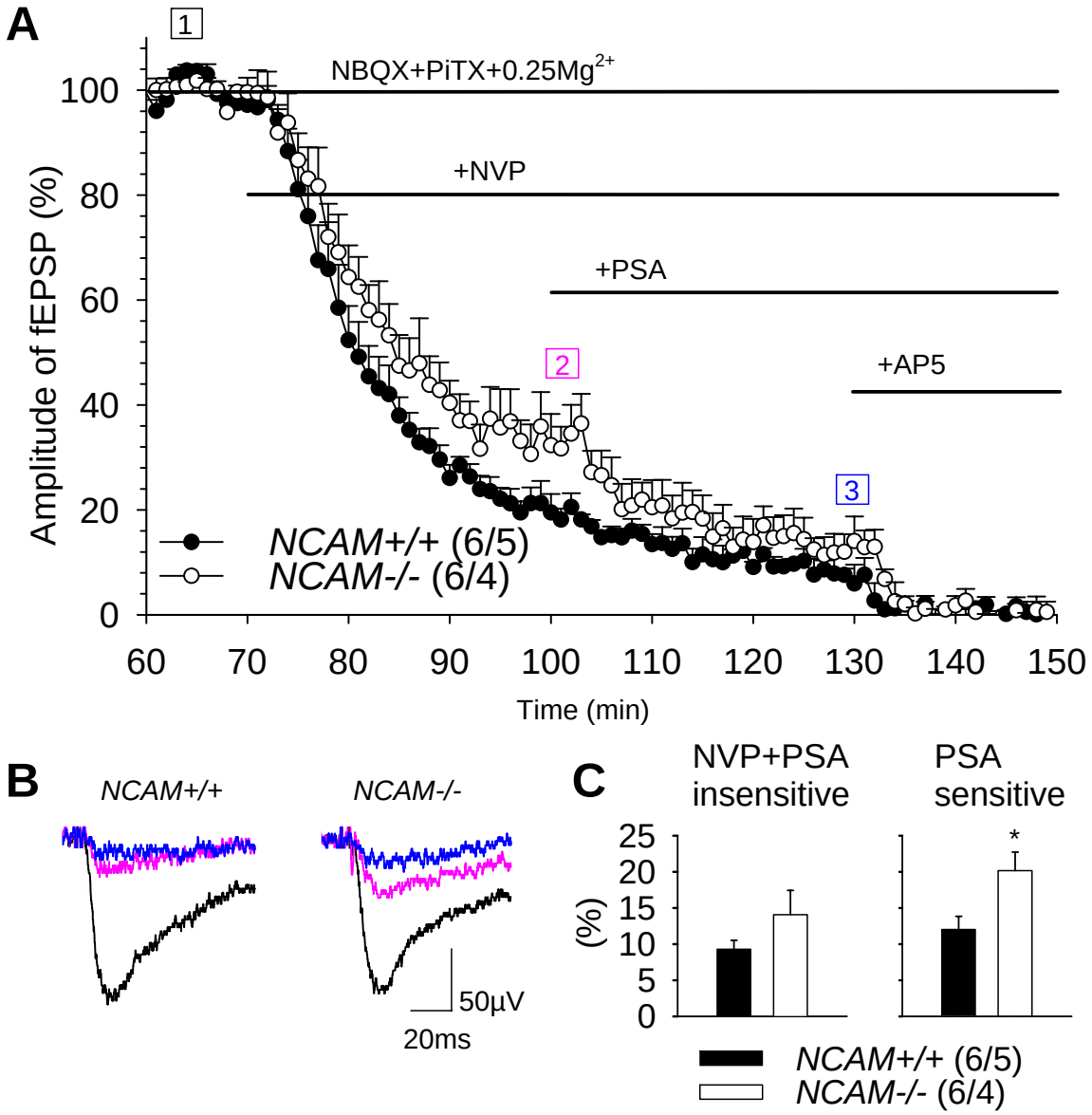

Figure 13. PSA more strongly inhibits NR2B-NMDA receptor mediated responses in NCAM-/- mice. *(A) NMDAR-mediated component [1], the amplitude of which was taken as 100%, was more strongly reduced by NVP in NCAM+/+ mice [2], whereas 10 µM PSA more strongly inhibited the residual component in NCAM-/- mice [3]. The amplitudes of components left after APV application were subtracted for both genotypes. (B) Representative traces corresponding to time intervals color-coded in (A). (C) Mean + SEM of the amplitudes of the NVP- and PSA-insensitive component, i.e. [3]/[1], and the PSA-sensitive component, i.e. ([2]-[3])/[1], in both genotypes. The latter component, presumably representing inhibition of extrasynaptic NR2B-NMDARs, was larger in NCAM-/- mice (*p<0.05, t-test). Numbers of tested slices and mice are indicated in parentheses.*

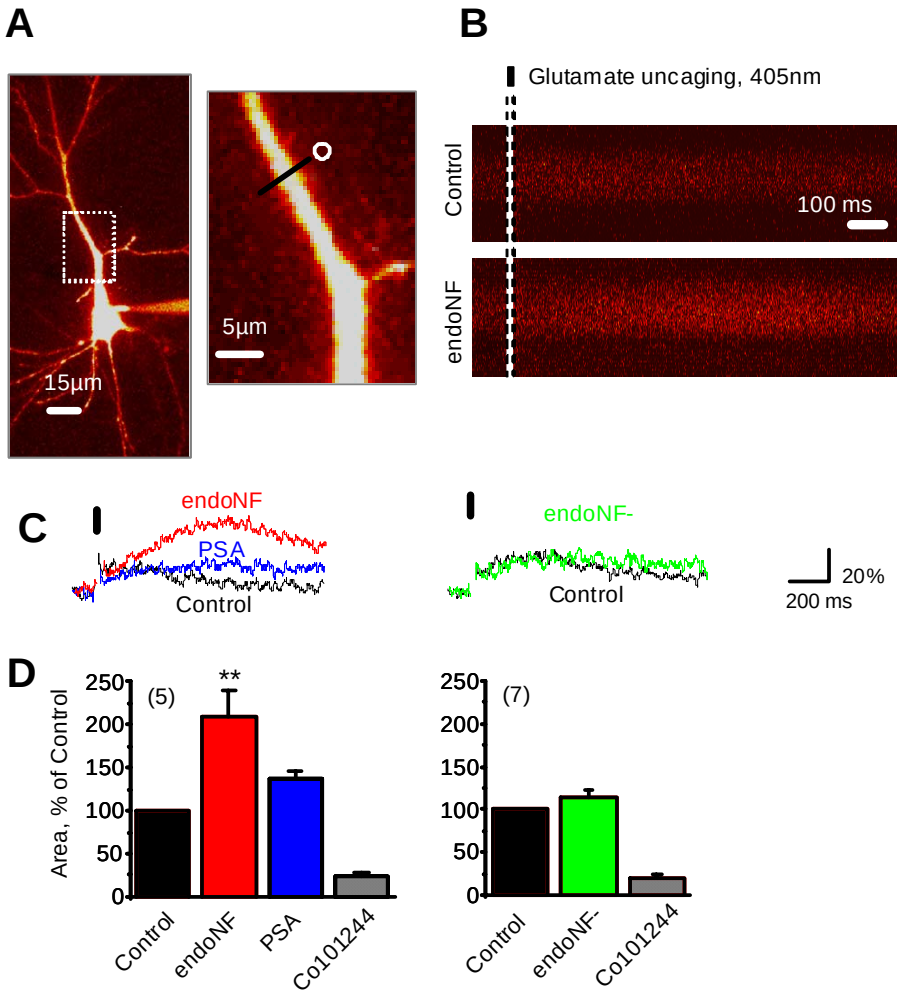

Figure 14. Enzymatic removal of PSA increased responses mediated by NR2B-NMDA receptors *(A) Left: CA1 pyramidal neuron filled with 250 µM Fluo4. The sample image obtained with high laser power to reveal the morphology. Dashed rectangle indicates the area of recordings (right image). Black line shows line scan position. The circle indicates the position of the uncaged spot. (B) Line-scan image obtained from selected part of the dendrite. White vertical line corresponds to the time of glutamate uncaging. Upper and lower panels show Ca^{2+} signal in control conditions (Control) and after active endoNF application (endoNF). Application of endoNF significantly increased the amount of fluorescence detected. (C) Representative traces from two neurons. Left: three sweeps showing Ca^{2+} transients in response to glutamate uncaging in control conditions, after active endoNF and after PSA application. EndoNF increased the magnitude of Ca^{2+} transients, while PSA reversed this effect. Right: Ca^{2+} transients recorded in another slice in control and after inactive endoNF (endoNF-) application. In both panels, the NR2B receptor antagonist Co101244 mostly inhibited the Ca^{2+} transients. (D) Summarized data obtained in experiments with application of active and inactive forms of endoNF (left and right panels, respectively). The active form of endoNF increased the area under the curve of the Ca^{2+} fluorescent signal more than twice (**p=0.01, paired t-test; numbers of recorded cells/slices are indicated in parentheses), while the effect of inactive form of endoNF was insignificant (p>0.1). Co101244 largely and to the same extent blocked Ca^{2+} transients after treatment with either active or inactive forms of endoNF, indicating that the effect of active endoNF on Ca^{2+} transient potentiation is mediated by NR2B receptors. Data were obtained in collaboration with Sergei Grebenyuk and Alexey Semyanov from the RIKEN Brain Science Institute, Saitama, Japan.*

3. Restoration of LTP NCAM-/- mice through modulation of NMDA receptor activity

Analysis of synaptic plasticity induced by theta-burst stimulation of Schaffer collaterals/commissural fibers at normal extracellular concentrations of Ca^{2+} (2.0 mM) and Mg^{2+} (1.5 mM) revealed impairment in CA1 LTP in NCAM-/- mice, as compared to NCAM+/+ mice (Figure 11). The observed deficit in synaptic transmission mediated by NR2A-NMDARs in NCAM-/- mice (Figure 12) may underlie the deficit in LTP, since LTP was restored in these mutants via elevation of extracellular Ca^{2+} concentrations from 2.0 to 2.5 mM (Salmen 2002), as has been done in a conditional NCAM mutant ablated in NCAM expression under control of the Ca^{2+}/calmodulin-dependent protein kinase (CaMKII) promoter after cessation of major developmental events in the third postnatal week (Bukalo et al., 2004). This is in line with a report showing a steep dependence of LTP in wild-type animals on extracellular Ca^{2+} concentrations between 0.8 to 1.0 mM: above 1.0 mM LTP can be successfully triggered and below 0.8 mM LTP could not be induced (Mulkeen et al., 1988). Thus, in NCAM-/- mice, the range of extracellular Ca^{2+} concentrations influencing LTP is shifted to higher values, presumably due to a deficit of Ca^{2+} influx via N2A-NMDARs. Next we used more specific ways to increase NMDAR-mediated Ca^{2+} influx to verify this idea. If an increase in extracellular Ca^{2+} concentrations would lead to increased Ca^{2+} influx via both NMDARs and voltage-gated Ca^{2+} channels, reduction in Mg^{2+} would more specifically affect NMDARs (via a relief of the Mg^{2+} block of these receptors). We therefore reduced extracellular Mg^{2+} concentrations from 1.5 to 0.75 mM and found that this treatment increased LTP in NCAM-/- mice (151.1±5.0%) to levels found in NCAM+/+ mice (155.9±7.6%) (Figure 15A,C). As another NMDAR-specific treatment, we used D-cycloserine (DCS), a partial agonist of the NMDAR glycine binding site, which is known to rescue deficits in NMDAR-dependent LTP in aged 23- to 27-month-old animals (Billard and Rouaud, 2007). DCS did not affect LTP in young 2.5-month-old NCAM+/+ mice (145.8±4.5%), but restored LTP levels in NCAM-/- mice to NCAM+/+ levels of 146.9±3.3% (Figure 16A,C). In contrast, NVP strongly inhibited LTP to 116.1±2.2% in NCAM+/+ mice and to 113.1±2.6% in NCAM-/- mice (Figure 17A,C), indicating that NR2A-NMDARs contribute predominantly to this form of synaptic plasticity in NCAM+/+ mice and have a smaller contribution in NCAM-/- mice. Importantly, NVP also fully abolished the potentiating effects of DCS on LTP in NCAM-/- mice (Figure 18A,C), suggesting that DCS mostly facilitated LTP in the mutant via NR2A-NMDARs. This is in agreement with the view that ambient concentrations of glycine and D-serine are sufficient to saturate the glycine binding site of NR2B- but not NR2A-NMDARs due to a higher

affinity of glycine and DCS binding to NR2B-NMDARs (Priestley et al., 1995). Higher levels of LTP in DCS plus NVP treated slices from NCAM+/+ mice (122.5±2.0%) as compared to NCAM-/- mice (113.7±3.2%) (Figure 18A,C), are in agreement with our data showing that NCAM+/+ mice have higher levels of synaptic transmission via NR2A-NMDARs than NCAM-/- mice (Figure 12A,C). These data suggest that residual activity of NR2A-NMDARs in the presence of DCS and NVP may be higher in NCAM+/+ than in NCAM-/- mice and facilitate induction of LTP. Application of the subunit non-specific antagonist of NMDARs, APV, fully blocked LTP in NCAM+/+ (101.3±5.2%) and NCAM-/- (100.8±3.6%) mice (Figure 19), confirming that this form of LTP is NMDAR-dependent in both genotypes.

Since our data demonstrate an increase in synaptic transmission through NR2B-NMDARs in NCAM-/- mice (Figure 12) and activation of extrasynaptic NR2B-NMDARs is known to induce synaptic depression (Massey et al., 2004), we next tested if inhibition of these receptors would normalize LTP in NCAM-/- mice. Indeed, application of the NR2B-NMDAR antagonist Ro 25-6981 increased LTP in NCAM-/- mice to 137.6±4.9%, a value not significantly different from the level of 138.4±3.3% recorded in NCAM+/+ mice (Figure 20A,C). We next recorded LTP in the presence of a glutamate scavenger, a substance known to reduce concentrations of extrasynaptic glutamate (Kullmann et al., 1996; Tsvetkov et al., 2004). This treatment also increased LTP in NCAM-/- mice to 136.8±3.2% being not significantly different from the level of 147.3±6.2% found in NCAM+/+ mice (Figure 21A,C). Thus, LTP in NCAM-/- mice can be restored by treatments that either increase transmission via NR2A-NMDARs or decrease transmission via extrasynaptic NR2B-containing receptors.

Next we investigated a possibility if intracellular signaling mediated by NCAM via direct interactions with fibroblast growth factor receptors (FGFR) is important for LTP induction, as it is for neurite outgrowth (Niethammer et al., 2002). To enhance FGFR signaling in NCAM-/- slices, we directly stimulated FGFR by basic FGF that was applied to slices at concentration of 25ng/ml. This treatment, however, affected neither STP (178.7±8.8%) nor LTP (125.4±3.1%) in NCAM-/- mice (Figure 22). In NCAM+/+ controls, STP was significantly higher (209.4±7.7%) than in NCAM-/- mice (Figure 22A,B). LTP in NCAM+/+ mice was not affected by FGF (146.2±6.0%) and was higher than in FGF-treated NCAM-/- mice (Figure 22A,C). These data do not support the hypothesis that a deficit in FGFR-mediated signaling in NCAM-/- mice underlies impairment in LTP.

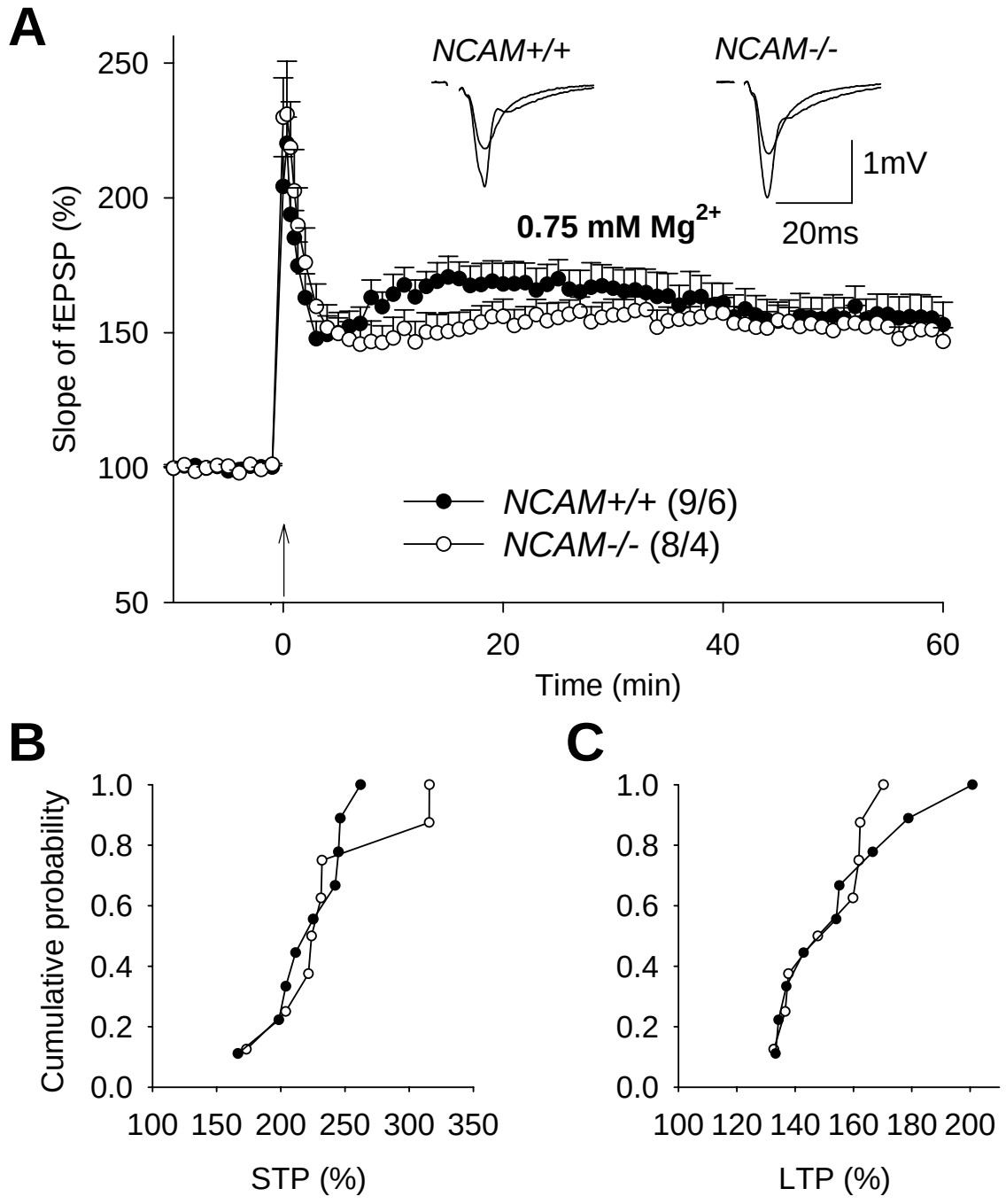

Figure 15. Impaired LTP in NCAM-/- mice is restored by facilitation of NMDA receptor activity through lowering the concentration of extracellular Mg^{2+}. *(A) Profiles of TBS-induced short- and long-term potentiation recorded in ACSF with reduced concentration of extracellular Mg^{2+} (0.75 mM instead of 1.5 mM). Note that TBS induces equal levels of LTP in the CA1 region of slices from NCAM-/- and NCAM+/+ mice. Traces on the top provide fEPSPs (average of 30 sweeps) collected before and 50-60 min after TBS administration. The mean slope of fEPSPs recorded 10 min before TBS is taken as 100% and arrow indicates delivery of TBS. Data represent mean + SEM, numbers of tested slices and mice are indicated in parentheses. (B-C) Cumulative plots representing levels of STP measured 1 min after TBS (B) and levels of LTP measured 50-60 min after TBS (C). Each symbol represents a single experiment. Cumulative probability at any given value x is the probability to observe potentiation less or equal to x. No significant difference between genotypes was found for either STP or LTP in this series of experiments.*

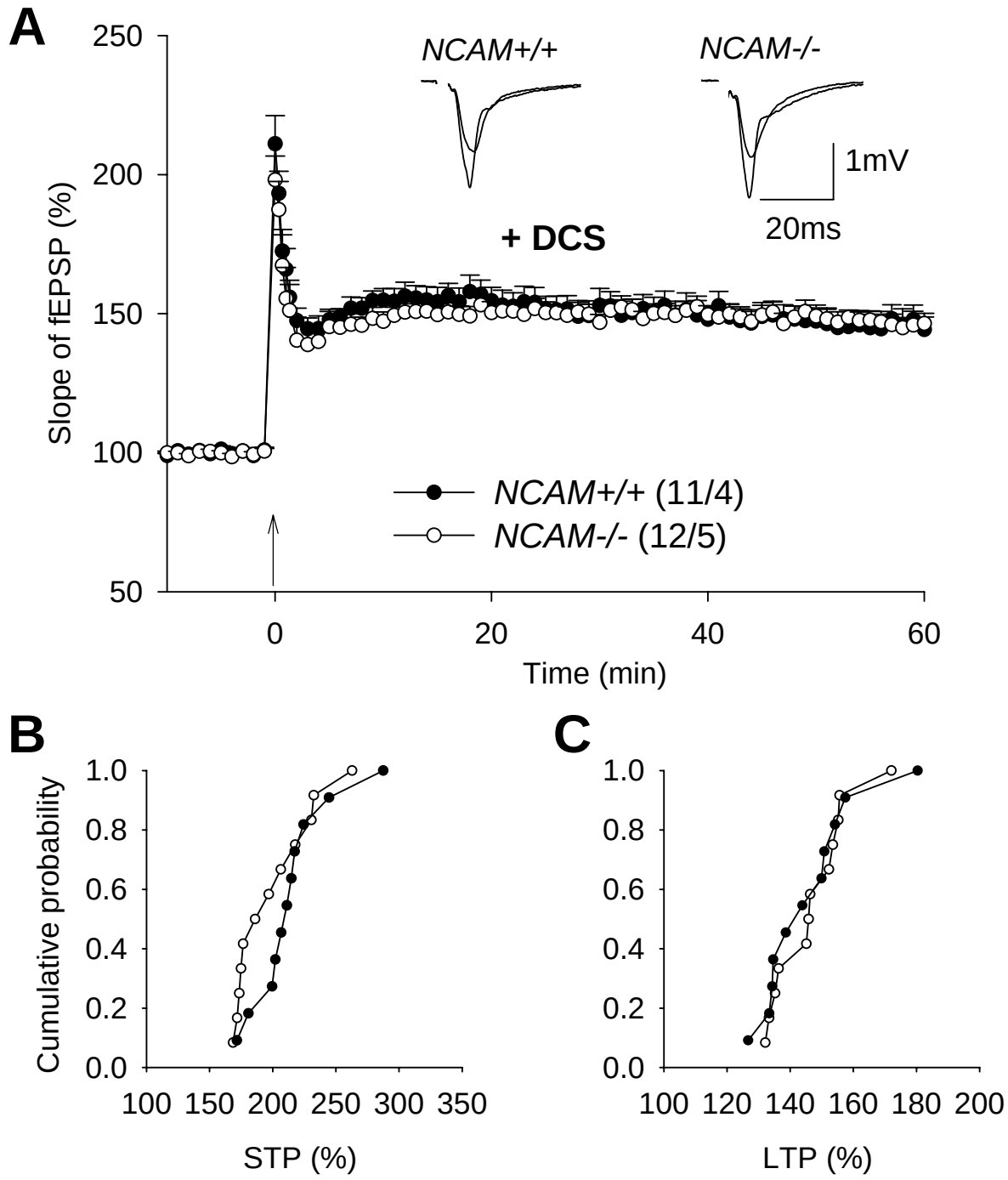

Figure 16. Restoration of impaired LTP in NCAM-/- mice via modulation of NMDA receptor by application of the NMDAR agonist D-cycloserine (DCS). *(A) Profiles of TBS-induced short- and long-term potentiation in the presence of DCS show restoration of LTP in NCAM-/- mice by DCS (40μM). Traces on the top provide fEPSPs (average of 30 sweeps) collected before and 50-60 min after TBS administration. The mean slope of fEPSPs recorded 10 min before TBS is taken as 100% and arrow indicates delivery of TBS. Data represent mean + SEM, numbers of tested slices and mice are indicated in parentheses. (B-C)Cumulative plots representing levels of STP measured 1 min after TBS (B) and levels of LTP measured 50-60 min after TBS (C). Each symbol represents a single experiment. Cumulative probability at any given value x is the probability to observe potentiation less or equal to x. No significant difference between genotypes was found for STP and LTP in this experiment.*

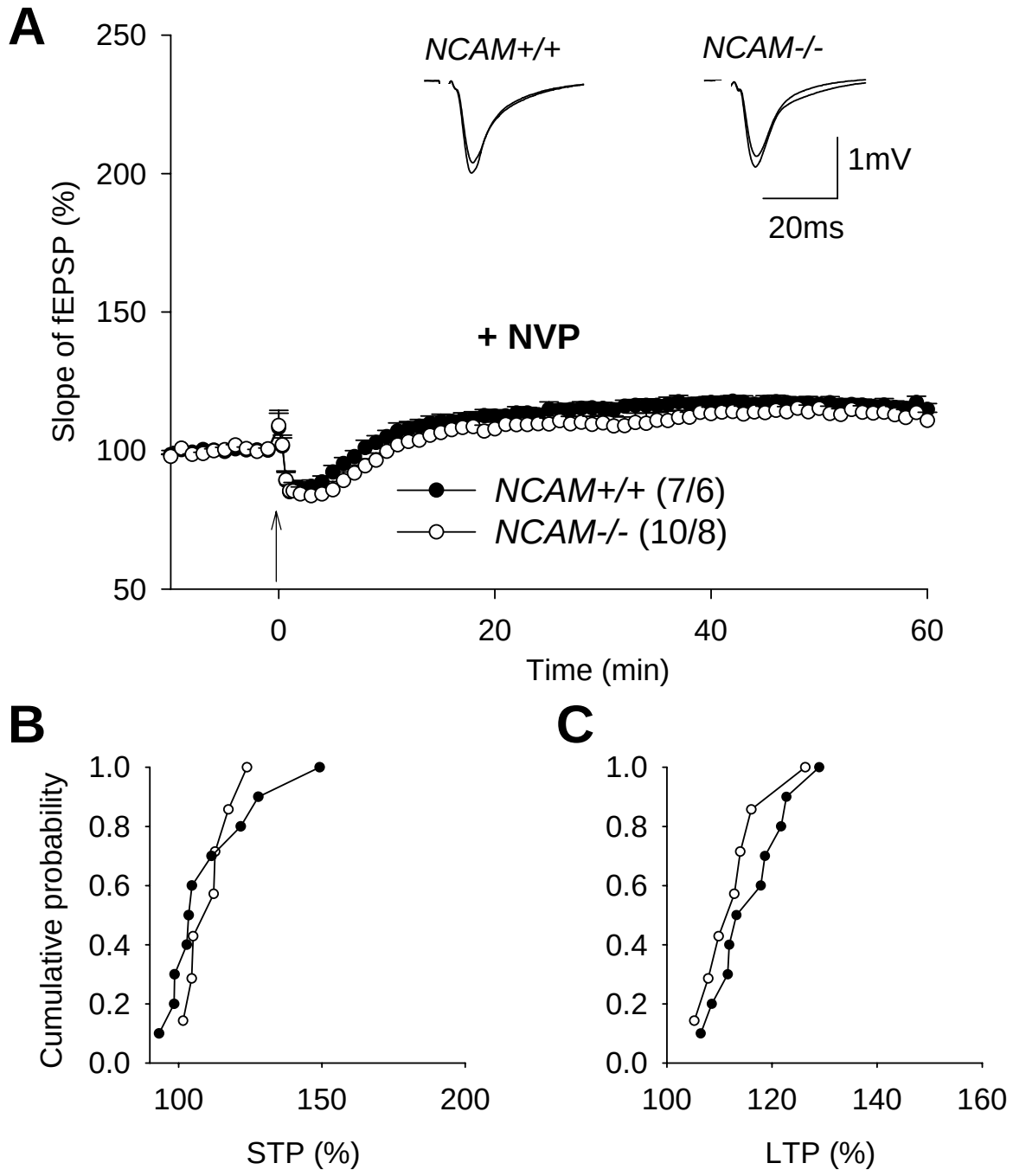

Figure 17. LTP is reduced to the same level in both genotypes by the NR2A-NMDA receptor antagonist NVP. *(A) Profiles of TBS-induced short-term potentiation, followed by short-term depression and long-term potentiation in the presence of NVP (NVP-AAMO77, 0.25 μM). Note strongly inhibited LTP in both genotypes indicating that NR2A-NMDARs contribute predominantly to this form of synaptic plasticity. Traces on the top provide fEPSPs (average of 30 sweeps) collected before and 50-60 min after TBS administration. The mean slope of fEPSPs recorded 10 min before TBS is taken as 100% and arrow indicates delivery of TBS. Data represent mean + SEM, numbers of tested slices and mice are indicated in parentheses. (B-C) Cumulative plots representing levels of STP measured 1 min after TBS (B) and levels of LTP measured 50-60 min after TBS (C). Each symbol represents a single experiment. Cumulative probability at any given value x is the probability to observe potentiation less or equal to x. No significant difference between genotypes was found for STP and LTP in this experiment.*

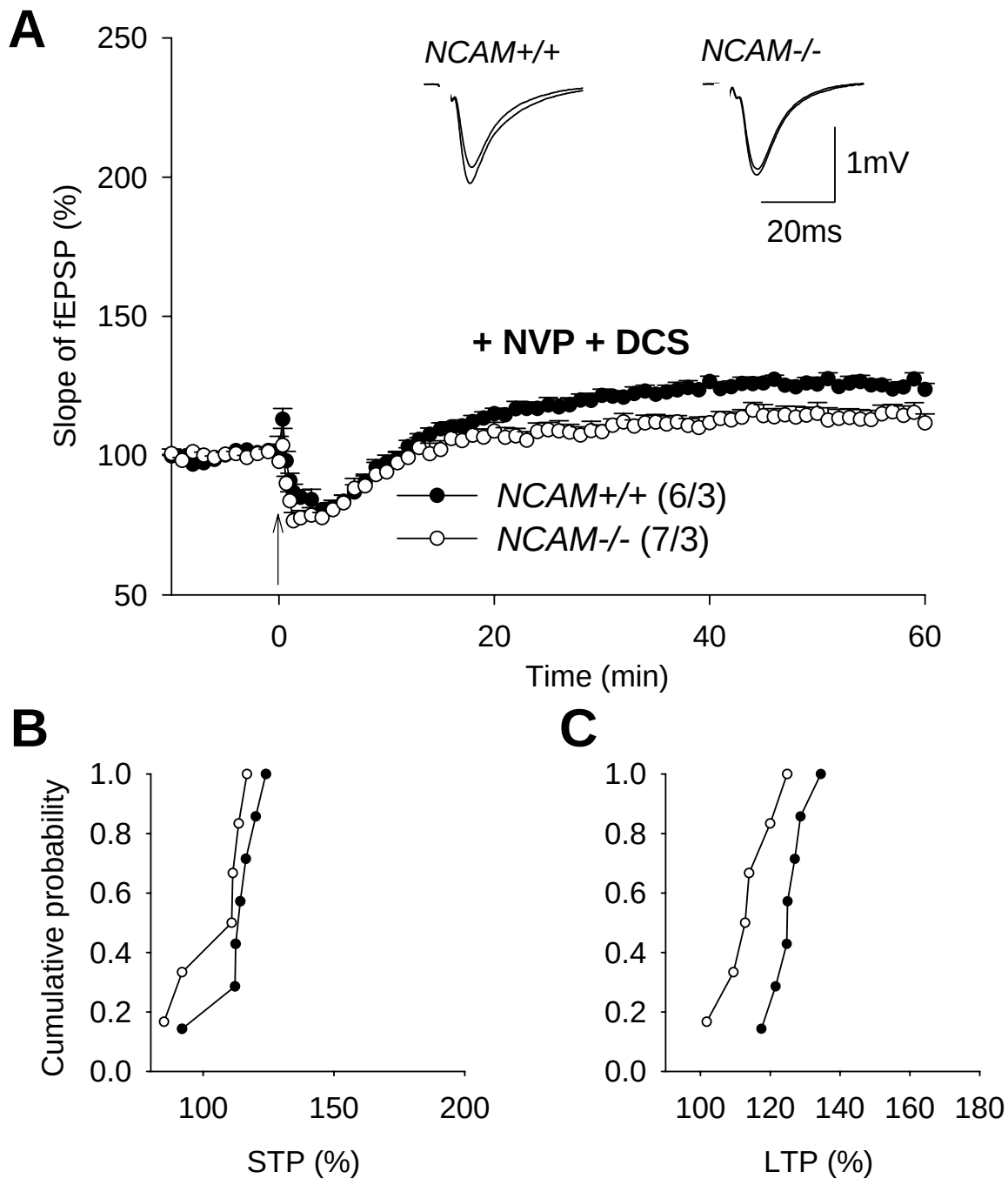

Figure 18. The NR2A-NMDA receptor antagonist NVP reduces LTP induced in the presence of DCS. *(A) Profiles of TBS-induced short-term potentiation, short-term depression and long-term potentiation in the presence of NVP (0.25μM) and DCS (40μM). Note that NVP fully abolished the potentiating effects of DCS on LTP in NCAM-/- mice, suggesting that DCS mostly facilitated LTP in the mutant via NR2A-NMDARs. Traces on the top provide fEPSPs (average of 30 sweeps) collected before and 50-60 min after TBS administration. The mean slope of fEPSPs recorded 10 min before TBS is taken as 100% and arrow indicates delivery of TBS. Data represent mean + SEM, numbers of tested slices and mice are indicated in parentheses. (B-C) Cumulative plots representing levels of STP measured 1 min after TBS (B) and levels of LTP measured 50-60 min after TBS (C). Each symbol represents a single experiment. Cumulative probability at any given value x is the probability to observe potentiation less or equal to x. No significant difference between genotypes was found for STP, but LTP was significantly lower in NCAM-/- mice.*

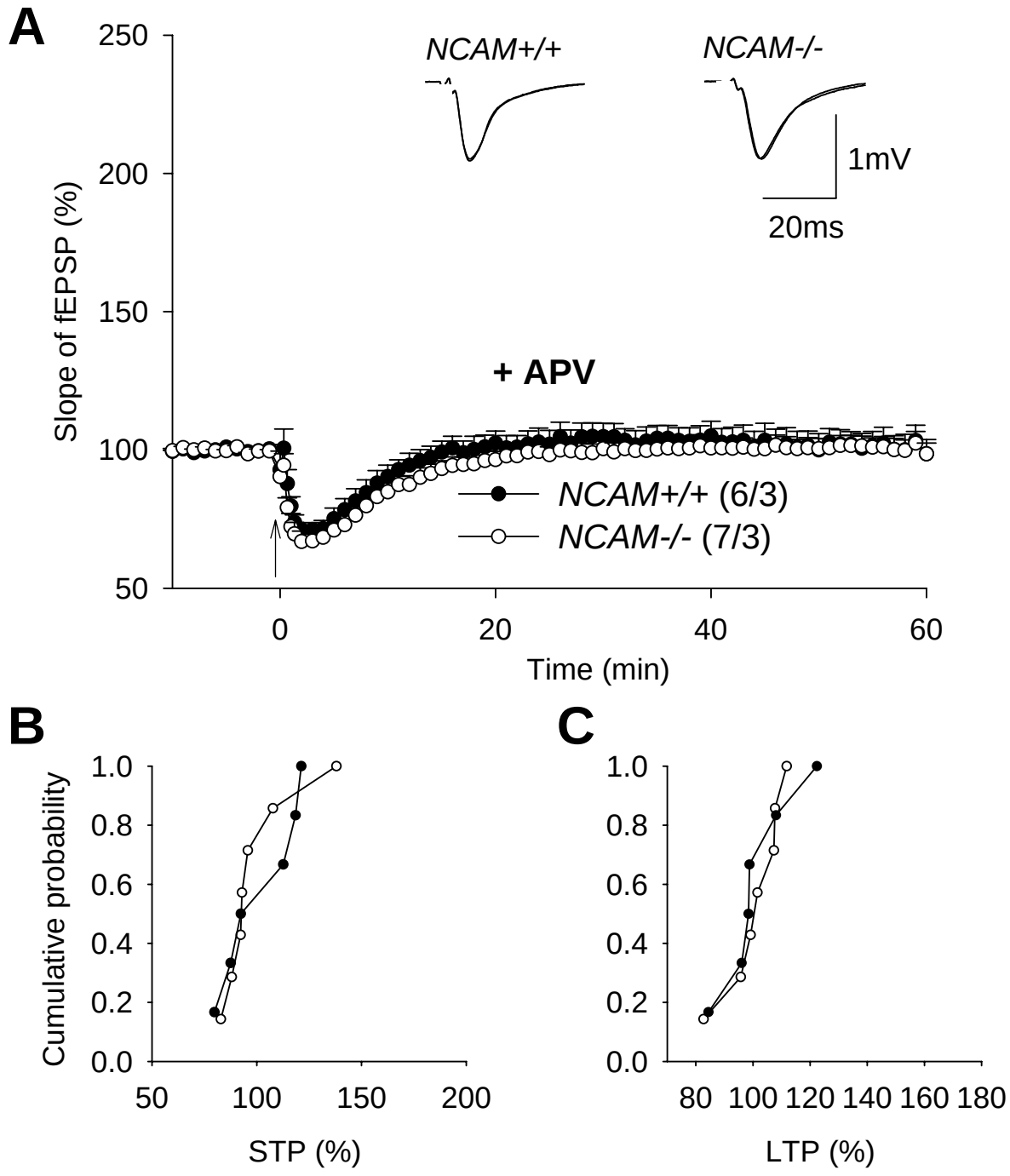

Figure 19. Application of the NMDA receptor subunit unspecific antagonist APV, fully blocked LTP in NCAM+/+ and NCAM-/- mice. *(A) Profiles of TBS-induced short-term depression in the presence of APV (50μM). Note that APV fully blocked STP and LTP in NCAM-/- and NCAM+/+ mice, confirming that these forms of synaptic plasticity are NMDAR dependent in both genotypes. Traces on the top provide fEPSPs (average of 30 sweeps) collected before and 50-60 min after TBS administration. The mean slope of fEPSPs recorded 10 min before TBS is taken as 100% and arrow indicates delivery of TBS. Data represent mean + SEM, numbers of tested slices and mice are indicated in parentheses. (B-C) Cumulative plots representing levels of STP measured 1 min after TBS (B) and levels of LTP measured 50-60 min after TBS (C). Each symbol represents a single experiment. Cumulative probability at any given value x is the probability to observe potentiation less or equal to x. No significant difference between genotypes was found for STP and LTP in this series of experiments.*

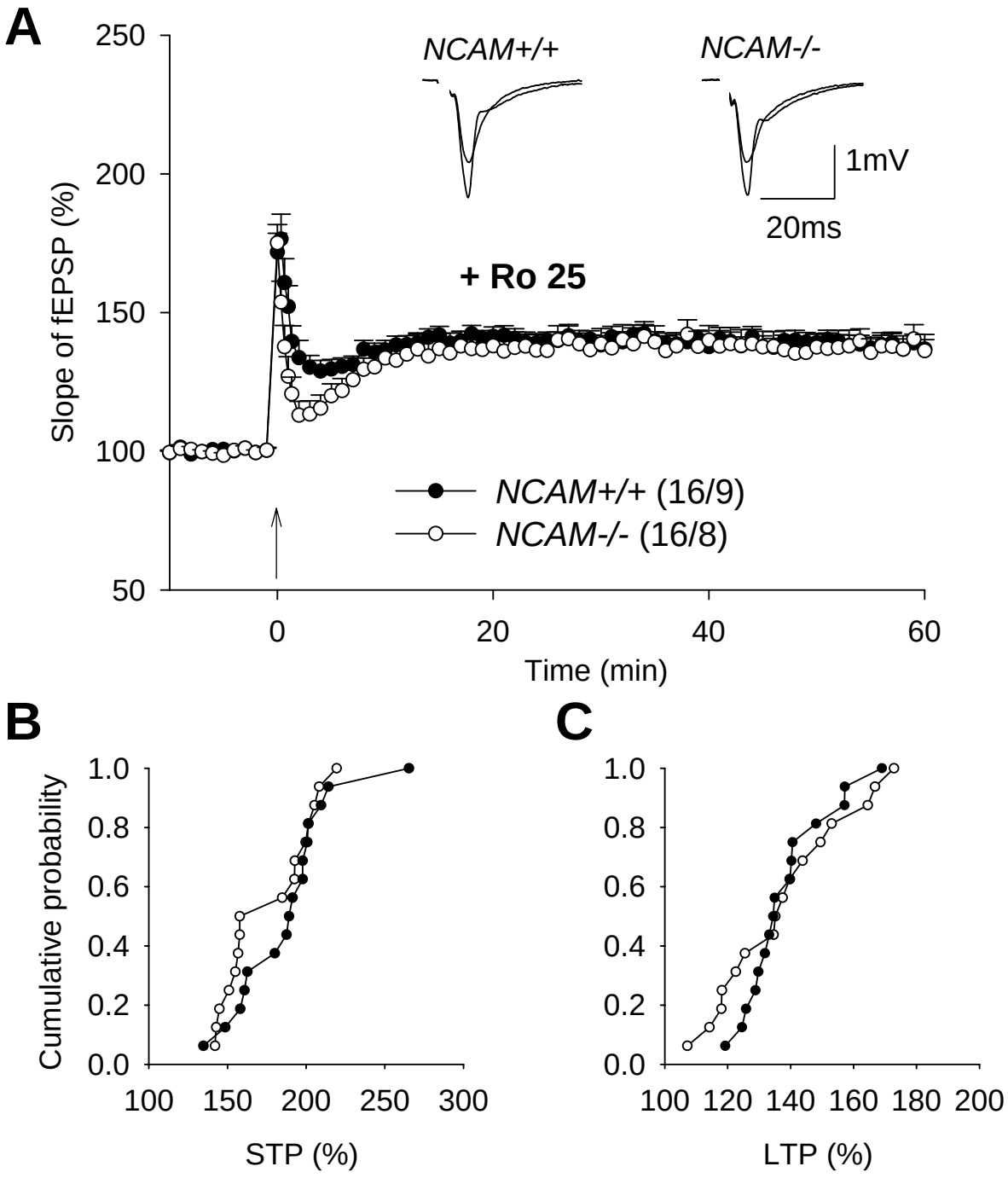

Figure 20. Restoration of impaired LTP in NCAM-/- mice via modulation of NMDARs by application of the NR2B-NMDA receptor selective antagonist Ro 25-6981 (Ro 25). *(A) Profiles of TBS-induced short- and long-term potentiation show restored LTP in NCAM-/- mice to the level of NCAM+/+ mice by application of Ro 25 (0.5μM). Traces on the top provide fEPSPs (average of 30 sweeps) collected before and 50-60 min after TBS administration. The mean slope of fEPSPs recorded 10 min before TBS is taken as 100% and arrow indicates delivery of TBS. Data represent mean + SEM, numbers of tested slices and mice are indicated in parentheses. (B-C)Cumulative plots representing levels of STP measured 1 min after TBS (B) and levels of LTP measured 50-60 min after TBS (C). Each symbol represents a single experiment. Cumulative probability at any given value x is the probability to observe potentiation less or equal to x. No significant difference between genotypes was found for STP and LTP in this series of experiments.*

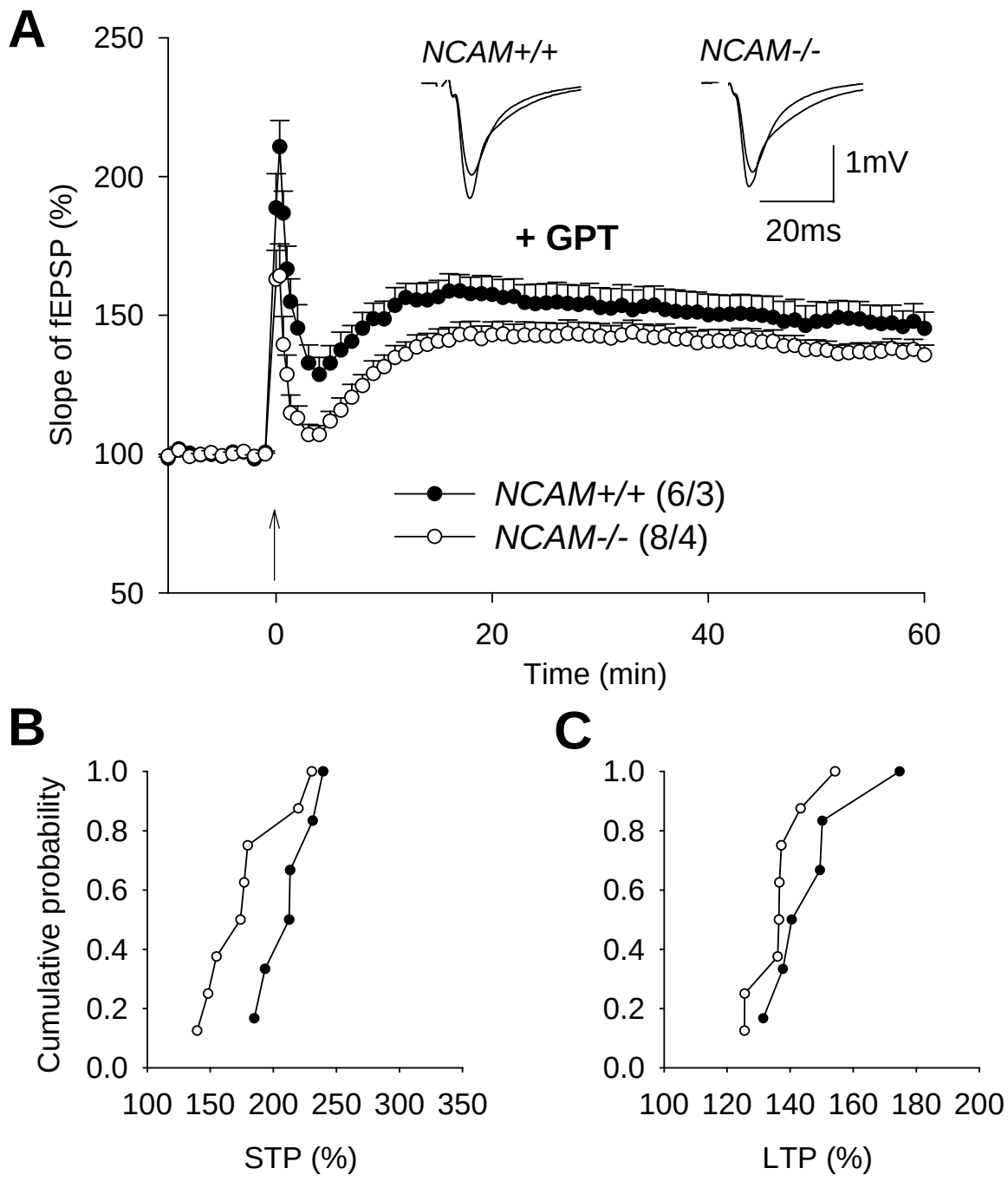

Figure 21. Restoration of impaired LTP in NCAM-/- mice by application of the glutamate scavenger, glutamic pyruvate transaminase (GPT). *(A) Profiles of TBS-induced short- and long-term potentiation show restored LTP in NCAM-/- mice by application of GPT (5 U/ml), a substance known to reduce concentrations of extrasynaptic glutamate. Traces on the top provide fEPSPs (average of 30 sweeps) collected before and 50-60 min after TBS administration. The mean slope of fEPSPs recorded 10 min before TBS is taken as 100% and arrow indicates delivery of TBS. Data represent mean + SEM, numbers of tested slices and mice are indicated in parentheses. (B-C) Cumulative plots representing levels of STP measured 1 min after TBS (B) and levels of LTP measured 50-60 min after TBS (C). Each symbol represents a single experiment. Cumulative probability at any given value x is the probability to observe potentiation less or equal to x. STP was slightly lower in slices from NCAM-/- mice but no difference between genotypes was found for LTP in this series of experiments.*

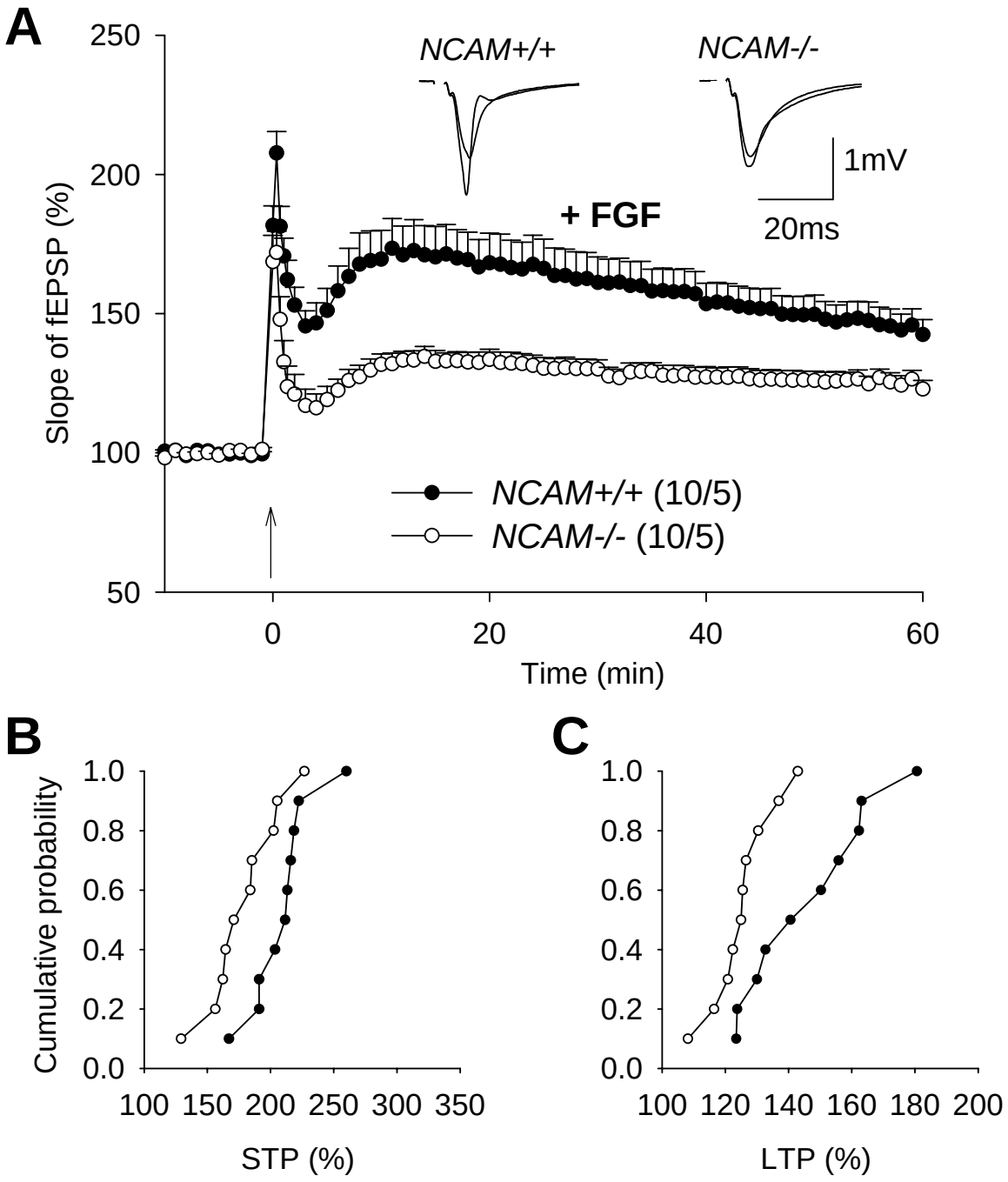

Figure 22. Administration of fibroblast growth factor (FGF) can not rescue impaired LTP in NCAM-/- mice. *(A) Profiles of TBS-induced short- and long-term potentiation show that the levels of STP and LTP in NCAM-/- mice are significantly lower than those in NCAM+/+ littermates after application of FGF (25 ng/ml). Have we checked this – how did you diluted? As I remember our stock is 1 mg/ml. Traces on the top provide fEPSPs (average of 30 sweeps) collected before and 50-60 min after TBS administration. The mean slope of fEPSPs recorded 10 min before TBS is taken as 100% and arrow indicates delivery of TBS. Data represent mean + SEM, numbers of tested slices and mice are indicated in parentheses. (B-C) Cumulative plots representing levels of STP measured 1 min after TBS (B) and levels of LTP measured 50-60 min after TBS (C). Each symbol represents a single experiment. Cumulative probability at any given value x is the probability to observe potentiation less or equal to x. Both STP and LTP were significantly impaired in slices from NCAM-/- mice.*

4. Modulation of NMDA receptors restores impaired LTD in *NCAM-/-* mice.

Next, we asked if abnormalities in NMDAR-mediated signaling also underlie impairment of LTD in NCAM-/- mice. To induce a robust NMDAR-dependent LTD in slices from adult mice, we used two trains of low-frequency stimulation (Eckhardt et al., 2000; Evers et al., 2002). This protocol reliably induced LTD of 26.5±3.4% in NCAM+/+ mice (Figure 23A,E). In contrast, LTD was completely abolished in NCAM-/- mice (4.0±3.9%; Figure 23A,E), as reported for the CaMKII/cre conditional NCAM deficient mice (Bukalo et al., 2004) and for PSA-depleted brain slices (Muller et al., 1996). Application of DCS restored LTD to 19.2±5.4% in NCAM-/- mice, while fully blocking LTD to 4.3±4.2% in NCAM+/+ mice (Figure 23B,E). Blockade of either NR2B- or NR2A-NMDARs by application of Ro 25-6981 (5.2±4.8% in NCAM+/+ and 1.3±4.8% in NCAM-/-) or NVP (4.6±6.5% in NCAM+/+ and 0.2±4.1%), respectively, inhibited LTD in both genotypes (Figure 23C,D,E). These data are consistent with the view that signaling via both NR2Aand NR2B-NMDARs is required for induction of this form of LTD and that the level of NMDAR-mediated synaptic transmission should be not too high and not too low to support induction of LTD. Thus, deficit in transmission via NR2A-containing receptors in NCAM-/- mice leads to impaired LTD in these mice that can be compensated by DCS. In NCAM+/+ mice, DCS facilitated NMDAR-mediated synaptic transmission to exceed the level under which LTD can be induced.

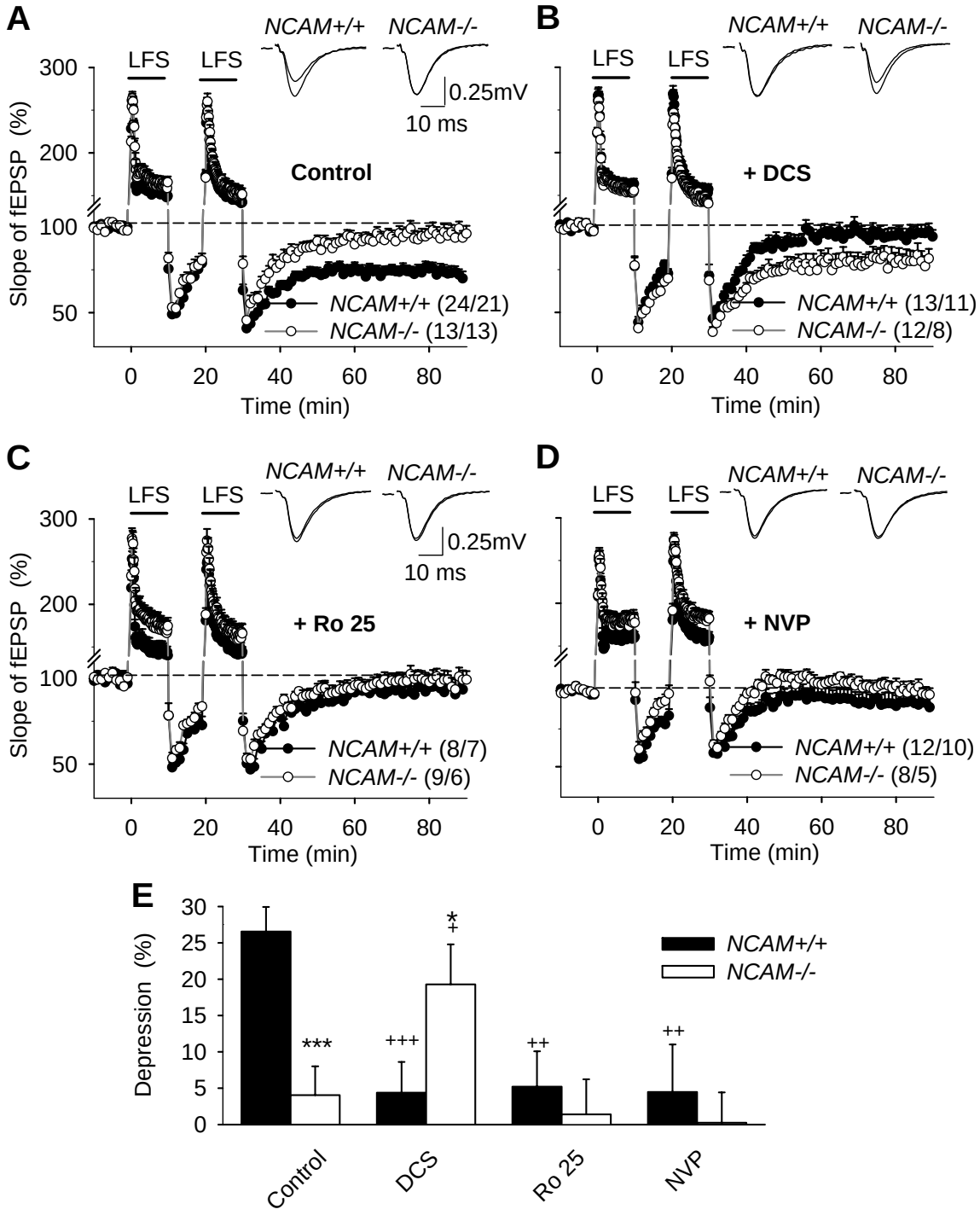

Figure 23. Modulation of NMDA receptor restores impaired LTD in NCAM-/- mice. *(A) Two trains of low-frequency stimulation (LFS, shown by horizontal bar) induce LTD in untreated slices from NCAM+/+ mice but not from NCAM-/- mice. (B) Restoration of LTD in NCAM-/- mice and impairment of LTD in NCAM+/+ mice by application of the NMDAR agonist D-cycloserine (DCS). (C-D) Inhibition of LTD in both genotypes by the NMDAR subtype selective antagonist Ro 25-6981 (Ro 25) (C) and NVP (D). (E) Mean + SEM of LTD levels recorded 50-60 min after induction of LTD in the presence of NR modulators. *p<0.05 and ***p<0.001, significant difference between NCAM+/+ and NCAM-/- mice treated by the same drug, +p<0.05, ++p<0.01, +++p<0.001, significant difference between control and pharmacologically treated mice of the same genotype, t-test. Numbers of tested slices and mice are indicated in parentheses in (A-D). Done in collaboration with Olena Bukalo from ZMNH, Hamburg, Germany.*

5. Restoration of impaired LTP in endoNF-treated hippocampal slices via modulation of NMDA receptors.

If a deficit in synaptic plasticity in NCAM-/- mice is due to the lack of PSA, it is plausible to expect that impaired LTP in PSA-deficient neurons would also be compensated by modulation of NMDARs. To test this hypothesis, we incubated hippocampal slices from NCAM+/+ mice for 2 hours with endoNF. This treatment resulted in sufficient removal of PSA which is diffusively expressed in the stratum radiatum of CA1 and CA3 and prominently expressed in mossy fibers in untreated slices or slices treated with the inactive mutated form of endoNF (Figure 24). Removal of PSA by endoNF did not affect significantly the level of STP which was 210.3±14.4% in sham treated slices and 183.9±6.5% in endoNF treated slices, respectively (Figure 25A,B) but, markedly impaired induction of LTP (Figure 25A,C), as previously reported for purified endoneuraminidase N (Becker et al., 1996; Muller et al., 1996). The amount of LTP in our condition in endoNF treated slices was significantly lower than in sham treated slices 120.1±2.1% and 143.6±2.6% respectively. As a negative control, inactive endoNF did not inhibit LTP (140.1±4.7%) and STP (198.8± 8.1%), as expected (Figure 26). Modulation of NMDARs with DCS (Figure 27) or blockade of NR2B-NMDARs with Ro 25-6981 (Figure 28) increased levels of LTP in endoNF-treated slices from 120.1±2.1% to 145.2±5.5% and 132.2±2.5%, respectively. These levels of LTP were not different from those observed after treatment with inactive endoNF (Figures 27 and 28). The levels of STP were not significantly affected by treatments with DCS (188±9.7%) and Ro 25 (177.3±13.2%). Thus, these data replicate results from the experiments in NCAM-/- mice and demonstrate that impaired LTP in either NCAM- or PSA-deficient slices is due to improper signaling via NMDARs.

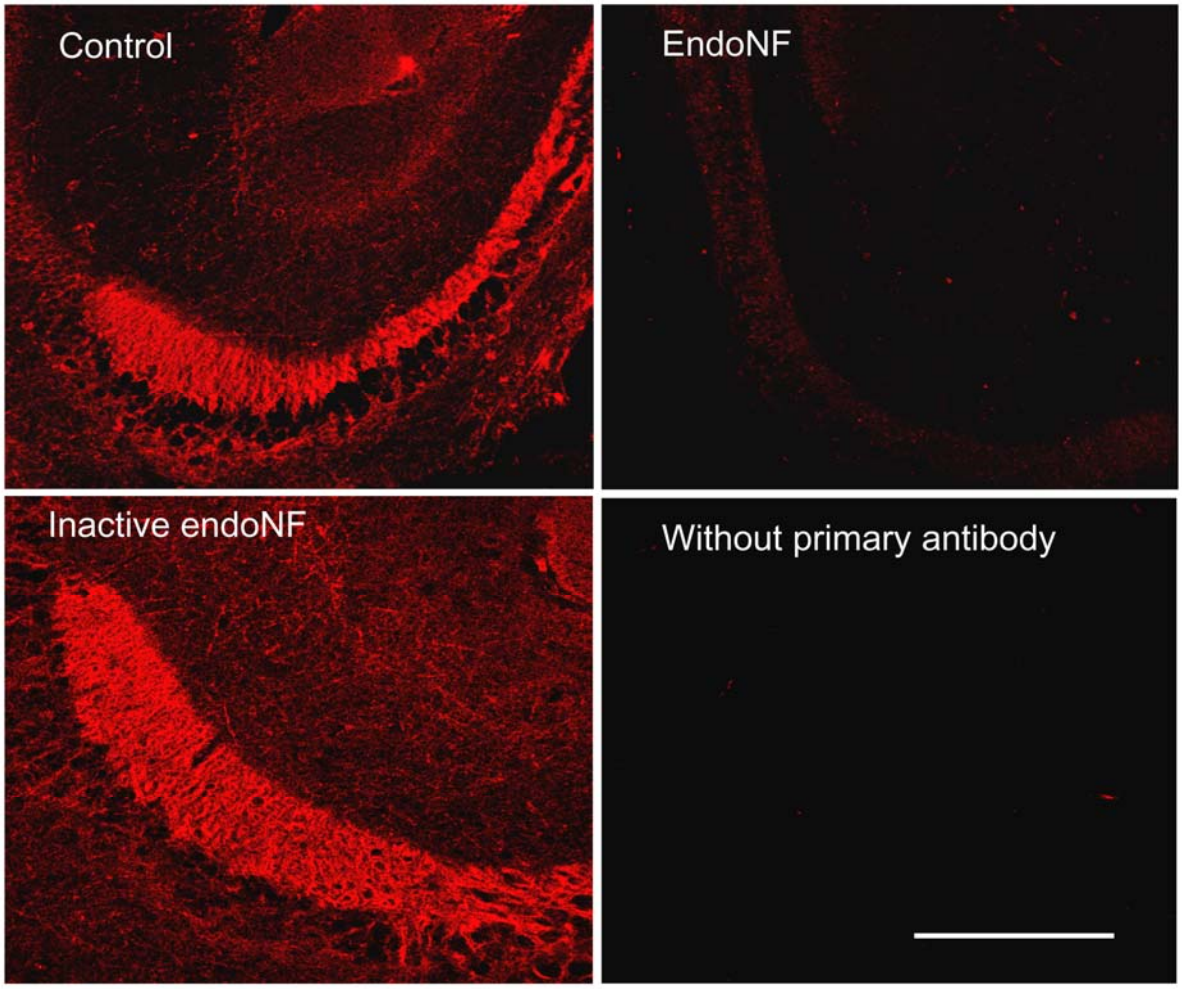

Figure 24. Removal of PSA in acute hippocampal slices by a two-hour incubation with endoNF. *In untreated control slices immunostaining for PSA conspicuously visualizes mossy fiber projections. Also there is diffuse immunolabeling in the strata radiatum and oriens. The same pattern is seen after treatment with inactive endoNF but no immunolabeling is seen after treatment with active endoNF or in slices stained with secondary antibodies only. Scale bar, 150 μm.*

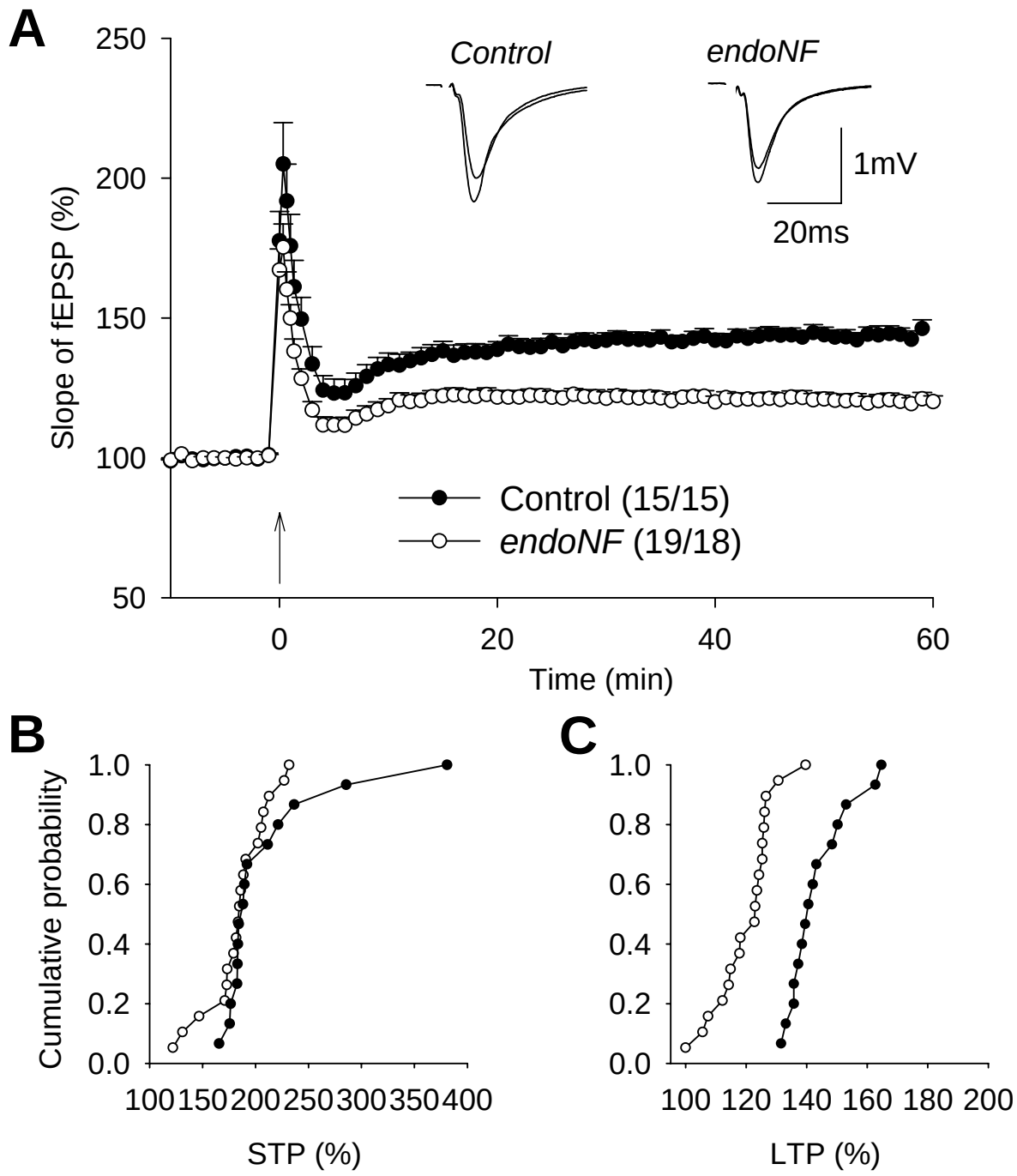

Figure 25. Impaired LTP in endoNF-treated hippocampal slices. *(A) Profiles of TBS-induced short- and long-term potentiation show impaired CA1 LTP in slices treated with the active form of endoNF, as compared to sham treated slices. Traces on the top provide fEPSPs (average of 30 sweeps) collected before and 50-60 min after TBS administration. The mean slope of fEPSPs recorded 10 min before TBS is taken as 100% and arrow indicates delivery of TBS. Data represent mean + SEM, numbers of tested slices and mice are indicated in parentheses. (B-C) Cumulative plots representing levels of STP measured 1 min after TBS (B) and levels of LTP measured 50-60 min after TBS (C). Each symbol represents a single experiment. Cumulative probability at any given value x is the probability to observe potentiation less or equal to x. No significant difference between sham and endoNF treated sclices was found for STP, but LTP was drastically impaired in endoNF treated slices.*

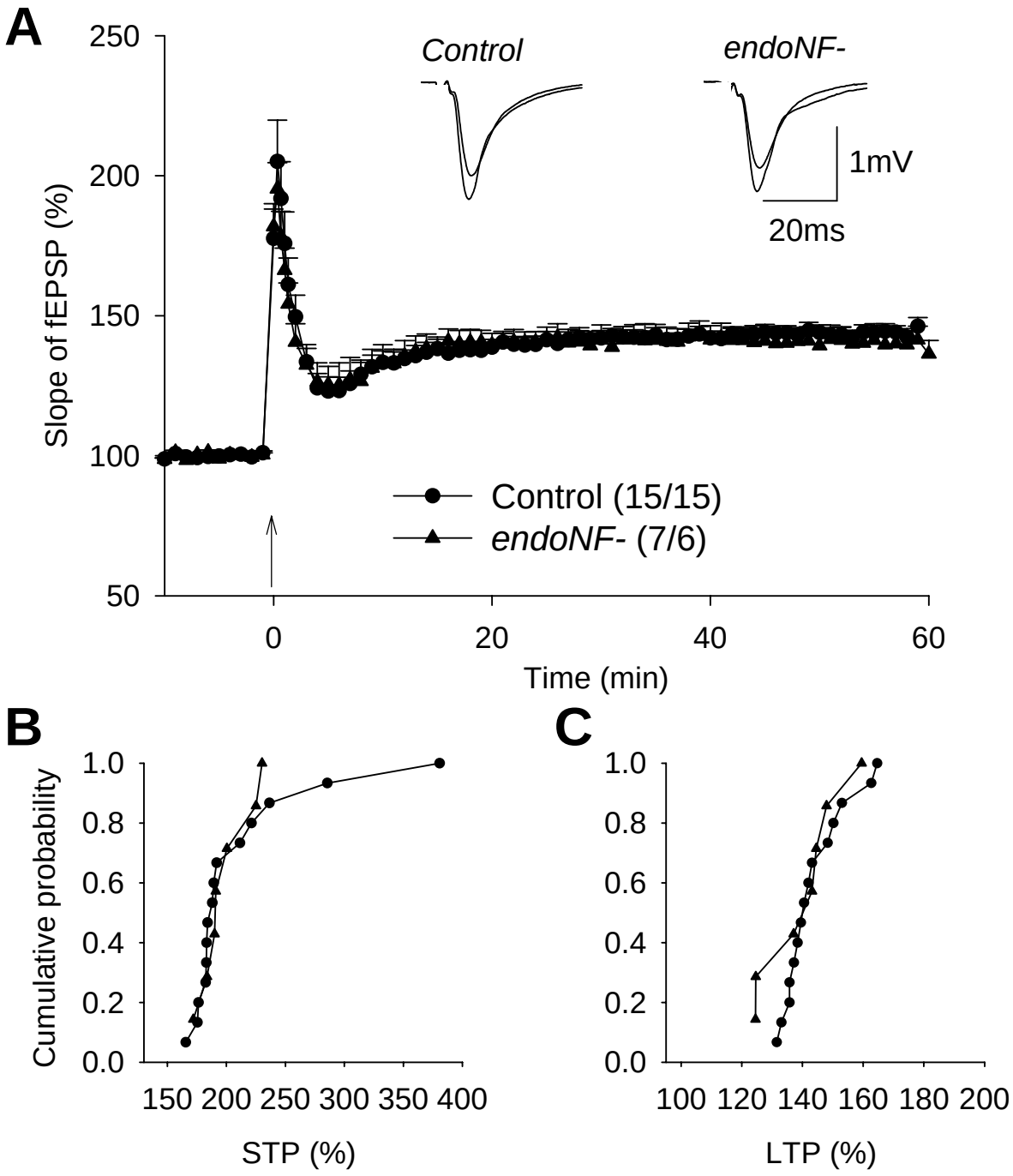

Figure 26. Inactive form of endoNF (endoNF-) does not affect the level of LTP. *(A) Profiles of TBS-induced short- and long-term potentiation show CA1 LTP in slices treated with sham, as compared to endoNF- treated slices. Traces on the top provide fEPSPs (average of 30 sweeps) collected before and 50-60 min after TBS administration. The mean slope of fEPSPs recorded 10 min before TBS is taken as 100% and arrow indicates delivery of TBS. Data represent mean + SEM, numbers of tested slices and mice are indicated in parentheses. (B-C)Cumulative plots representing levels of STP measured 1 min after TBS (B) and levels of LTP measured 50-60 min after TBS (C). Each symbol represents a single experiment. Cumulative probability at any given value x is the probability to observe potentiation less or equal to x. No significant difference between sham and endoNF- treated slices was found for STP and LTP in this series of experiments.*

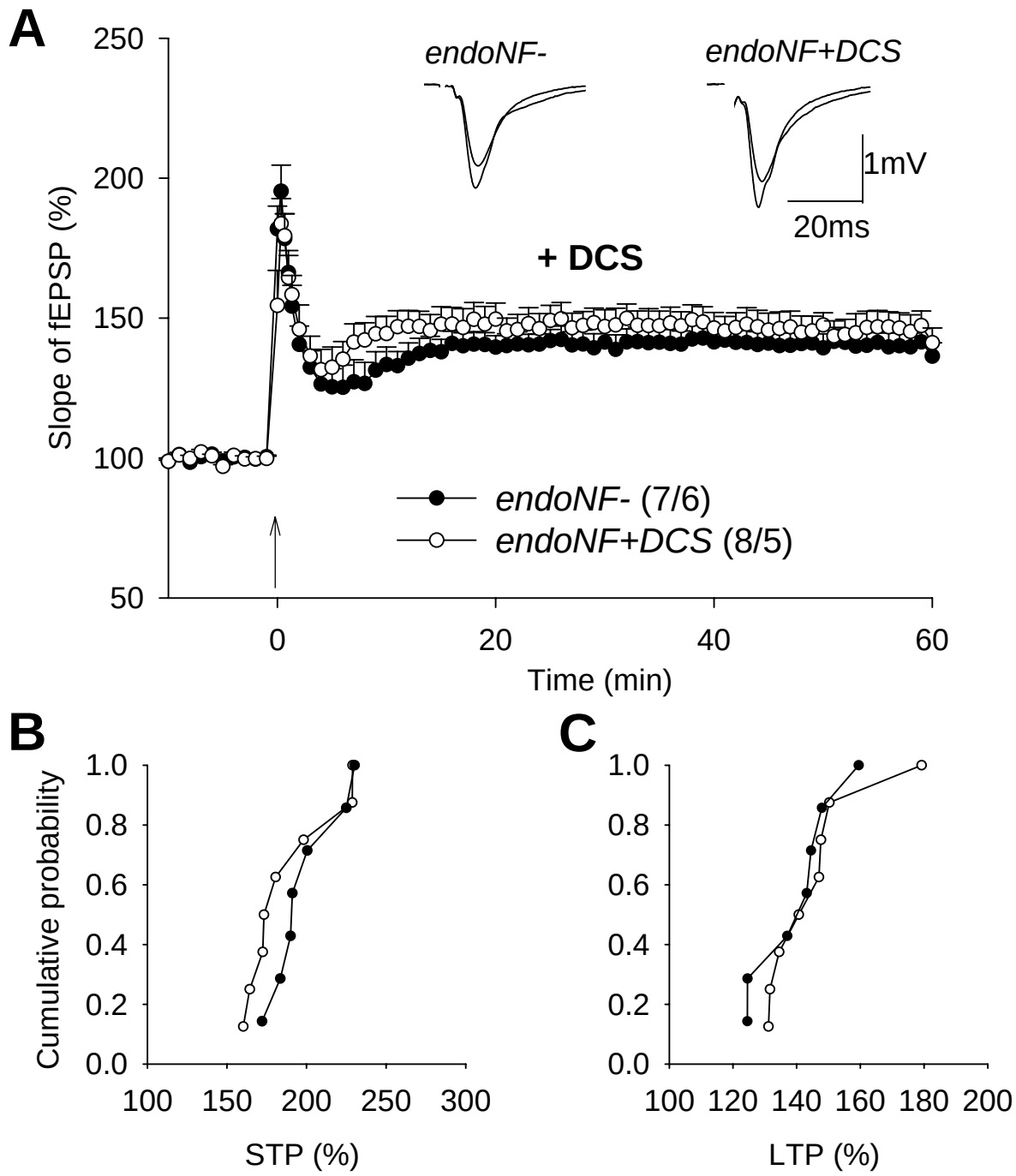

Figure 27. Restoration of LTP in endoNF-treated slices to normal levels by application of the NMDA receptor agonist DCS. *(A) A profile of TBS-induced short- and long-term potentiation shows restored LTP in active endoNF treated slices by application of 40μM DCS. Traces on the top provide fEPSPs (average of 30 sweeps) collected before and 50-60 min after TBS administration. The mean slope of fEPSPs recorded 10 min before TBS is taken as 100% and arrow indicates delivery of TBS. Data represent mean + SEM, numbers of tested slices and mice are indicated in parentheses. (B-C)Cumulative plots representing levels of STP measured 1 min after TBS (B) and levels of LTP measured 50-60 min after TBS (C). Each symbol represents a single experiment. Cumulative probability at any given value x is the probability to observe potentiation less or equal to x. No significant difference between sham and endoNF treated slices was found for STP and LTP in this series of experiments.*

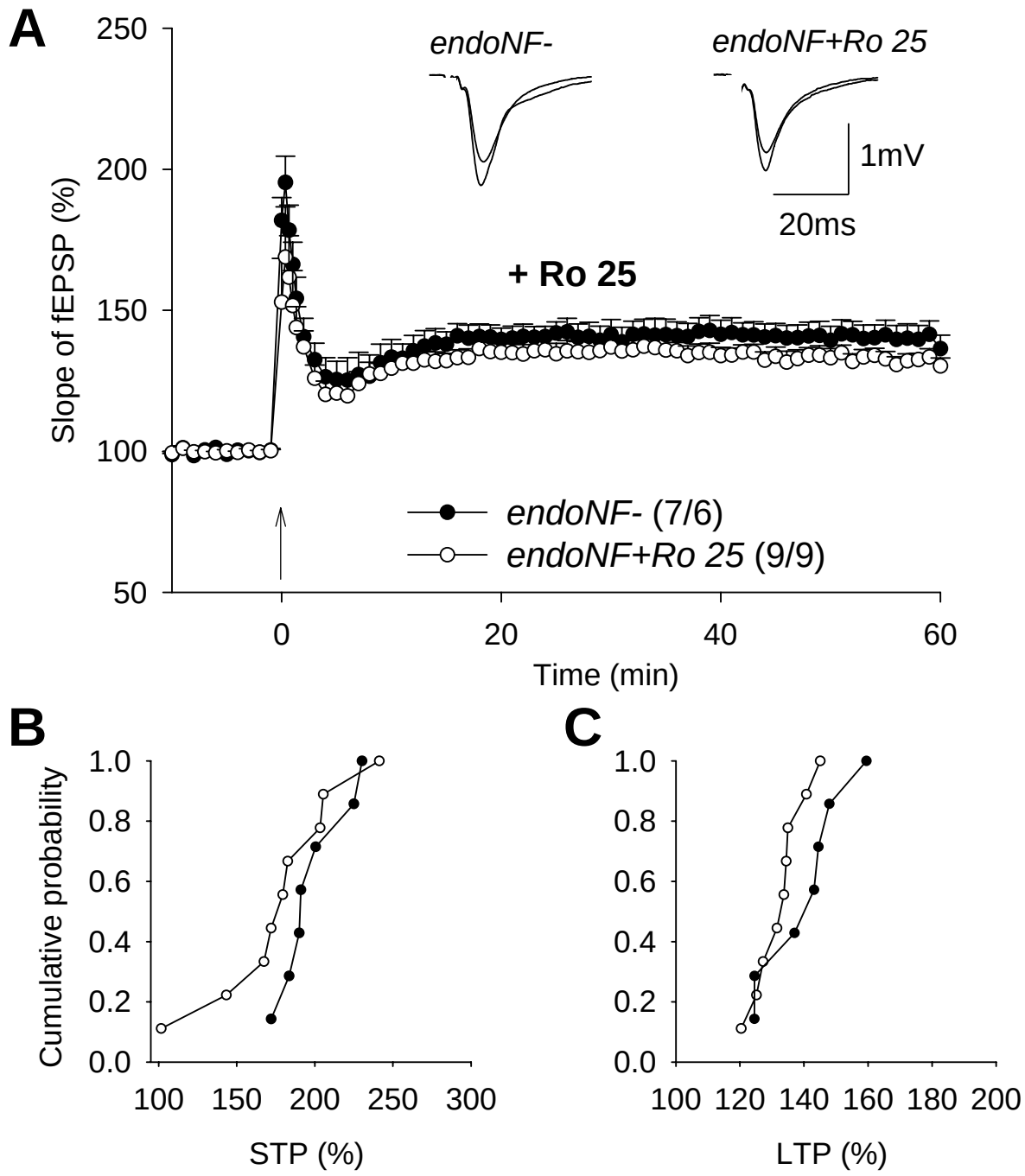

Figure 28. Restoration of LTP in endoNF-treated slices by application of the NR2B-NMDA receptor antagonist Ro 25. *(A) Profiles of TBS-induced short- and long-term potentiation in the presence of Ro 25. Note that LTP in active endoNF treated slices is restored to control levels by application of Ro 25 (0.5μM). Traces on the top provide fEPSPs (average of 30 sweeps) collected before and 50-60 min after TBS administration. The mean slope of fEPSPs recorded 10 min before TBS is taken as 100% and arrow indicates delivery of TBS. Data represent mean + SEM, numbers of tested slices and mice are indicated in parentheses. (B-C) Cumulative plots representing levels of STP measured 1 min after TBS (B) and levels of LTP measured 50-60 min after TBS (C). Each symbol represents a single experiment. Cumulative probability at any given value x is the probability to observe potentiation less or equal to x. No significant difference between sham and endoNF treated slices was found for STP and LTP in this series of experiments.*

6. Deficit in PSA is a key feature of NCAM-/- mice that leads to impairment of LTP via activation of the Ras-GRF1/p38 mitogen-activated protein kinase signaling cascade

6.1. Upregulation of p38 MAPK signaling in the hippocampus of NCAM-/- mice

Our experiments with Ro-25 and GTP support the view that impaired LTP in both NCAM- and PSA-deficient slices is due to improper signaling via extrasynaptic NMDARs. We next asked which molecules downstream of extrasynaptic NR2B-NMDARs mediate this effect. Previous reports highlighted p38 mitogen-activated protein kinase (MAPK) as a key player in synaptic depression (Bolshakov et al., 2000; Hsieh et al., 2006; Zhu et al., 2002). We therefore investigated the levels of active MAPKs in the hippocampus of *NCAM-/-* mice using an activation-specific antibody. We found a more than 5-fold upregulation of p38 MAPK phosphorylation (Figure 29A,B), whereas p38 protein levels (Figure 29A,B) and levels of protein and phosphorylated p42/44 MAPKs (Figure 29B) were not significantly changed.

6.*2. Impaired LTP in PSA deficient slices can be restored by the antagonist of p38 MAPK*

Since we found that phospo-p38 is upregulated in NCAM-/- brains and since it is known that p38 MAPK is important mediator in LTD signaling (Bolshakov et al., 2000; Hsieh et al., 2006; Zhu et al., 2002; Giese et al., 2001), we suggested that improved signaling mediated by extrasynaptic NMDARs can lead to overactivation of p38 MAPK cascade and therefore impair LTP in NCAM and or PSA deficient slices. To prove this hypothesis we applied the inhibitor of p38 MAPK activity SB203580 in slices from NCAM-/- mice and indeed this treatment restored LTP in *NCAM-/-* mice from 125.0±1.6% to 137.2±6.1% (Figure 30A,C), i.e. to the level of wild-type control (140.0±3.4%). Next we asked if we can rescue impaired LTP in endoNF treated slices in the same way like we did for NCAM-deficient slices. Also, LTP was restored to normal level (Figure 31A,C) by addition of SB203580 to endoNF-treated slices: there was an increase from 120.1±2.1% to 133.5±3.7%, which was not significantly different from LTP in sham treated slices (139.4±3.6%).

The Ca^{2+}-dependent Ras-guanine releasing factor (GRF) 1 mediates activation of p38 MAPK by NR2B-NRs (Li et al., 2006). We therefore studied LTP in mice deficient in *Ras-GRF1*. In contrast to wild-type mice, enzymatic removal of PSA in this mutant did not impair LTP (135.3±2.9% in untreated versus 133.3±2.5% in endoNF-treated mutants) (Figure 32A,C), suggesting that enhanced NR2B-NMDAR activation of p38 MAPK via Ras-GRF1 is responsible for reduction of LTP in the absence of NCAM/PSA.

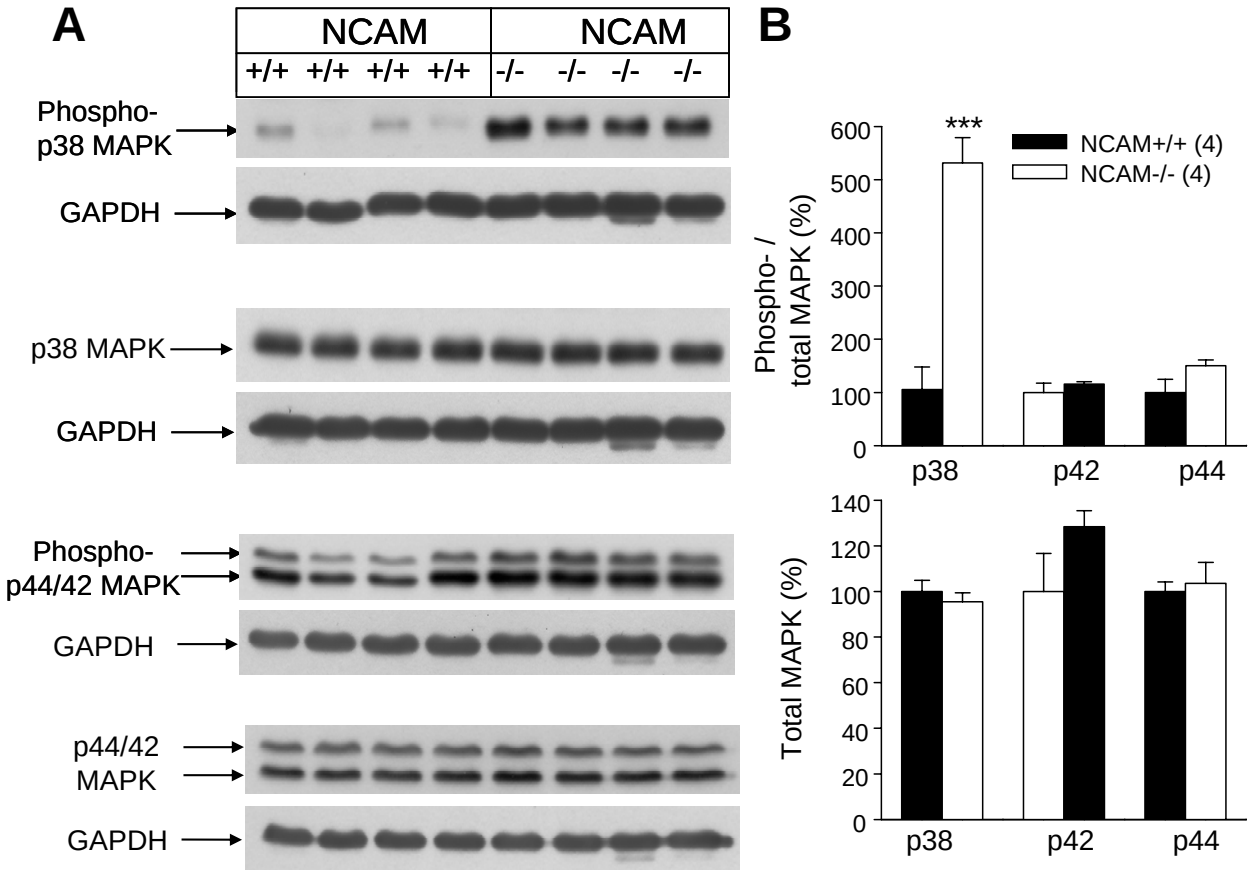

Figure 29. Upregulation of p38 MAPK signaling in the hippocampus of NCAM-/- mice. *(A) Western blots showing levels of phosphorylated (phospho) and total p38 and p42/p44 MAPK proteins in the hippocampi of NCAM+/+ and NCAM-/- mice. Blots were stripped and reblotted with GAPDH antibody as a loading control. The intensity of GAPDH signal was used for normalization of corresponding MAPK signals. (B) Quantification of the levels of phosphorylated and total p38, p42 and p44 in NCAM+/+ and NCAM-/- mice. ***p<0.001, significant difference between genotypes. Number of mice is indicated in parentheses. These experiments were performed in collaboration with Meifang Xiao from ZMNH, Hamburg, Germany.*

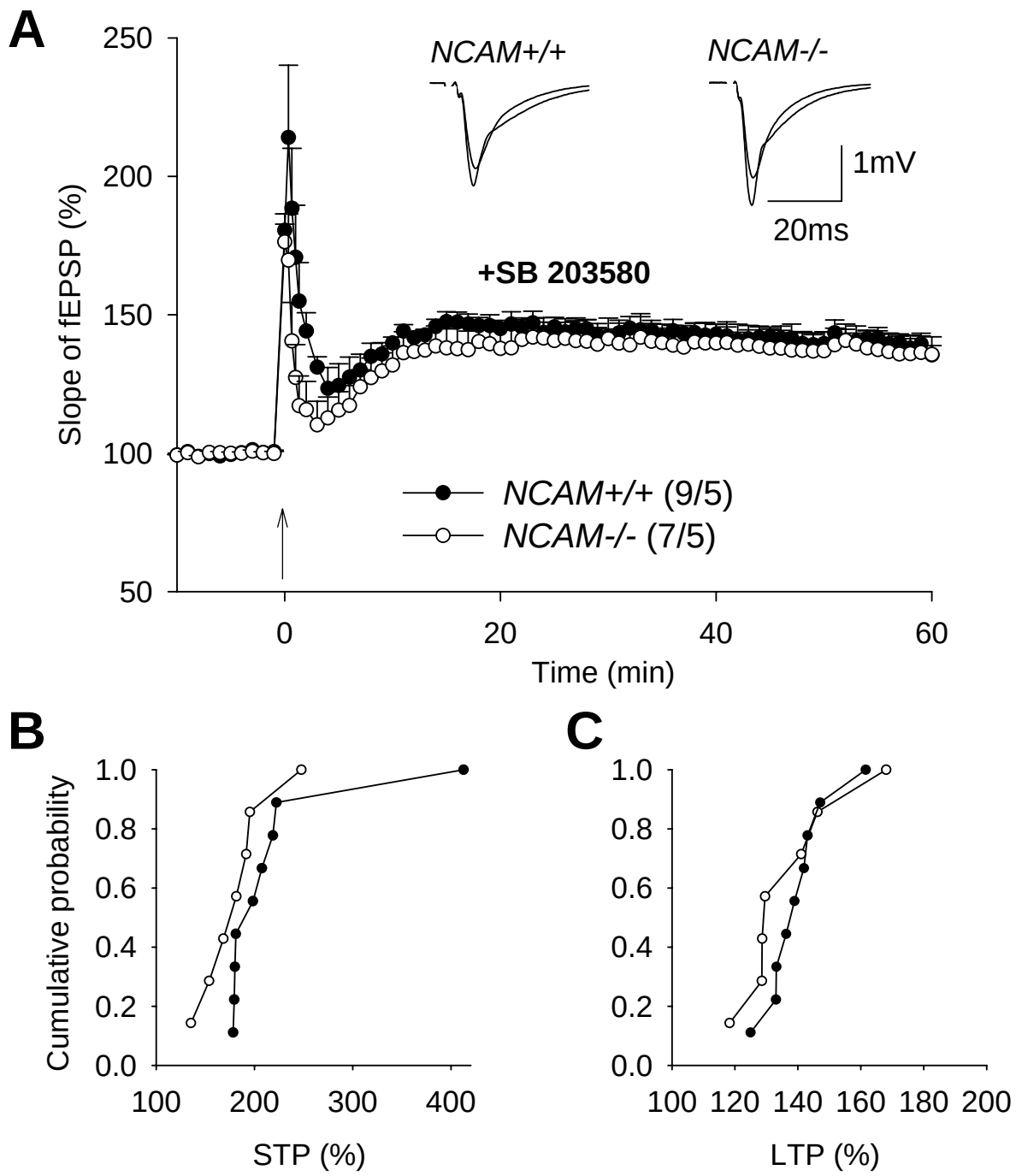

Figure 30. Restoration of impaired LTP in NCAM-/- mice by application of p38 MAPK inhibitor SB 203580. *(A) Profiles of TBS-induced short- and long-term potentiation in the presence of SB 203580 (10μM). Note that LTP in NCAM-/- mice is restored to NCAM+/+ levels by blockade of p38 MAPK activity. Traces on the top provide fEPSPs (average of 30 sweeps) collected before and 50-60 min after TBS administration. The mean slope of fEPSPs recorded 10 min before TBS is taken as 100% and arrow indicates delivery of TBS. Data represent mean + SEM, numbers of tested slices and mice are indicated in parentheses. (B-C) Cumulative plots representing levels of STP measured 1 min after TBS (B) and levels of LTP measured 50-60 min after TBS (C). Each symbol represents a single experiment. Cumulative probability at any given value x is the probability to observe potentiation less or equal to x. No significant difference between genotypes was found for STP and LTP in this series of experiments.*

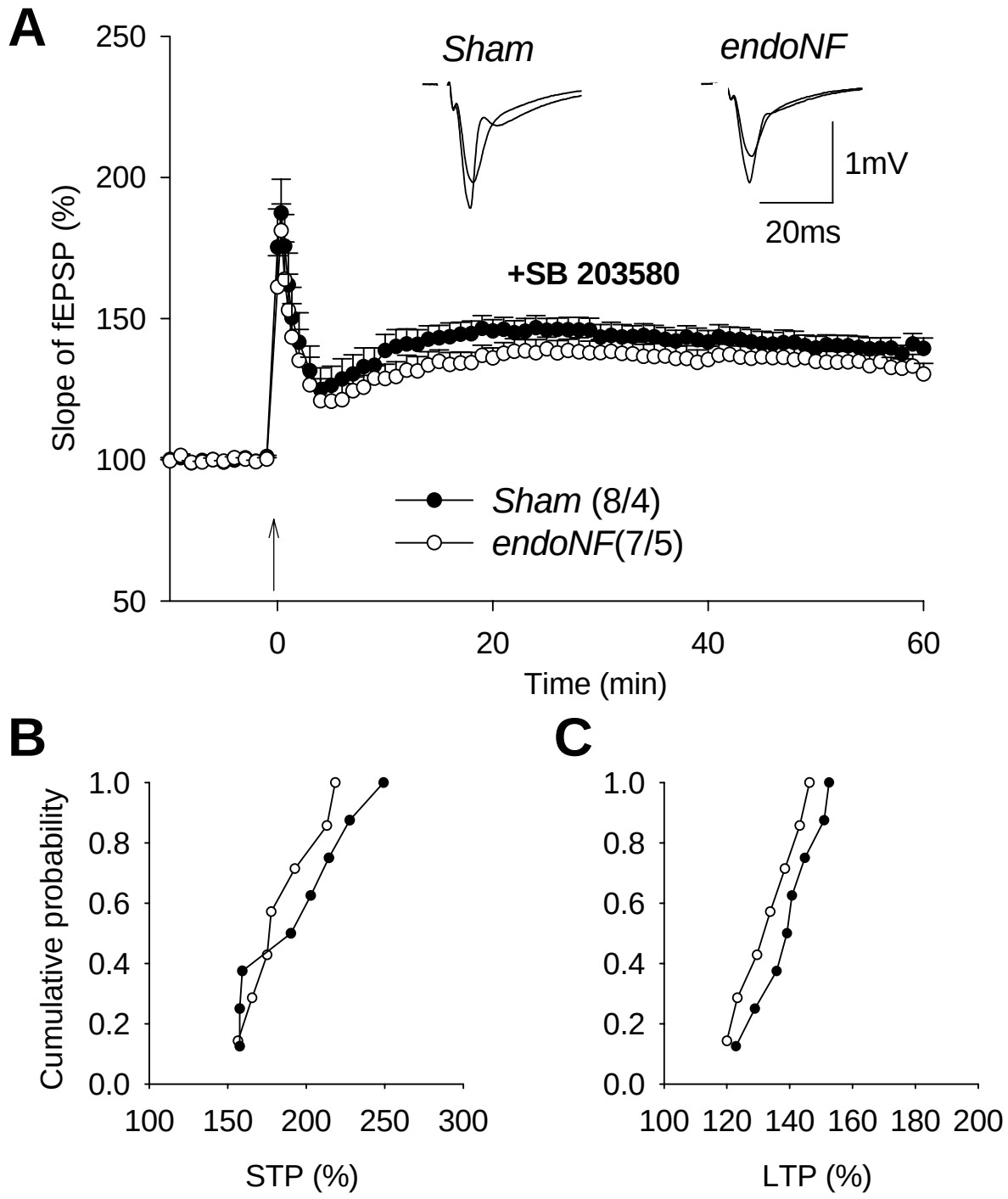

Figure 31. Restoration of LTP in endoNF-treated slices by application of p38 MAPK inhibitor SB 203580. *(A) Profile of TBS-induced short- and long-term potentiation in the presence of SB 203580**.** Note that LTP in active endoNF treated slices was restored by application of 10μM SB 203580. Traces on the top provide fEPSPs (average of 30 sweeps) collected before and 50-60 min after TBS administration. The mean slope of fEPSPs recorded 10 min before TBS is taken as 100% and arrow indicates delivery of TBS. Data represent mean + SEM, numbers of tested slices and mice are indicated in parentheses. (B-C) Cumulative plots representing levels of STP measured 1 min after TBS (B) and levels of LTP measured 50-60 min after TBS (C). Each symbol represents a single experiment. Cumulative probability at any given value x is the probability to observe potentiation less or equal to x. No significant difference between sham and endoNF treated slices was found for STP and LTP in this series of experiments.*

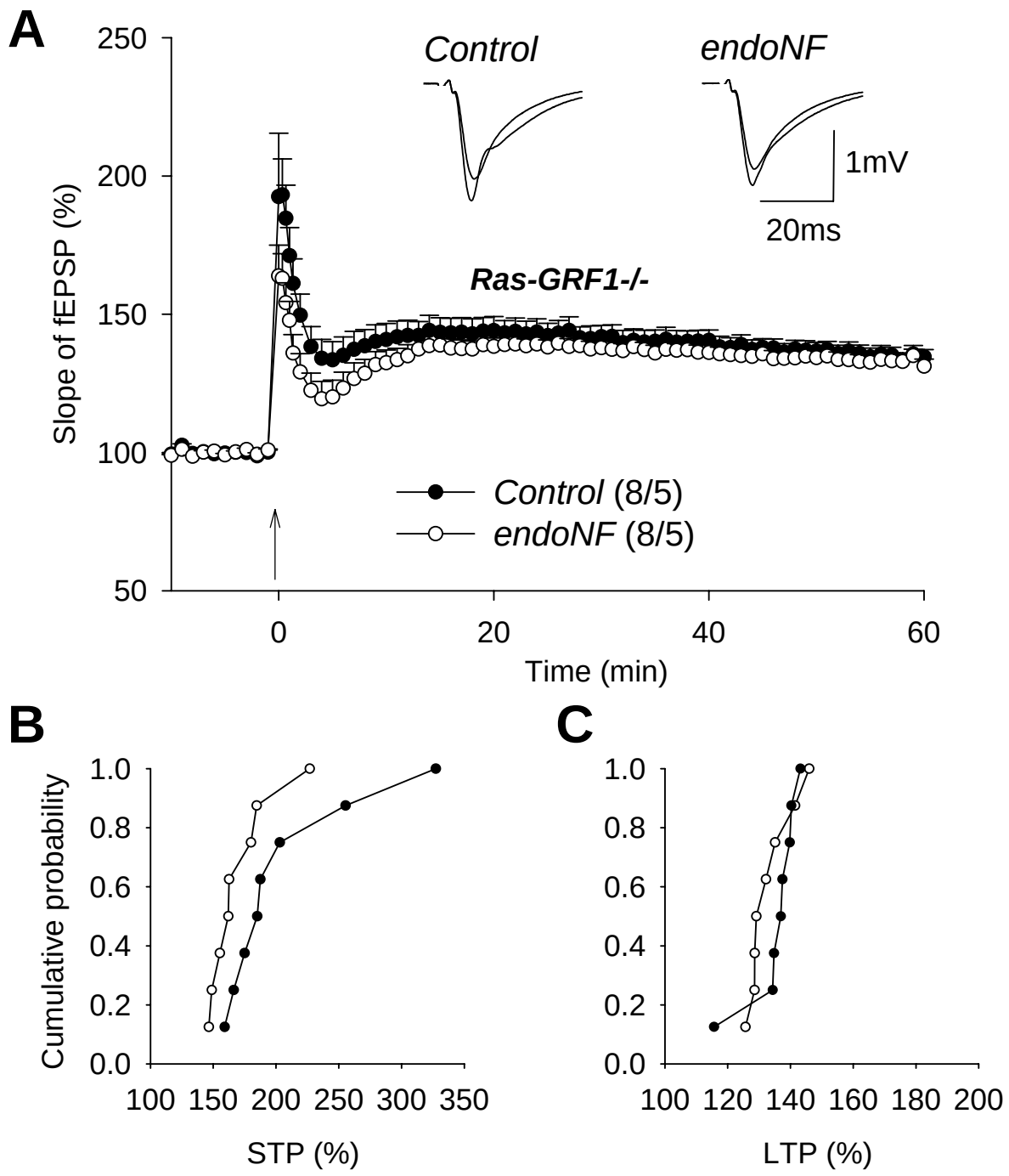

Figure 32. LTP is normal in endoNF-treated slices from Ras-GRF1-/- mice. *(A) Profiles of TBS-induced short- and long-term potentiation in Ras-GRF1-/- mice. Note that endoNF treatment does not affect LTP in this mutant. Traces on the top provide fEPSPs (average of 30 sweeps) collected before and 50-60 min after TBS administration. The mean slope of fEPSPs recorded 10 min before TBS is taken as 100% and arrow indicates delivery of TBS. Data represent mean + SEM, numbers of tested slices and mice are indicated in parentheses. (B-C) Cumulative plots representing levels of STP measured 1 min after TBS (B) and levels of LTP measured 50-60 min after TBS (C). Each symbol represents a single experiment. Cumulative probability at any given value x is the probability to observe potentiation less or equal to x. No significant difference between sham and endoNF treatment were found for STP and LTP in slices from Ras-GRF1-/- mice.*

7. Age-dependent role of NCAM in long-term synaptic plasticity.

Recent data show that LTP signaling in the CA1 subfield of the hippocampus of post-pubescent mice is mediated by Ras-GRF but in pre-pubescent mice it is Ras-GRF independent (Li et al., 2006). Since we found that PSA-NCAM restrains signaling via Ras-GRF1, we examined whether the role of NCAM in synaptic plasticity could be age-dependent. First, we investigated the role of NCAM in synaptic plasticity in 2.5 weeks old mice. Theta-burst stimulation induced a robust LTP in slices from NCAM+/+ (144.2±7.1%) as well as NCAM-/- (142.7±5.9%) mice (Figure 33A,C; Figure 40A). Maximal potentiation during 1 minute after TBS was also equal between two genotypes: 221.2±9.5% and 218.7±9.6% for NCAM+/+ and NCAM-/- mice, respectively (Figure 33A,B). These findings indicate that in contrast to adult animals, 2.5-week-old NCAM-/- mice are normal in terms of synaptic plasticity. To investigate if ablation of NCAM has further age-related effects, we recorded LTP in 12 and 24-month-old NCAM+/+ and NCAM-/- mice. TBS induced a robust LTP in 12-month-old NCAM+/+ mice (144.4±3.6%), whereas the level of LTP in 12-month-old NCAM-/- mice was drastically impaired in comparison to wild-type littermates (115.9±3.1%). This level was significantly lower than the LTP level recorded in 2.5-month-old NCAM-/- mice (Figure 34A,C; Figure 40A). STP following TBS was also significantly lower in 12-month-old NCAM-/- mice (178.7±7.8%) than in NCAM+/+ mice (219.8±8.6) (Figure 34A,B). Further we asked if we can rescue impaired STP and LTP in 12-month-old NCAM-/- mice using NMDAR-modulators as we did in 2.5-month-old NCAM-/- mice. Indeed, stimulation of NR2A-NMDARs with NMDAR agonist DCS and blockade of NR2B-NMDARs with Ro 25 rescued impaired phenotype seen in 12-month-old NCAM-/- mice. Administration of DCS restored levels of STP and LTP in NCAM-/- from 178±7.8% (STP) and 115.9±3.1% (LTP) to 233.6±15.6% and 137.1±2.1%, respectively, being not significantly different from the levels in NCAM+/+ mice (STP of 260.2±26.3% and LTP of 144.7±7.1%) (Figure 35, 40B). Administration of Ro 25 restored the level of STP in NCAM-/- (216.8±5.0%) to the similar level as seen for NCAM+/+ mice (200.7±12.7%) (Figure 36A,B). The level of LTP was only partially restored (129.6±3.1%) by Ro 25 treatment in NCAM-/-, that was still significantly lower than seen in NCAM+/+ mice (139.1±2.2) (Figure 36A,C; Figure 40C). Similarly, the application of p38 MAPK inhibitor SB203580 to slices from NCAM-/- restored the levels of STP completely (216.8±9.6%) (Figure 37A,B), whereas LTP was only partially increased (129.7±2.8%) (Figure 37A,C. Figure 40D) but remained lower than in NCAM+/+ littermates (137.9±1.6%).

RESULTS

Further we studied 24-month-old age NCAM-/- mice. LTP induced by TBS in 24-month-old NCAM+/+ mice (132.7±3.6%) was significantly lower than in all younger age groups of NCAM+/+ mice analyzed (Figure 38A,C; Figure 40A), whereas STP was normal (208.5±9.1%) (Figure 38A,B). Age-dependent reduction of LTP in 24-mounth-old NCAM+/+ mice was well compensated by NMDAR agonist DCS treatment, which rescued LTP to the level seen in younger animals (144.3±3.7) (Figure 39; Figure 40B). Similar effect was seen in 23- to 27-month-old rats (Billard and Rouaud, 2007). Interestingly the level of STP and LTP in 24-month-old NCAM-/- mice was further reduced (167.6±13.1% and 109.5±2.9% respectively, Figure 38; Figure40A), indicating a strong NCAM-related age dependent deficit. DCS was able to rescue STP in 24-month-old NCAM-/- mice completely (215.0±22.4) (Figure 39A,B) i.e. to the level of their age-matched treated wild-type controls (237.6±11.5%), whereas LTP was only partially recovered (from 109.5±2.9% to 126.8±3.7%) (Figure 39A,C; Figure 40B).

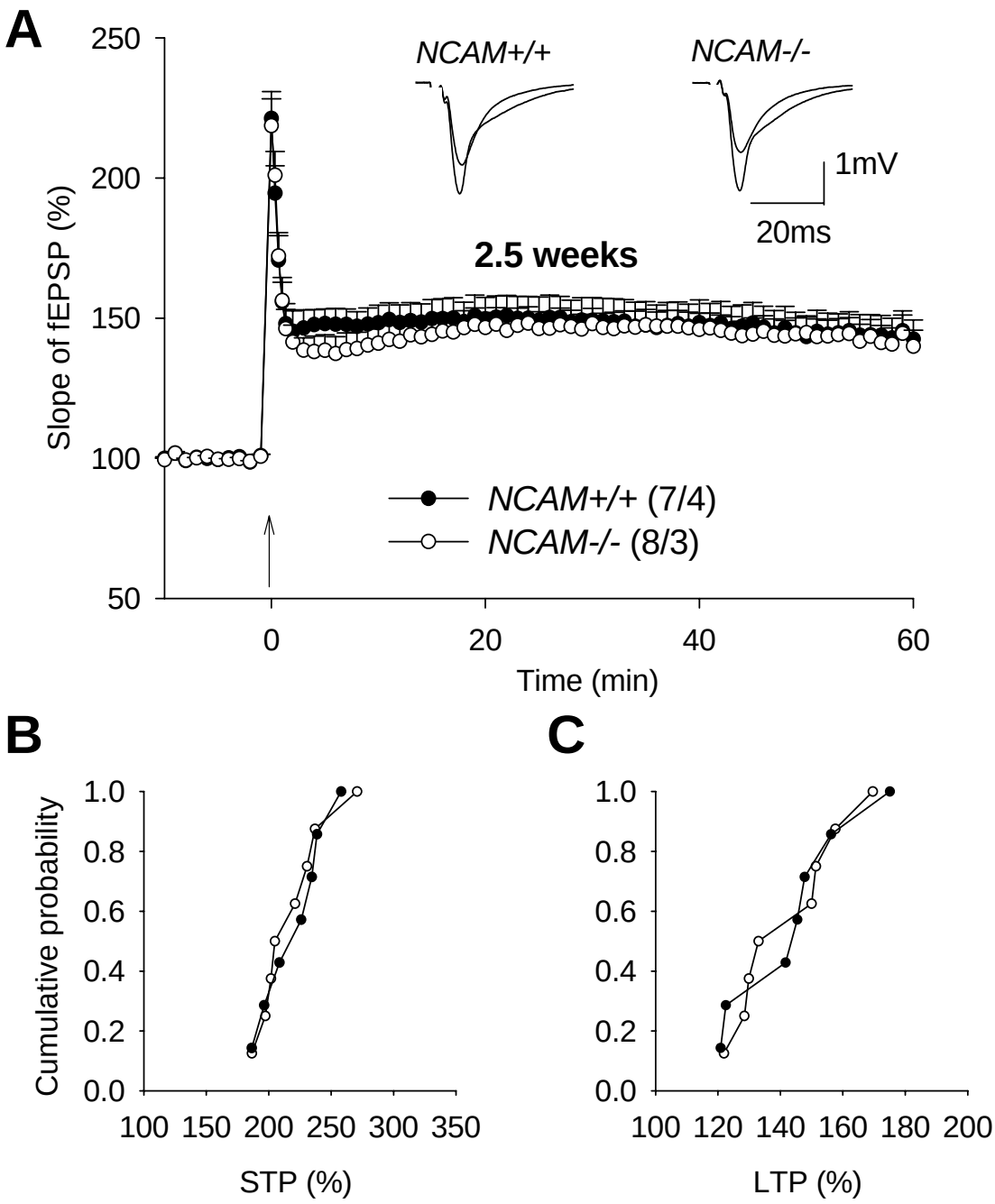

Figure 33. The level of LTP is normal in slices from 2.5-week-old NCAM-/- mice. *(A) Profiles of TBS-induced short- and long-term potentiation, which show that TBS elicited a robust CA1 LTP in 2.5-week old NCAM+/+ and NCAM-/- mice. Traces on the top provide fEPSPs (average of 30 sweeps) collected before and 50-60 min after TBS administration. The mean slope of fEPSPs recorded 10 min before TBS is taken as 100% and arrow indicates delivery of TBS. Data represent mean + SEM, numbers of tested slices and mice are indicated in parentheses. (B-C)Cumulative plots representing levels of STP measured 1 min after TBS (B) and levels of LTP measured 50-60 min after TBS (C). Each symbol represents a single experiment. Cumulative probability at any given value x is the probability to observe potentiation less or equal to x. No significant difference between genotypes was found for STP and LTP in this series of experiments.*

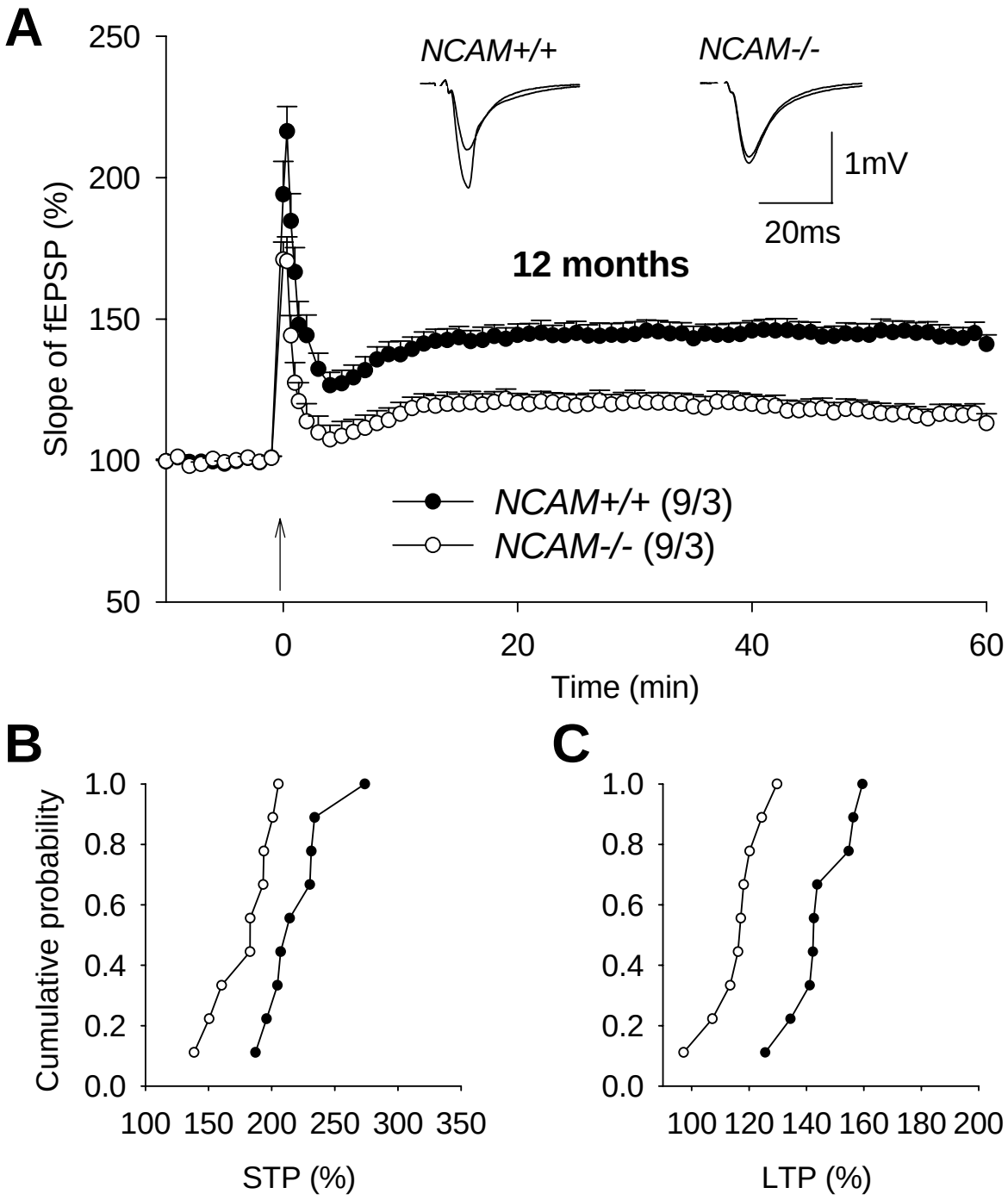

Figure 34. LTP is impaired in 12-month-old NCAM-/- mice. *(A) Profiles of TBS-induced short- and long-term potentiation show that both STP and LTP are impaired in NCAM-/- mice. Traces on the top provide fEPSPs (average of 30 sweeps) collected before and 50-60 min after TBS administration. The mean slope of fEPSPs recorded 10 min before TBS is taken as 100% and arrow indicates delivery of TBS. Data represent mean + SEM, numbers of tested slices and mice are indicated in parentheses. (B-C) Cumulative plots representing levels of STP measured 1 min after TBS (B) and levels of LTP measured 50-60 min after TBS (C). Each symbol represents a single experiment. Cumulative probability at any given value x is the probability to observe potentiation less or equal to x.*

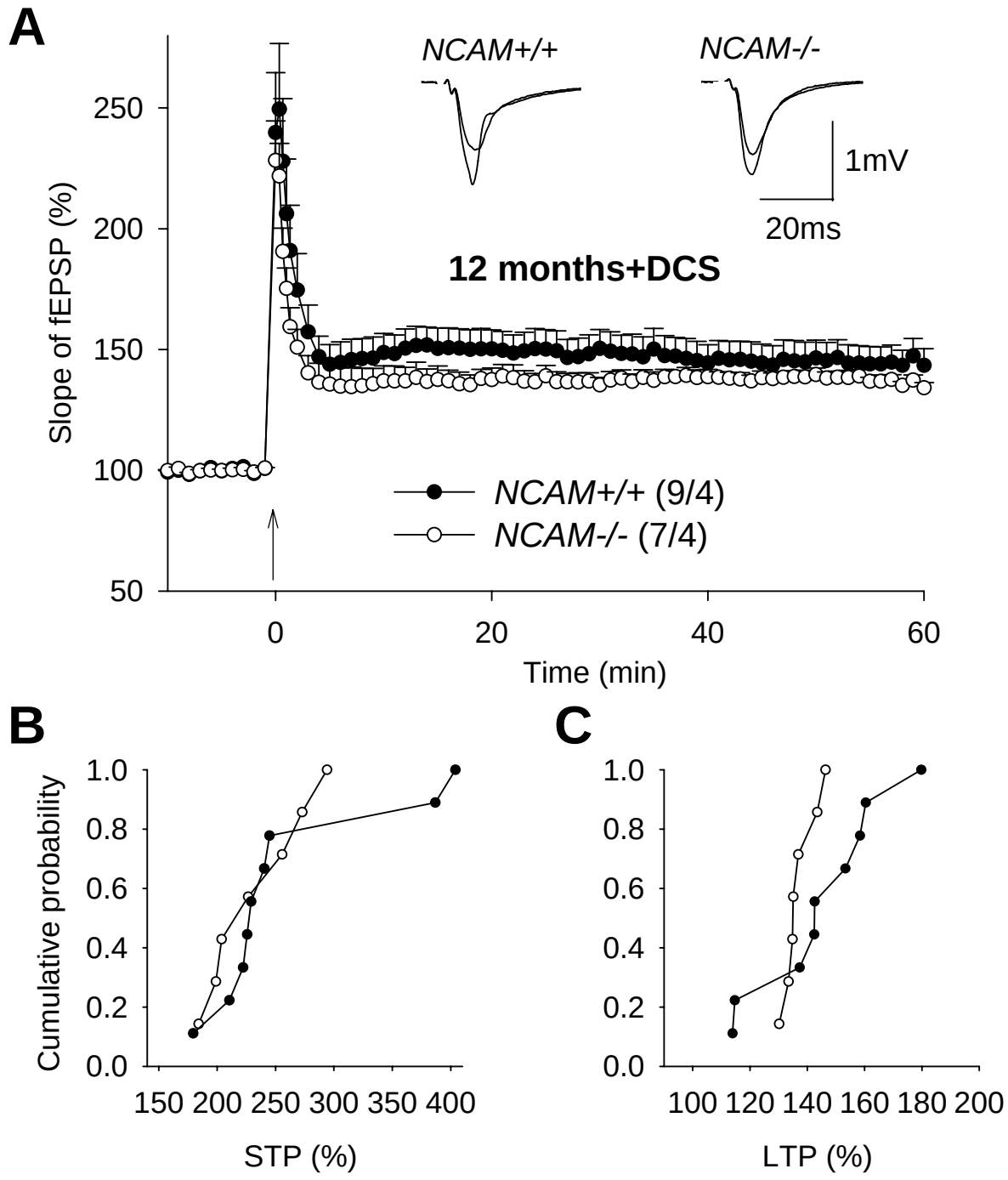

Figure 35. Restoration of impaired LTP in 12-month-old NCAM-/- mice via modulation of NMDA receptors by application of the NMDA receptor agonist D-cycloserine (DCS). *(A) Profiles of TBS-induced short- and long-term potentiation in the presence of DCS (40μM). Note that both STP and LTP are improved in NCAM-/- mice to the levels seen in NCAM+/+ mice. Traces on the top provide fEPSPs (average of 30 sweeps) collected before and 50-60 min after TBS administration. The mean slope of fEPSPs recorded 10 min before TBS is taken as 100% and arrow indicates delivery of TBS. Data represent mean + SEM, numbers of tested slices and mice are indicated in parentheses. (B-C) Cumulative plots representing levels of STP measured 1 min after TBS (B) and levels of LTP measured 50-60 min after TBS (C). Each symbol represents a single experiment. Cumulative probability at any given value x is the probability to observe potentiation less or equal to x.*

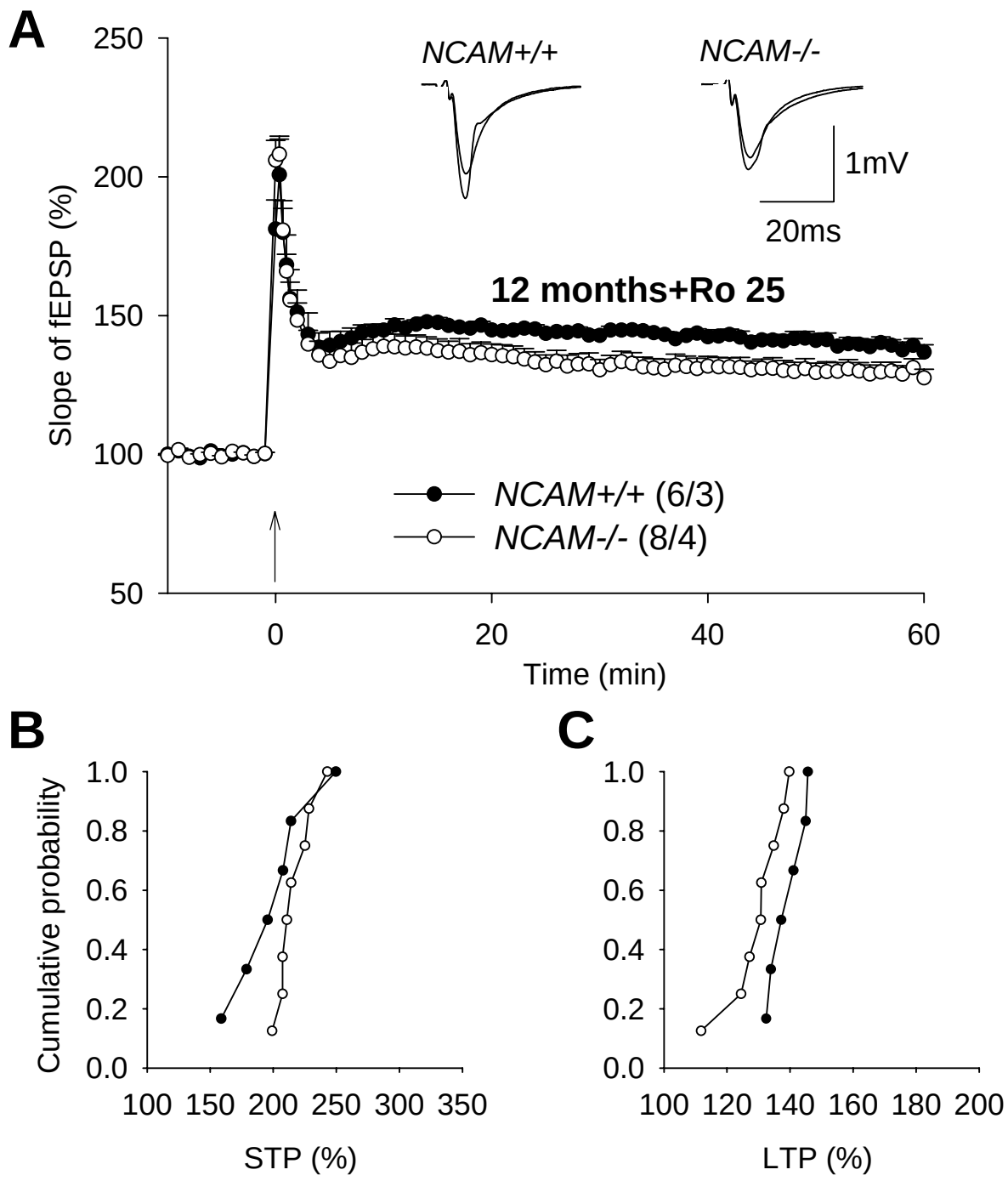

Figure 36. Partial restoration of impaired LTP in 12-month-old NCAM-/- mice via modulation of NMDA receptors by application of the NR2B-NMDA receptor selective antagonist Ro 25-6981 (Ro 25). *(A) Profiles of TBS-induced short- and long-term potentiation in the presence of 0.5μM Ro 25. Traces on the top provide fEPSPs (average of 30 sweeps) collected before and 50-60 min after TBS administration. The mean slope of fEPSPs recorded 10 min before TBS is taken as 100% and arrow indicates delivery of TBS. Data represent mean + SEM, numbers of tested slices and mice are indicated in parentheses. (B-C) Cumulative plots representing levels of STP measured 1 min after TBS (B) and levels of LTP measured 50-60 min after TBS (C). Each symbol represents a single experiment. Cumulative probability at any given value x is the probability to observe potentiation less or equal to x. No significant difference between genotypes was found for STP, but LTP was lower in slices from NCAM-/- mice in this series of experiments.*

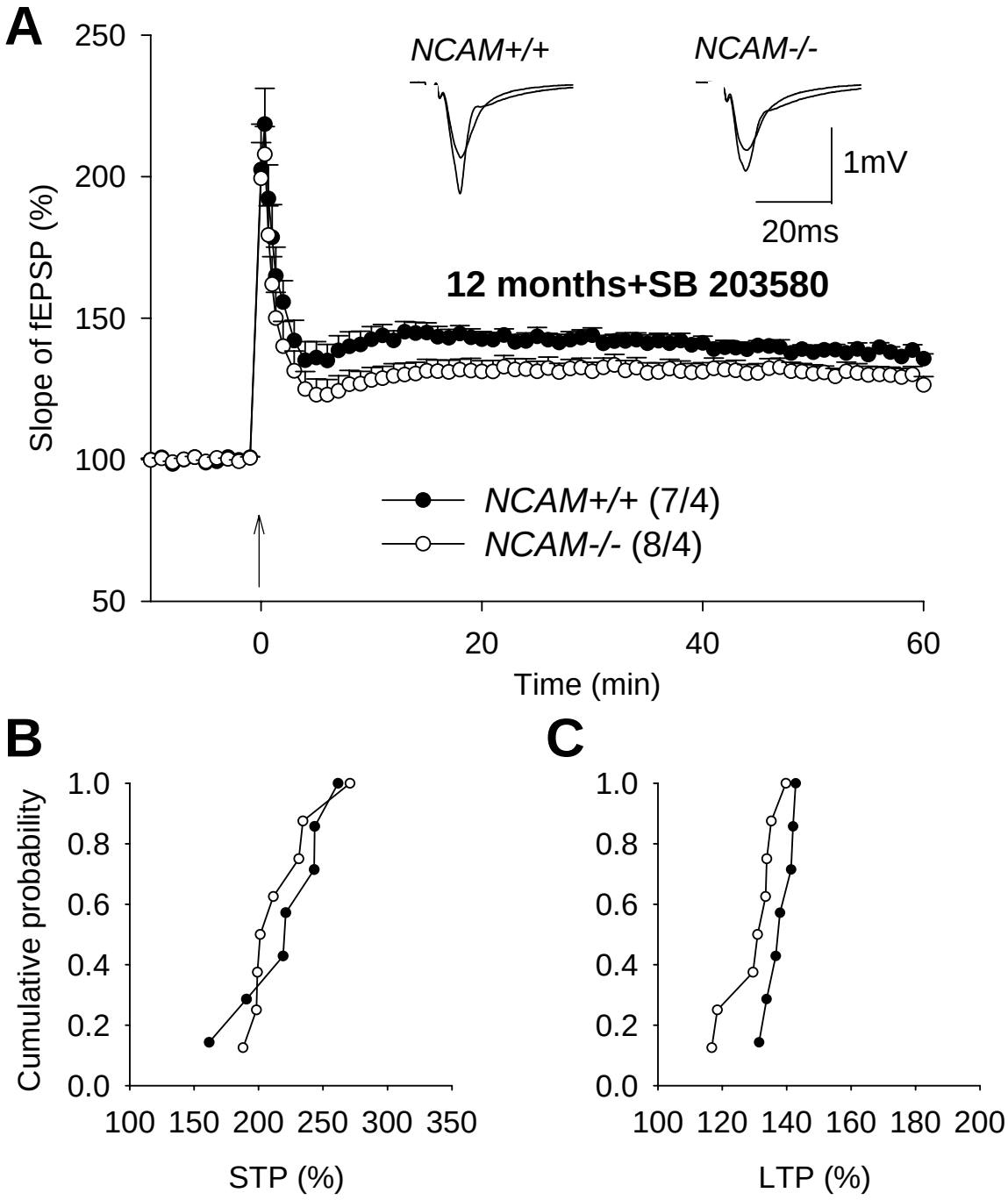

Figure 37. Partial restoration of impaired LTP in 12-month-old NCAM-/- mice by application of the p38 MAPK inhibitor SB 203580. *(A) Profiles of TBS-induced short- and long-term potentiation in 12-month-old NCAM-/- mice in the presence of 10μM SB 203580. Traces on the top provide fEPSPs (average of 30 sweeps) collected before and 50-60 min after TBS administration. The mean slope of fEPSPs recorded 10 min before TBS is taken as 100% and arrow indicates delivery of TBS. Data represent mean + SEM, numbers of tested slices and mice are indicated in parentheses. (B-C) Cumulative plots representing levels of STP measured 1 min after TBS (B) and levels of LTP measured 50-60 min after TBS (C). Each symbol represents a single experiment. Cumulative probability at any given value x is the probability to observe potentiation less or equal to x. No significant difference between genotypes was found for STP, but LTP was lower in slices from NCAM-/- mice in this series of experiments.*

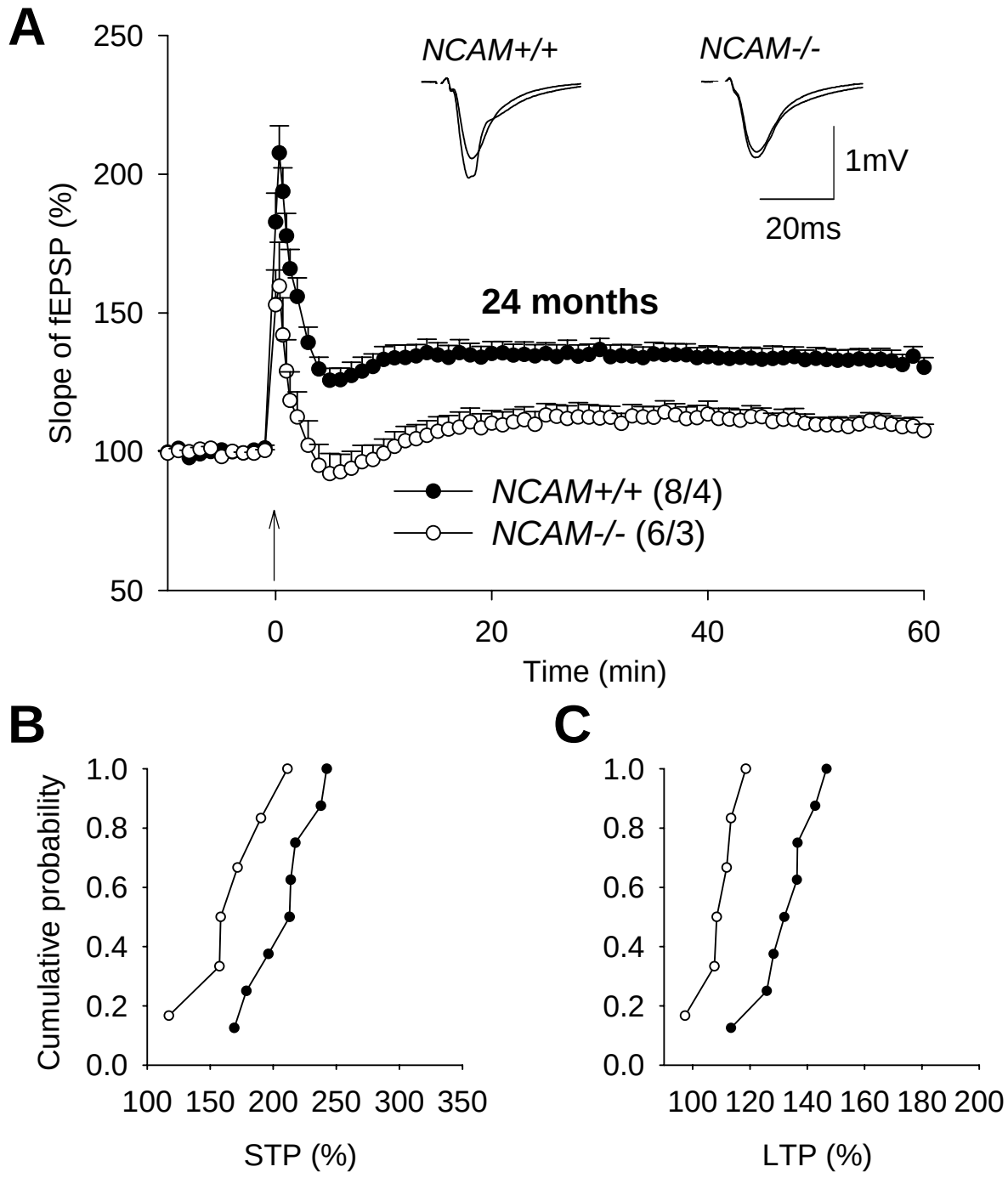

Figure 38. Impaired LTP in slices from 24-month-old NCAM+/+ and NCAM-/- mice. *(A) Profiles of TBS-induced short- and long-term potentiation, which show that STP and LTP are drastically impaired in NCAM-/- mice. Traces on the top provide fEPSPs (average of 30 sweeps) collected before and 50-60 min after TBS administration. The mean slope of fEPSPs recorded 10 min before TBS is taken as 100% and arrow indicates delivery of TBS. Data represent mean + SEM, numbers of tested slices and mice are indicated in parentheses. (B-C) Cumulative plots representing levels of STP measured 1 min after TBS (B) and levels of LTP measured 50-60 min after TBS (C). Each symbol represents a single experiment. Cumulative probability at any given value x is the probability to observe potentiation less or equal to x. Both LTP and STP levels are lower in NCAM-/- than in NCAM+/+ mice.*

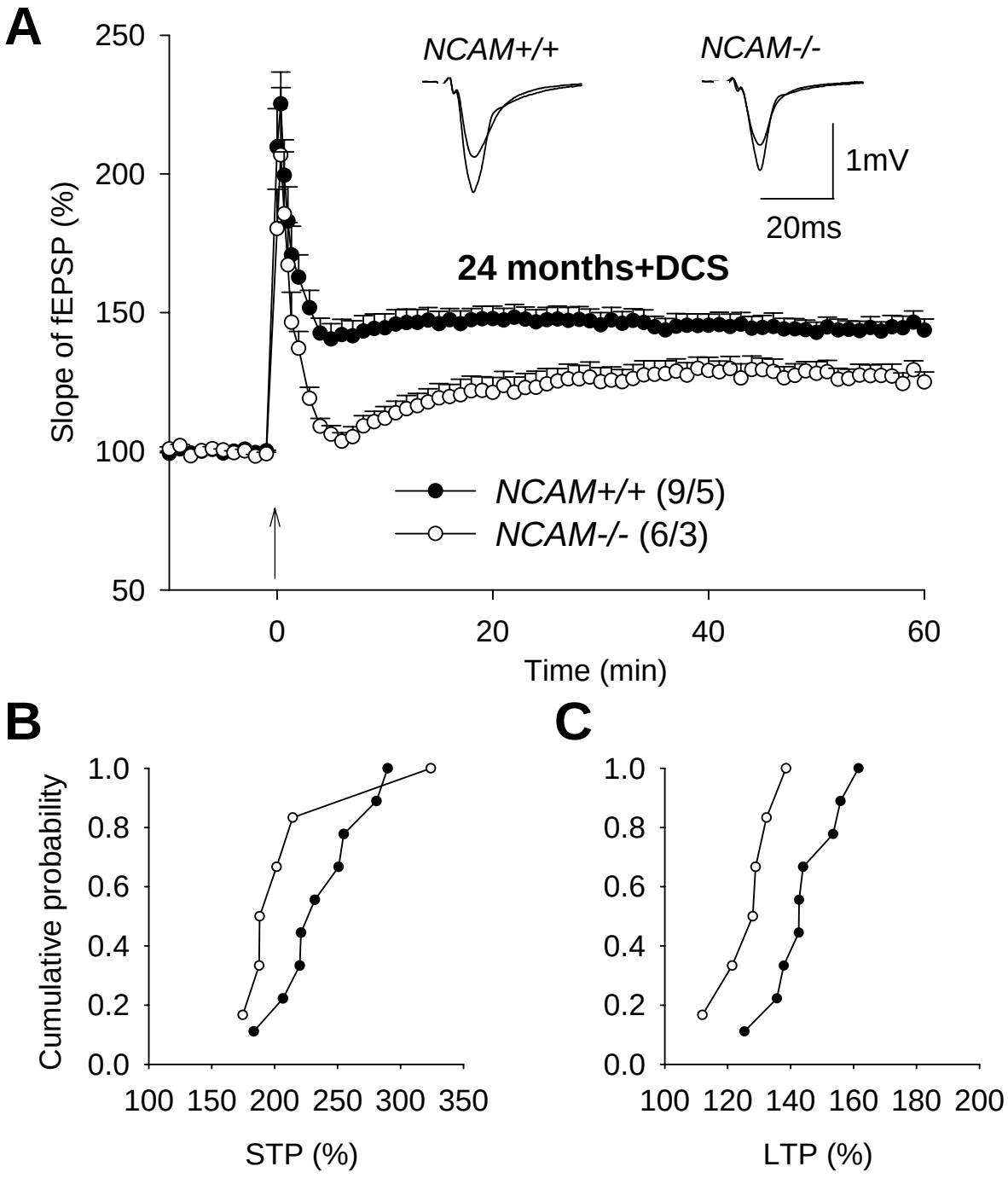

Figure 39. Slight improvement of impaired LTP in 24-month-old NCAM-/- mice via modulation of NMDA receptors by application of the NMDA receptor agonist D-cycloserine (DCS)*. (A) Profiles of TBS-induced short- and long-term potentiation, which show normal LTP in 24-month-old NCAM+/+ and partially restored LTP in slices from 24-month-old NCAM-/- mice in the presence of 40μM DCS. Traces on the top provide fEPSPs (average of 30 sweeps) collected before and 50-60 min after TBS administration. The mean slope of fEPSPs recorded 10 min before TBS is taken as 100% and arrow indicates delivery of TBS. Data represent mean + SEM, numbers of tested slices and mice are indicated in parentheses. (B-C) Cumulative plots representing levels of STP measured 1 min after TBS (B) and levels of LTP measured 50-60 min after TBS (C). Each symbol represents a single experiment. Cumulative probability at any given value x is the probability to observe potentiation less or equal to x. No significant difference between genotypes was found for STP, but LTP was lower in slices from NCAM-/- mice in this series of experiments.*

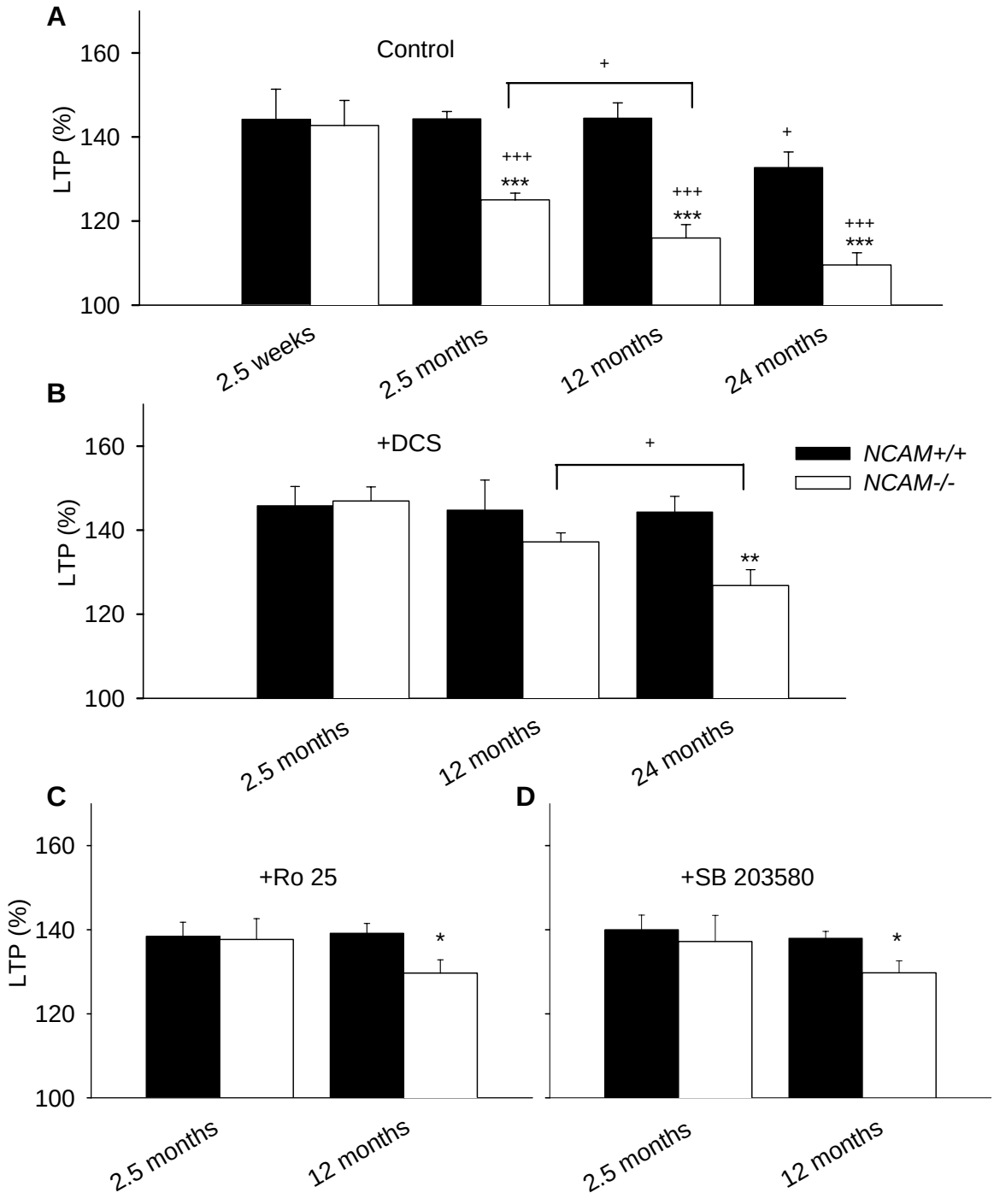

Figure 40. Age-dependent deficit of LTP in NCAM-deficient mice. *Statistical summary bars show mean values + SEM of the LTP levels recorded in slices from NCAM+/+ and NCAM-/- mice 50-60 minutes after TBS stimulation. (A) From left to the right; TBS elicited a robust LTP in 2.5-week-old NCAM+/+ and NCAM-/- mice. The level of LTP does not decline in 2.5- and 12-month-old MCAM+/+ but is significantly lower in slices from 24-month-old NCAM+/+ mice, whereas the level of LTP in NCAM-/- mice progressively declines in 2.5-, 12- and 24-month-old NCAM-/- mice. (B) The graph shows that the LTP levels are completely recovered by the administration of the NMDAR agonist DCS (40μM)*

*in 24-month-old NCAM+/+ mice, and in 2.5- and 12-month-old NCAM-/- mice. However, DCS could not fully rescue LTP in slices form 24-month-old NCAM-/- mice. (C) LTP levels fully recover to the level of NCAM+/+ mice by application of Ro 25 (0.5μM) in slices from 2.5- month-old NCAM-/- mice, while there is only partial improvement in LTP in 12-month-old NCAM-/- mice. (D) LTP is fully rescued to the level of NCAM+/+ mice in the presence of SB 203580 (10μM) in slices from 2.5-month-old NCAM-/- mice, whereas in 12-month-old NCAM-/- mice this treatment leads only to partial restoration of LTP. *p<0.05, **p<0.01, ***p<0.001, significant difference between NCAM+/+ and NCAM-/- mice treated in the same way; +p<0.05, +++p<0.001, significant difference between untreated control and pharmacologically treated slices from mice of the same genotype, t-test.*

VIII. Discussion

In the present study we investigated mechanisms by which PSA-NCAM regulates synaptic plasticity. Despite that the basal synaptic transmission, paired-pulse facilitation and short-term potentiation (Figures 9,10) were normal in NCAM-/- mice, the levels of long-term potentiation and depression were significantly lower in NCAM-/- mice as compared to NCAM+/+ littermates (Figures 42A,23E), showing a specificity of abnormalities in long-term synaptic plasticity in the mutant. Furthermore, the present study suggests that NCAM is involved in regulating the balance in signaling between two major subtypes of NMDARs, since a deficiency in NCAM increases the NR2B subunit-mediated transmission at the expense of the NR2A subunit-mediated one. Our working model linking disbalance of NMDAR mediated signaling in NCAM-/- mice to a reduction in LTP is shown in Figure 41.

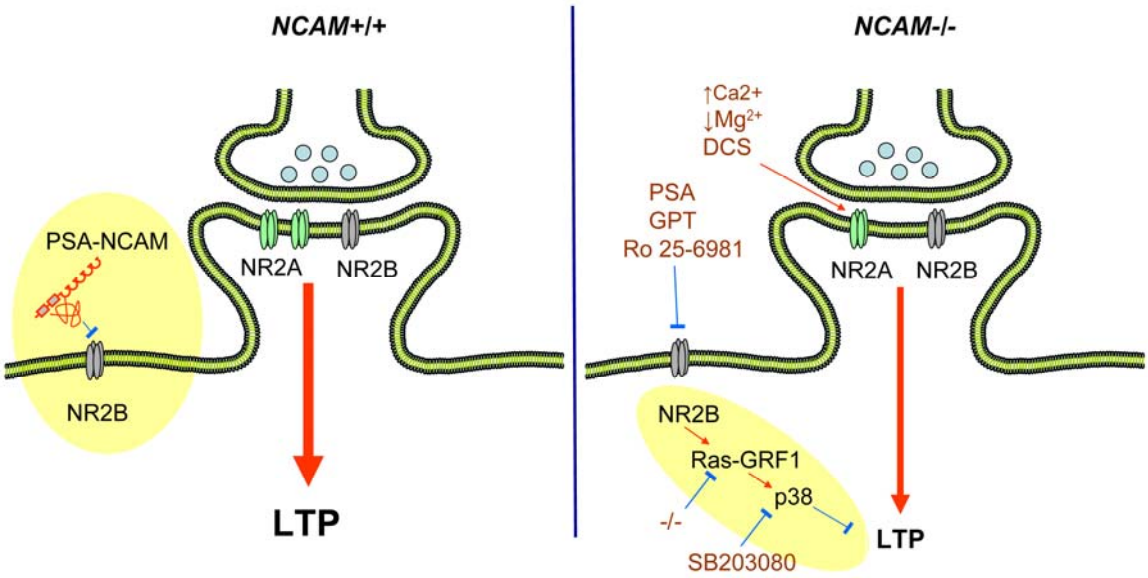

Figure 41. Model for PSA-NCAM mediated modulation of signaling via NMDA receptors. *Endogenous and exogenous molecules are shown in black and brown, respectively. Stimulatory and inhibitory relationships are shown in red and blue, respectively. In NCAM+/+ mice, PSA-NCAM inhibits extrasynaptic NR2B-NMDARs. In NCAM-/- mice, enhanced signaling occurs via extrasynaptic NR2B-NMDARs and reduced signaling via NR2A-NMDARs. This model is supported by data from experiments with increasing Ca2+ and decreasing Mg2+ extracellular concentrations, or application of DCS, Ro 25-6981, GPT, PSA, or SB203580, which change the balance in signaling via NR2A- and NR2B-mediated pathways in favor of the NR2A-mediated pathway, which restores LTP in NCAM-/- mice. Similarly, LTP is restored in endoNF-treated slices from NCAM+/+ mice by DCS, Ro 25-6981 and SB 203580 and by genetic ablation of Ras-GRF1.*

DISCUSSION

Briefly, in wild-type animals, NCAM-associated PSA inhibits activation of extrasynaptic NR2B-NMDARs at low concentrations of glutamate, presumably via a competition with glutamate for the ligand binding site (Hammond et al., 2006). As such, signaling via synaptic NMDARs predominantly contributes to the induction of LTP. In the absence of NCAM or PSA, extrasynaptic NR2B-NMDARs become more active resulting in activation of p38 MAPK, which together with reduced signaling via NR2A-NMDARs impairs LTP. Thus, in addition to the well recognized anti-adhesive property of PSA, being critically important for modulation of cell interactions during development (Rutishauser, 2008), PSA regulates synaptic plasticity in adults via modulation of a specific subset of glutamate receptors, rather than the L-type Ca^{2+} channels or FGF receptors.

The reduction in synaptic NR2A-mediated signaling during induction of LTP in NCAM-/- mice is in agreement with the following data: (1) The NVP-sensitive component of LTP is smaller in NCAM-/- mice than in NCAM+/+ mice (Figure 42A). (2) In adult wild-type mice, NR2A-NMDARs are the predominant NMDARs (Figure 12) at the postsynaptic density (Petralia et al., 2005), where they are major contributors to the induction of LTP at CA3-CA1 synapses (Kohr et al., 2003; Li et al., 2006; Liu et al., 2004). In young animals and at other synapses, however, there may be a substantial contribution of NR2B-NMDARs in LTP (Kohr et al., 2003; Zhao et al., 2005). (3) Expression of NMDARs in the synaptosomal fraction and the number of immunogold labeled NMDARs at the postsynaptic density are reduced in NCAM-/- versus NCAM+/+ mice (Sytnyk et al., 2006). (4) Facilitation of NR2A-NMDARs by DCS restores levels of LTP in NCAM/PSA deficient slices to levels seen in slices from wild-type mice (Figure 42A,B). NVP also fully abolishes the potentiating effects of DCS on LTP in NCAM-/- mice (Figure 42A). Also, the data showing restoration of LTP in NCAM/PSA deficient slices by BDNF (Muller et al., 2000) are consistent with our findings, since BDNF may facilitate the activity of molecules downstream of Ca^{2+} entry via synaptic NMDARs, such as CaMKII (Liu et al., 1999). Facilitation of NMDARs via a relief of the Mg^{2+} block of these receptors restores levels of LTP in NCAM deficient slices to levels seen in slices from wild-type mice (Figure 42A).

The increase in extrasynaptic NR2B-mediated signaling in NCAM/PSA deficient slices is supported by numerous observations: (1) PSA suppresses opening of native ifenprodil/Ro 25-6981-sensitive NMDARs by low concentrations of glutamate (Hammond et al., 2006). (2) The NVP-insensitive component is larger in hippocampal slices of NCAM-/- mice than in NCAM+/+ mice (Figure 12). (3) PSA more strongly inhibits NR2B-NMDAR mediated responses in NCAM-/- mice (Figure 13). (4) Removal of PSA increases

Ca^{2+} transients mediated by NR2B-NMDARs in the aspiny part of dendrites (Figure 14). (5) Mice deficient in the glial glutamate transporter GLT-1 have an increased extracellular concentration of glutamate and impaired LTP (Katagiri et al., 2001). (6) Inhibition of NR2B-NMDARs with Ro 25-6981 restores levels of LTP in NCAM or PSA deficient slices to the levels seen in slices from wild-type mice (Figure 42A,B). (7) Reduction of extrasynaptic glutamate concentrations by the glutamate scavenger GTP restores LTP in NCAM-/- mice (Figure 42A). (8) A substantial fraction of NR2B-NMDARs is located extrasynaptically in the adult hippocampus (reviewed by Kohr, 2006). (9) The synaptic pool of NMDARs activates the extracellular signal-regulated kinases, whereas the extrasynaptic pool triggers a signaling pathway that results in the inactivation of this pathway (Ivanov et al., 2006). The suppressive effect of extrasynaptic NR2B receptors on synaptic potentiation thus may be important for maintaining input specificity of synaptic modifications recruited during learning.

Our data in endoNF treated slices replicate results from the experiments in NCAM-/- mice and demonstrate that impaired LTP in either NCAM- or PSA-deficient slices is due to improper signaling via NMDARs. Modulation of NMDARs with DCS (Figure 42B) or blockade of NR2B-NMDARs with Ro 25-6981 (Figure 42B) increased levels of LTP in endoNF-treated slices to the wild-type levels.

The following data support the view that the mechanisms downstream of extrasynaptic NR2B-NMDARs in NCAM/PSA deficient slices involve signaling via Ras-GRF1 to the Rac effector p38 MAPK: (1) The level of phosphorylated p38 MAPK is upregulated in NCAM deficient mice (Figure 29). (2) An inhibitor of p38 restores levels of LTP in PSA or NCAM-deficient slices to those seen in wild-type mice (Figure 42C,D). (3) Ras-GRF1 is shown to mediate synaptic depression through p38 MAPK (Li et al., 2006). (4) PSA deficiency does not lead to impaired LTP in *Ras-GRF1-/-* mice (Figure 42D).

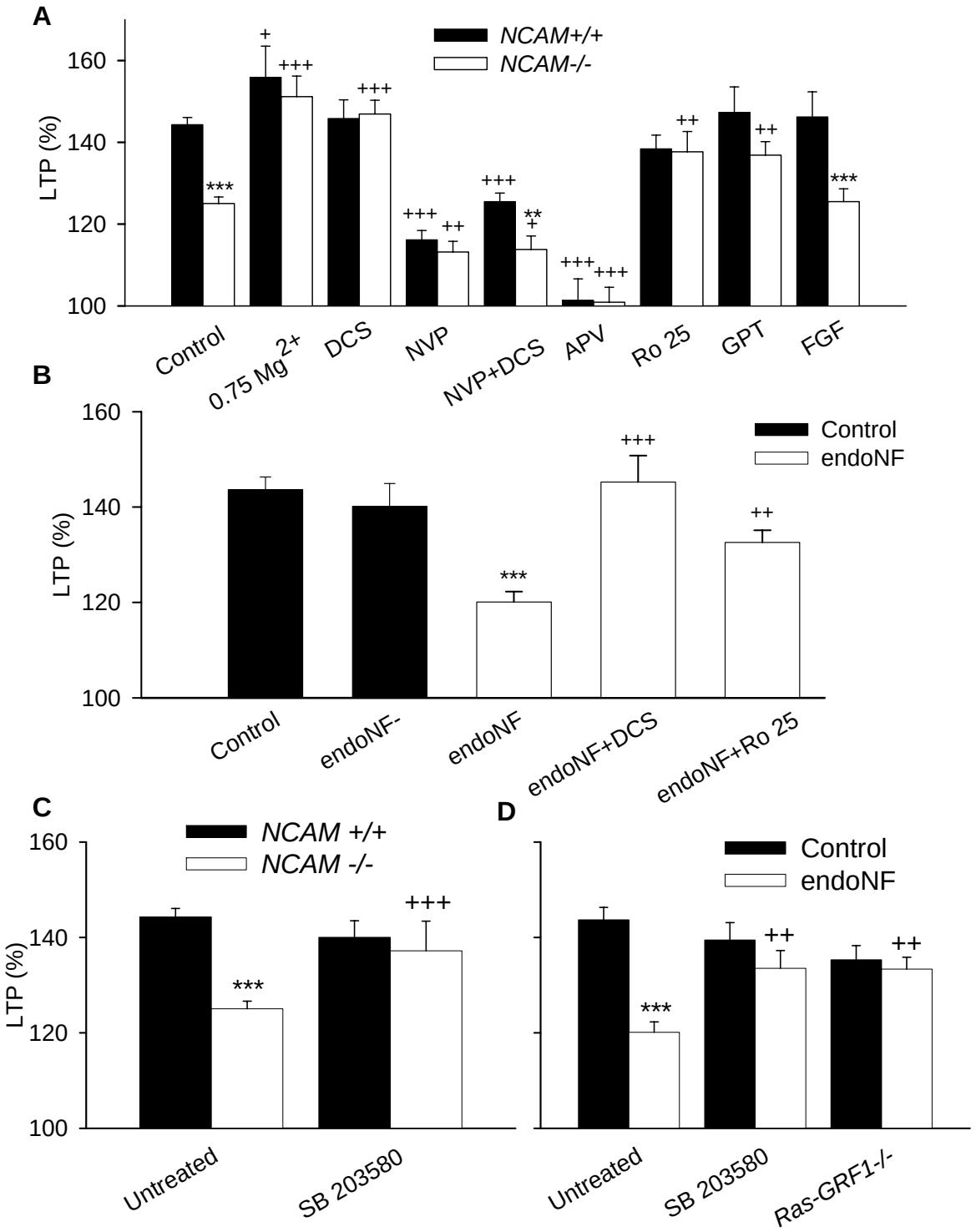

Figure 42. Summary graph showing restoration of impaired LTP in NCAM-/- and endoNF-treated hippocampal slices via modulation of NMDA receptors and downstream signaling cascades. *(A) Mean + SEM of LTP levels in slices from NCAM+/+ and NCAM-/- mice, recorded 50-60 min after TBS in the presence of NMDAR modulators. The graph shows that LTP is impaired in slices from NCAM-/- mice. TBS induces equal LTP in NCAM-/- and NCAM+/+ mice in presence of decreased concentration of Mg^{2+} or in presence of NMDAR agonist DCS. LTP is reduced to the same levels in both genotypes by the NR2A-NMDAR antagonist NVP and by the NMDAR subtype unspecific antagonist APV. NVP also reduces LTP induced in the presence of DCS. The NR2B-NMDAR selective*

*antagonist Ro 25-6981 or glutamate scavenger glutamic pyruvate transaminase is also able to restore LTP in NCAM-/- slices. Application of fibroblast growth factor can not rescue impaired LTP in NCAM-/- mice. **p<0.01, ***p<0.001, significant difference between NCAM+/+ and NCAM-/- mice treated in the same way; +p<0.05, ++p<0.01, +++p<0.001, significant difference between untreated control and pharmacologically treated mice of the same genotype, t-test. (B) Mean + SEM of LTP levels in slices treated with endoNF recorded 50-60 min after TBS in the presence of NMDAR modulators. TBS induced robust LTP in wild type slices treated with sham or with inactive form of endoNF, whereas the level of LTP in slices treated with active endoNF was significantly lower. The NMDAR modulators DCS and Ro 25-6981 was able to restore impaired LTP in endoNF treated slices. ***p<0.001, significant difference between control and endoNF-treated slices, ++p<0.01, +++p<0.001, significant effects of DCS and Ro 25 on endoNF-treated slices, t-test. (C) Mean + SEM of LTP levels recorded 50-60 min after TBS in SB 203580 treated and untreated slices from NCAM+/+ and NCAM-/- mice. ***p<0.001, significant difference between slices from NCAM+/+ and NCAM-/- mice, +++p<0.001, significant effects of SB 203580, t-test. (D) Mean + SEM of LTP levels recorded 50-60 min after TBS in endoNF treated and control slices from wild-type and Ras-GRF1-/- mice. Slices from wild-type mice were either pharmacologically untreated or treated with SB 203580. ***p<0.001, significant difference between control and endoNF-treated slices. ++p<0.01, significant effects of Ras-GRF1 deficiency and SB 203580, t-test.*

Recently, activation of p38 MAPK signaling has also been shown to mediate impairment in LTP by the tumor necrosis factor α (Butler et al., 2004) and Aβ (Hsieh et al., 2006; Wang et al., 2004), a peptide generated from the amyloid precursor protein, which is widely believed to underlie the pathophysiology of Alzheimer's disease. Although p38 MAPK is thought to be involved in the removal of synaptic AMPA and NMDARs, the specific p38 substrates that mediate these effects in response to tumor necrosis factor α, Aβ, or activation of NMDARs remain to be identified. Among the many molecules signaling downstream of p38 are transcription factors, protein kinases and the small GPTase Rab5, which is essential for early endocytosis (Shi and Gaestel, 2002). An attractive hypothesis is that activation of p38 MAPK may accelerate glutamate receptor endocytosis by stimulating the formation of the guanyl nucleotide dissociation inhibitor-Rab5 complex (Huang et al., 2004) (Figure 43).

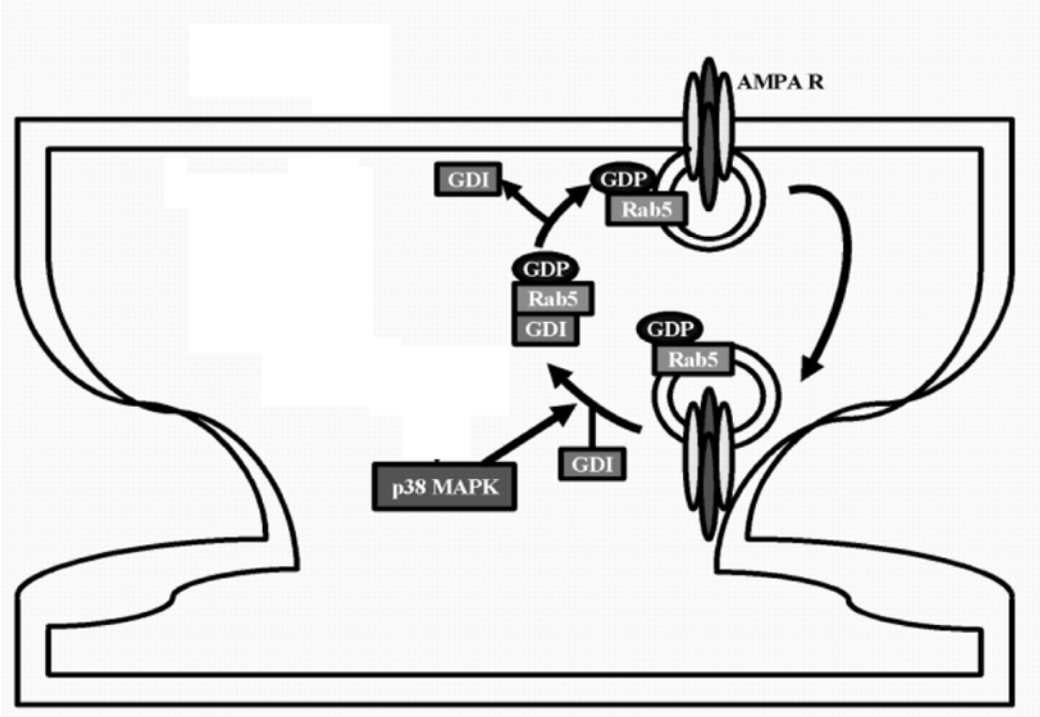

Figure 43. Hypothetical model showing possible mechanism mediated by the p38 MAPK signaling pathway. *Activated p38 MAPK facilitates the loss of surface AMPA receptor by stimulating the formation of the GDI-Rab5 complex, which has been identified as an important component of the machinery controlling endocytotic vesicle formation and limiting the recycling of receptor back to the plasma membrane (adapted from Huang et al., 2004).*

Our pharmacological analysis of LTD in wild-type mice supports the view that both NR2A- and NR2B-NMDARs are involved in the induction of LTD in the adult by low-frequency stimulation (Figure 23). The same conclusion was derived for induction of LTD in adult rats (Fox et al., 2006). However, in hippocampal slices from young rats NR2B-NMDARs are not required for the induction of LTD (Bartlett et al., 2007; Morishita et al., 2007). Impaired LTD in NCAM-/- mice is noteworthy, since an excess in signaling via extrasynaptic NR2B-NMDARs in NCAM-/- mice could promote induction of LTD, as found in DA rats (Massey et al., 2004). Thus, impaired LTD in NCAM-/- mice is most likely due to a deficit in signaling via NR2A-NMDARs, which could be restored by DCS (Figure 23B,E). In contrast, in NCAM+/+ mice, application of DCS increased signaling via NMDARs to levels above the threshold for induction of LTD and, thus, impaired induction of LTD (Figure 23B,E). As levels of basal excitatory synaptic transmission are normal in NCAM-/- mice (Figure 9), it is unlikely that the increased basal activity of p38 MAPK results in depression and thus occludes LTD induced by low-frequency stimulation.

DISCUSSION

To test whether facilitation of NR2A-NMDAR signaling can normalize cognitive deficits in NCAM deficient (NCAM-/-) mice, our group used a combination of systemic administration of D-cycloserine (DCS), an agonist of glycine-site of NMDARs, and a newly developed repetitive fear conditioning paradigm (Senkov 2007). Pretraining injection of DCS dose-dependently (3, 10 and 20 mg/kg, b.w.) rescued not only impaired retrieval of contextual memory after both repetitive fear conditionings at either 1st or 7th test day, but also improved discrimination of contexts compared to vehicle-injected NCAM-/- or DCS-injected wild-type mice. In addition, DCS facilitated tone memory, especially discrimination of tones. To verify whether a suppression of excessive NR2B-NMDAR activity in NCAM-/- mice would restore impaired contextual memory, we injected intrahippocampally a selective blocker of NR2B-NMDARs, Ro25-6981 (0.5 µl, 20µg/µl). Pretraining injection of Ro25-6981 in NCAM-/- mice resulted in a restoration of contextual memory as well as facilitated contextual discrimination after training. Thus, pharmacological treatments affecting a balance in NR2A/NR2B-NMDAR signaling restore not only synaptic plasticity in vitro but also fear memory in NCAM-/- mice.

This study is the first to highlight an age-dependent role of NCAM in hippocampal synaptic plasticity. We show that (1) there is a stronger LTP deficit in 24- and 12-month-old NCAM-/- mice as compared to 2.5-month-old NCAM-/- mice (Figure 40A). (2) Short-term potentiation is exclusively impaired in aged (12 and 24-month-old) NCAM-/- mice (Figure 34A,B; Figure 38A,B), but not in younger mice (Figure 33A,B; Figure 11A,B). (3) Impaired LTP in aged NCAM-/- mice could not be fully rescued by treatments that are fully effective in 2.5-month-old NCAM-/- mice, although STP was fully recovered. (4) LTP is normal in acute slices from 2.5-week-old NCAM-/- mice (Figure 33A,C; Figure 40A). This is in contrast to impaired CA1 LTP observed in organotypic slices treated with endo-N and impaired glutamate-induced LTP in dissociated NCAM-/- neurons cultured for 2-3 weeks (Muller et al. 1996; Dityatev et al. 2000). Possibly, a lack of neuromodulatory inputs in these experimental systems may lead to earlier and more pronounced effects of PSA/NCAM deficiency on synaptic plasticity. Normal LTP in slices from 2.5-week-old but not from older mice correlates with “maturation” of mechanisms related to signaling via Ras-guanine nucleotide-releasing factor 1 (Ras-GRF1) and Ras-GRF2. The latter contributes predominantly to the induction of NMDAR-dependent LTP, whereas Ras-GRF1 contributes predominantly to the induction of NMDAR dependent LTD in the CA1 subfield of the hippocampus of post-pubescent mice. In contrast, neither Ras-GRF protein influences synaptic plasticity in prepubescent mice (Li et al., 2006).

It remains, however, to be identified which additional mechanisms are impaired in aged NCAM-/- mice. One noteworthy in this respect finding from our laboratory is that NCAM-/- cornu ammonis receive abnormally high cholinergic input in one-year-old but not in adolescent mice (Yuliya Tereschenko, personal communication). This age-dependent increase in cholinergic innervation may be of a compensatory nature to counteract impairment in cholinergic transmission in aged NCAM-/- mice. NCAM may regulate membrane targeting, clustering or functional properties of particular neurotransmitter receptors, for example, the alpha7 nicotinic acetylcholine receptor. Another possibility is that NCAM is important for acetylcholine release, since compensatory production of cholinergic fibers may reflect a deficit in transmitter release. This hypothesis is supported by data on abnormal organization of the neuromuscular junction and impaired evoked release of acetylcholine vesicles at physiological rates of motor nerve stimulation in NCAM-/- mice (Rafuse et al., 2000; Polo-Parada et al., 2001). At motor endplates, NCAM interacts with agrin which is crucial for organization of cholinergic synapses (Huh and Fuhrer, 2002). The notion that cholinergic transmission is impaired in the absence of NCAM is also attractive in functional terms: cholinergic transmission modulates anxiety as well as learning and memory formation (File et al., 2000), and previous work has shown that NCAM-deficient mice are more anxious and have deficient memory compared to wild-type littermates (Cremer et al., 1994; Stork et al., 1997; 1999; Bukalo et al., 2004). Thus, further studies are warranted to investigate how NCAM supports cholinergic functions during aging.

NCAM is a strong candidate gene for schizophrenia. In addition to a deficit in PSA expression (Barbeau et al., 1995), a polymorphism in the promoter region of the polysialyltransferase *ST8SiaII* gene is associated with schizophrenia (Arai et al., 2006; Tao et al., 2007). Furthermore, patients with schizophrenia also have higher concentrations of the soluble cleaved extracellular domain of NCAM in prefrontal cortex, cingulate cortex, hippocampus, and cerebrospinal fluid (Vawter et al., 2001). NCAM-/- mice have enlarged lateral ventricles and deficits in prepulse inhibition of the acoustic startle (Wood et al., 1998), reminiscent of findings in schizophrenic patients. Our findings showing abnormalities in NMDAR-mediated signaling in NCAM/PSA deficient animals are remarkable in this context, since NMDAR antagonists induce negative and positive symptoms of schizophrenia and the glycine NMDAR site agonists are effective tools for treatment of negative symptoms (Javitt, 2006). Thus, our data put forward the view that abnormalities in NMDAR signaling in NCAM/PSA deficient brains may underlie some

cognitive abnormalities in schizophrenia. Furthermore, our findings suggest that approaches which normalize the balance between NR2A- and NR2B-NMDARs function by inhibition of the p38 MAPK pathway may provide a promising approach to treatment of schizophrenia associated with dysregulation of NCAM

IX. Reference list

Abraham WC, Williams JM (2003) Properties and mechanisms of LTP maintenance. Neuroscientist 9(6): 463-74.

Akazawa C, Shigemoto R, Bessho Y, Nakanishi S, Mizuno N (1994) Differential expression of five Nmethyl- D-aspartate receptor subunit mRNAs in the cerebellum of developing and adult rats. J Comp Neurol 347, 150-160.

Andersen P (1960) Interhippocampal impulses. II. Apical dendritic activatin of CA1 neurons. Acta Physiol Scand 48:178-208.

Andersen P, Bliss TVP, Skrede KK (1971) Lamellar organization of hippocampal excitatory pathways. Exp Brain Res 13:222-238.

Angata K, Suzuki M, Fukuda M (1998) Differential and cooperative polysialylation of the neural cell adhesion molecule by two polysialyltransferases, PST and STX. J Biol Chem 273: 28524-28532.

Anson LC, Chen PE, Wyllie DJ, Colquhoun D, Schoepfer R (1998) Identification of amino acid residues of the NR2A subunit that control glutamate potency in recombinat NR1/NR2A NMDA receptors. J Neurosci 18, 581-589.

Arai M, Yamada K, Toyota T, Obata, N, Haga S, Yoshida Y, Nakamura K, Minabe Y, Ujike H, Sora I, Ikeda K, Mori N, Yoshikawa T, Itokawa M (2006) Association between polymorphisms in the promoter region of the sialyltransferase 8B (SIAT8B) gene and schizophrenia. Biol Psychiatry 59, 652-659.

Bading H, Greenberg ME (1991) Stimulation of protein tyrosine phosphorylation by NMDA receptor activation. Science 253, 912-914.

Balak K, Jacobson M, Sunshine J, Rutishauser U (1987) Neural cell adhesion molecule expression in Xenopus embryos. Dev Biol 119:540-50.

Barbeau D, Liang JJ, Robitalille Y, Quirion R, Srivastava L K (1995) Decreased expression of the embryonic form of the neural cell adhesion molecule in schizophrenic brains. Proc Natl Acad Sci USA 92, 2785-2789.

Barnes CA, Rao G, McNaughton BL (1996) Functional integrity of NMDA-dependent LTP induction mechanisms across the life-spam of F-344 rats. Learn Mem 3:124-137

Bartlett TE, Bannister NJ, Collett VJ, Dargan SL, Massey PV, Bortolotto ZA, Fitzjohn SM, Bashir ZI, Collingridge GL, Lodge D (2007) Differential roles of NR2A and NR2B-containing NMDA receptors in LTP and LTD in the CA1 region of two-week old rat hippocampus. Neuropharmacology 52, 60-70.

Bear MF, Malenka RC (1994) Synaptic plasticity: LTP and LTD. Curr Opin Neurobiol. 4(3):389-99.

REFERENCE LIST

Becker CG, Artola A, Gerardy-Schahn R, Becker T, Welzl H, Schachner M (1996) The polysialic acid modification of the neural cell adhesion molecule is involved in spatial learning and hippocampal long-term potentiation. J Neurosci Res 45: 143-152.

Behe P, Stern P, Wyllie DJ, Nassar M, Schoepfer R, Colquhoun D (1995) Determination of NMDA NR1 subunit copy number in recombinant NMDA receptors. Proc R Soc Lond B Biol Sci 262, 205-213.

Berberich S, Punnakkal P, Jensen V, Pawlak V, Seeburg PH, Hvalby Q, Köhl G (2005) Lack of NMDA receptor subtype selectivity for hippocampal long-term potentiation. J Neurosci. 20;25(29):6907-10.

Billard JM, Rouaud E (2007) Deficit of NMDA receptor activation in CA1 hippocampal area of aged rats is rescued by D-cycloserine. Eur J Neurosci 25, 2260-2268.

Bliss TVP, Collingridge GL (1993) A synaptic model of memory: long-term potentiation in the hippocampus. Nature 361:31-39.

Bliss TVP, Gardner-Medwin AR (1973) Long-lasting potentiation of synaptic transmission in the dentate area of the unanaestetized rabbit following stimulation of the perforant path. J Physiol (Lond) 232(2): 357-74.

Bliss TVP, Lomo T (1973) Long-lasting potentiation of synaptic transmission in the dentate area of the anaesthetized rabbit following stimulation of the perforant path." J Physiol (Lond) 232(2): 331-56.

Bock E, Edvardsen K, Gibson A, Linnemann D, Lyles JM, Nybroe O (1987) Characterization of soluble forms of NCAM. FEBS Lett 225: 33-36.

Bolshakov VY, Carboni L, Cobb MH, Siegelbaum SA, Belardetti F (2000) Dual MAP kinase pathways mediate opposing forms of long-term plasticity at CA3-CA1 synapses. Nat Neurosci 3, 1107-1112.

Brackenbury R, Thiery JP, Rutishauer U, Edelman GM (1977) Adhesion among neural cells of the chick embryo. I. An immunological assay for molecules involved in cell-cell binding. J Biol Chem. 10;252(19):6835-40.

Brümmendorf T, Rathjen FG (1995) Cell adhesion molecules 1: immunoglobulin superfamily. Protein Profile. 2(9):963-1108.

Bruses JL, Rutishauser U (2201) Roles, regulation, and mechanism of polysialic acid function during neural development. Biochimie. 83(7):635-43.

Buchsbaum RJ, Connolly BA, Feig LA (2002) Interaction of Rac exchange factors Tiam1 and Ras-GRF1 with a scaffold for the p38 mitogenactivated protein kinase cascade. Mol Cell Biol 22:4073– 4085.

Bukalo O, Dityatev A (2006) Analysis of neural cell functions in gene knockout mice - electrophysiological investigation of synaptic plasticity in acute hippocampal slices. Methods in Enzymology. 417:52-66.

REFERENCE LIST

Bukalo O, Fentrop N, Lee AY, Salmen B, Law JW, Wotjak CT, Schweizer M, Dityatev A, Schachner M (2004) Conditional ablation of the neural cell adhesion molecule reduces precision of spatial learning, long-term potentiation, and depression in the CA1 subfield of mouse hippocampus. J Neurosci 24, 1565-1577.

Burg MA, Halfter W, Cole GJ (1995) Analysis of proteoglycan expression in developing chicken brain: characterization of a heparan sulfate proteoglycan that interacts with the neural cell adhesion molecule. J Neurosci Res 41: 49-64.

Butler MP, O'Connor JJ, Moynagh PN (2004) Dissection of tumornecrosis factor-alpha inhibition of long-term potentiation (LTP) reveals a p38 mitogen-activated protein kinase-dependent mechanism which maps to earlybut not late-phase LTP. Neuroscience 124, 319-326.

Buttner B, Kannicht C, Reutter W, Horstkorte R (2003) The neural cell adhesion molecule is associated with major components of the cytoskeleton. Biochem Biophys Res Commun 310: 967-971.

Carroll RC, Beattie EC, Xia H, Lüscher C, Altschuler Y, Nicoll RA, Malenka RC, Zastrow M (1999) Dynamin-dependent endocytosis of ionotropic glutamate receptors. Proc Natl Acad Sci U S A 96(24): 14112-7.

Castillo PE, Malenka RC, Nicoll RA (1997) Kainate receptors mediate a slow postsynaptic current in hippocampal CA3 neurons. Nature 388:182-186.

Chandler LJ, Sutton G, Dorairaj RN, Norwood D (2001) N-methyl D-aspartate receptor-mediated bidirectional control of extracellular signal-regulated kinase activity in cortical neuronal cultures. J Biol Chem 276, 2627-2636.

Chatterton JE (2002) Excitatory glycine receptors containing the NR3 family of NMDA receptor subunits. Nature 30 , 715-719.

Chazal G, Durbec P, Jankovski A, Rougon G, Cremer H (2000) Consequences of neural cell adhesion molecule deficiency on cell migration in the rostral migratory stream of the mouse. J Neurosci 20:1446–1457.

Chen HX, Otmakhov N, Lisman J (1999) Requirements for LTP induction by pairing in hippocampal CA1 pyramidal cells. J Neurophysiol 82(2): 526-32.

Cole GJ, Akeson R (1989) Identification of a heparin binding domain of the neural cell adhesion molecule N-CAM using synthetic peptides. Neuron 2: 1157-1165.

Cole GJ, Loewy A, Cross NV, Akeson R, Glaser L (1986) Topographic localization of the heparin-binding domain of the neural cell adhesion molecule N-CAM. J Cell Biol 103: 1739-1744.

Collingridge GL, Kehl SJ, McLennan H (1983) Excitatory amino acids in synaptic transmission in the Schaffer collateral-commissural pathway of the rat hippocampus. J Physiol 334:33-46.

REFERENCE LIST

Cossart R, Epsztein J, Tyzio R, Becq H, Hirsch J, Ben-Ari Y, Crepel V (2002) Quantal release of glutamate generates pure kainate and mixer AMPA/kainate EPSCs in hippocampal neurons. Neuron 35:147-159.

Cossart R, Esclapez M, Hirsch JC, Bernard C, Ben-Ari Y (1998) GluR5 kainate receptor activation in interneurons increases tonic inhibition of pyramidal cells. Nat Neurosci 1:470-478.

Cremer H, Chazal G, Carleton A, Goridis C, Vincent JD, Lledo PM (1998) Long-term but not short-term plasticity at mossy fiber synapses is impaired in neural cell adhesion molecule-deficient mice. Proc Natl Acad Sci U S A 95: 13242-13247.

Cremer H, Chazal G, Goridis C, Represa A (1997) NCAM is essential for axonal growth and fasciculation in the hippocampus. Mol Cell Neurosci 8:323–335.

Cremer H, Lange R, Christoph A, Plomann M, Vopper G, Roes J, Brown R, Baldwin S, Kraemer P, Scheff S, and et al. (1994). Inactivation of the NCAM gene in mice results in size reduction of the olfactory bulb and deficits in spatial learning. Nature 367, 455-459.

Crossin KL, Krushel LA (2000) Cellular signaling by neural cell adhesion molecules of the immunoglobulin superfamily. Dev Dyn. 218(2):260-79.

Crossin KL, Krushel LA (2000) Cellular signaling by neural cell adhesion molecules of the immunoglobulin superfamily. Dev Dyn 218: 260-279.

Cunningham BA, Hemperly JJ, Murray BA, Prediger EA, Brackenbury R, Edelman GM (1987) Neural cell adhesion molecule: structure, immunoglobulin-like domains, cell surface modulation, and alternative RNA splicing. Science. 15;236(4803):799-806.

D'Eustachio P, Owens GC, Edelman GM, Cunningham BA (1985) Chromosomal location of the gene encoding the neural cell adhesion molecule (N-CAM) in the mouse. Proc Natl Acad Sci U S A 82:7631-5.

Das S, Sasaki YF, Rothe T, Premkumar LS, Takasu M, Crandall JE, Dikkes P, Conner DA, Rayudu PV, Cheung W (1998) Increased NMDA current and spine density in mice lacking the NMDA receptor subunit NR3A. Nature 393, 377-381.

Davies J, Francis AA, Jones AW, Watkins JC (1981) 2-Amino-5-phosponovalerate (2AP5), a potent and selective antagonist of amino acid-induced and synaptic excitation. Neurosci Lett 21:77-81.

Delling M, Wischmeyer E, Dityatev A, Sytnyk V, Veh RW, Karschin A, Schachner M (2002) The neural cell adhesion molecule regulates cellsurface delivery of G-protein-activated inwardly rectifying potassium channels via lipid rafts. J Neurosci 22:7154–7164.

Deupree DL, Turner DA, Watters CL (1991) Spatial performance correlates with in vitro potentiation in young and aged Fisher 344 rats. Brain Res 554:1-9

Dingledine R, Borges K, Bowie D, Traynelis SF (1999) The glutamate receptor ion channels. Pharmacol Rev 51, 7-61.

REFERENCE LIST

Dityatev A, Dityateva G, Schachner M (2000) Synaptic strength as a function of post- versus presynaptic expression of the neural cell adhesion molecule NCAM. Neuron 26: 207-217.

Dityatev A, Dityateva G, Sytnyk V, Delling M, Toni N, Nikonenko I, Muller D, Schachner M (2004) Polysialylated neural cell adhesion molecule promotes remodeling and formation of hippocampal synapses. J Neurosci 24: 9372-9382.

Doyle E, Nolan PM, Bell R, Regan CM (1992) Intraventricular infusions of anti-neural cell adhesion molecules in a discrete posttraining period impair consolidation of a passive avoidance response in the rat. J Neurochem 59: 1570-1573.

Dudek SM, BearMF (1992) Homosynaptic long-term depression in area CA1 of hippocampus and effects of N-methyl-D-aspartate receptor blockade. Proc Natl Acad Sci U S A 89(10): 4363-7.

Dunah AW, Luo J, Wang YH, Yasuda RP, Wolfe BB (1998) Subunit composition of N-methyl-Daspartate receptors in the central nervous system that contain the NR2D subunit. Mol Pharmacol 53, 429-437.

DurbecP, Cremer H (2001) Revisiting the function of PSA-NCAM in the nervous system. Mol. Neurobiol. 24, 53-64.

Eckhardt M, Bukalo O, Chazal G, Wang L, Goridis C, Schachner M, Gerardy-Schahn R, Cremer H, Dityatev A (2000) Mice deficient in the polysialyltransferase ST8SiaIV/PST-1 allow discrimination of the roles of neural cell adhesion molecule protein and polysialic acid in neural development and synaptic plasticity. J Neurosci 20: 5234-5244.

Eckhardt M, Muhlenhoff M, Bethe A, Koopman J, Frosch M, Gerardy-Schahn R (1995) Molecular characterization of eukaryotic polysialyltransferase-1. Nature 373: 715-718.

Emptage N, Bliss TV, Fine A (1999) Single synaptic events evoke NMDA receptor-mediated release of calcium from internal stores in hippocampal dendritic spines. Neuron 22(1):115-24.

Evers MR, Salmen B, Bukalo O, Rollenhagen A, Bosl MR, Morellini F, Bartsch U, Dityatev A, Schachner M (2002) Impairment of L-type Ca2+ channel-dependent forms of hippocampal synaptic plasticity in mice deficient in the extracellular matrix glycoprotein tenascin-C. J Neurosci 22, 7177-7194.

Fam NP, Fan W-T, Wang Z, Zhang L-J, Chen Z, Moran MF (1997) Cloning and characterization of Ras-GRF2, a novel guanine nucleotide exchange factor for Ras. Mol Cell Biol 17:1396 –1406.

Fan WT, Koch CA, de Hoog CL, Fam NP, Moran MF (1998) The exchange factor Ras-GRF2 activates Ras-dependent and Rac-dependent mitogenactivated protein kinase pathways. Curr Biol 8:935–938.

Farnsworth CL, Freshney NW, Rosen LB, Ghosh A, Greenberg ME, Feig LA (1995) Calcium activation of Ras mediated by the neuronal exchange factor Ras-GRF. Nature 376:524 –527.

REFERENCE LIST

File SE, Kenny PJ, Cheeta S (2000) The role of the dorsal hippocampal serotonergic and cholinergic systems in the modulation of anxiety. Pharmacol Biochem Behav 66, 65-72.

Finne J, Finne U, Deagostini-Bazin H, Goridis C (1983) Occurrence of alpha 2-8 linked polysialosyl units in a neural cell adhesion molecule. Biochem Biophys Res Commun 112: 482-487.

Finne J, Makela PH (1985) Cleavage of the polysialosyl units of brain glycoproteins by a bacteriophage endosialidase. Involvement of a long oligosaccharide segment in molecular interactions of polysialic acid. J Biol Chem 260: 1265-1270.

Forrest D, Yuzaki M, Soares HD, Ng L, Sheng M, Stewart CL, Morgan JI, Connor JA, Curran T (1994) Targeted disruption of NMDA receptor 1 gene abolishes NMDA response and results in neonatal death. Neuron 13, 325-338.

Fox CJ, Russell KI, Wang YT, Christie BR (2006) Contribution of NR2A and NR2B NMDA subunits to bidirectional synaptic plasticity in the hippocampus in vivo. Hippocampus 16, 907-915.

Freedman R (2003) Schizophrenia. N Engl J Med 349:1738–1749.

Freund TF, Buzsaki G (1996) Interneurons of the hippocampus. Hippocampus 6:347-470.

Frosch M, Gorgen I, Boulnois GJ, Timmis KN, Bitter-Suermann D (1985) NZB mouse system for production of monoclonal antibodies to weak bacterial antigens: isolation of an IgG antibody to the polysaccharide capsules of Escherichia coli K1 and group B meningococci. Proc Natl Acad Sci USA 82:1194 –1198.

Gennarini G, Hirn M, Deagostini-Bazin H, Goridis C (1984a) Studies on the transmembrane disposition of the neural cell adhesion molecule N-CAM. The use of liposome-inserted radioiodinated N-CAM to study its transbilayer orientation. Eur J Biochem 2;142:65-73.

Gennarini G, Rougon G, Deagostini-Bazin H, Hirn M, Goridis C (1984b) Studies on the transmembrane disposition of the neural cell adhesion molecule N-CAM. A monoclonal antibody recognizing a cytoplasmic domain and evidence for the presence of phosphoserine residues. Eur J Biochem 2;142:57-64.

Giese KP, Friedman E, Telliez JB, Fedorov NB, Wines M, Feig LA, Silva AJ (2001) Hippocampus-dependent learning and memory is impaired in mice lacking the Ras-guanine nucleotide-releasing factor 1 (Ras-GRF1). Neuropharmacology 41:791– 800.

Gilmore JH, van Tol J, Kliewer MA, Silva SG, Cohen SB, Hertzberg BS, Chescheir NC (1998) Mild ventriculomegaly detected in utero with ultrasound: clinical associations and implications for schizophrenia. Schizophr Res 33:133–140.

Goodman CS (1996) Mechanisms and molecules that control growth cone guidance. Annu. Rev. Neurosci. 19:341-77., 341-377.

REFERENCE LIST

Gordon-Weeks PR, Fischer I (2000) MAP1B expression and microtubule stability in growing and regenerating axons. Microsc Res Tech. 15;48(2):63-74.

Gower HJ, Barton CH, Elsom VL, Thompson J, Moore SE, Dickson G, Walsh FS (1988) Alternative splicing generates a secreted form of N-CAM in muscle and brain. Cell 55: 955-964.

Grumet M, Flaccus A, Margolis RU (1993) Functional characterization of chondroitin sulfate proteoglycans of brain: interactions with neurons and neural cell adhesion molecules. J Cell Biol 120: 815-824.

Gustafsson B, Asztely F, Hanse E, Wigström H (1989) Onset characteristics of long-term potentiation in the guinea-pig hippocampal CA1 region invitro. Eur J Neurosci 1:382-394.

Gustafsson B, Wigström H (1986) Hippocampal long-lasting potentiation produced by pairing single volleys and brief conditioning tetani evoked in separate afferents. J Neurosci 6(6): 1575-82.

Gustafsson B, Wigström H, Abraham WC, Huang YY (1987) Long-term potentiation in the hippocampus using depolarizing current pulses as the conditioning stimulus to single volley synaptic potentials. J Neurosci 7(3): 774-80.

Hammond M, Sims C, Kodeeswaran P, Suppiramaniam V, Schachner M, Dityatev A (2006) NCAM associated polysialic acid inhibits NR2B-containing NMDA receptors and prevents glutamate-induced cell death. J Biol Chem 281: 34859-69.

Hardigham GE, Arnold FJ, Bading H (2001) A calcium microdomain near NMDA receptors: on switch for ERK-dependent synapse-to-nucleus communication. Nat Neurosci 4, 565-566.

He HT, Barbet J, Chaix JC, Goridis C (1986) Phosphatidylinositol is involved in the membrane attachment of NCAM-120, the smallest component of the neural cell adhesion molecule. EMBO J 5: 2489-2494.

He Q, Meiri KF (2002) Isolation and characterization of detergent-resistant microdomains responsive to NCAM-mediated signaling from growth cones. Mol Cell Neurosci 19: 18-31.

Hildebrandt H, Becker C, Murau M, Gerardy-Schahn R, Rahmann H (1998) Heterogeneous expression of the polysialyltransferases ST8Sia II and ST8Sia IV during postnatal rat brain development. J Neurochem 71: 2339-2348.

Hinkle CL, Diestel S, Lieberman J, Maness PF (2006) Metalloprotease-induced ectodomain shedding of neural cell adhesion molecule (NCAM). J Neurobiol 66:1378–1395

Hinkle CL, Maness PF (2006) Regulation of neural cell adhesion molecule function by ectodomain shedding. In: Pandalai SG (ed) Recent research developments in molecular and cellular biology. Research Signpost, Kerala, India, pp 121–136.

REFERENCE LIST

Hollmann M (1999) Structure of ionotropic glutamate receptors. Ionotropic glutamate receptors in the CNS. Edited by Jonas P, Monyer H. Berlin: Springer 1-98.

Horstkorte R, Schachner M, Magyar JP, Vorherr T and Schmitz B (1993) The fourth immunoglobulin-like domain of NCAM contains a carbohydrate recognition domain for oligomannosidic glycans implicated in association with L1 and neurite outgrowth. J Cell Biol 121:1406-1421.

Hsieh H, Boehm J, Sato C, Iwatsubo T, Tomita T, Sisodia S, Malinow R (2006) AMPAR removal underlies Abeta-induced synaptic depression and dendritic spine loss. Neuron 52, 831-843.

Huang YY, Kandel ER (2005) Theta frequency stimulation induces a local form of late phase LTP in the CA1 region of the hippocampus. Learn Mem. 12(6):587-93.

Huang CC, You JL, Wu MY, Hsu KS (2004) Rap1-induced p38 mitogen-activated protein kinase activation facilitates AMPA receptor trafficking via the GDI.Rab5 complex. Potential role in (S)-3,5-dihydroxyphenylglycene-induced long term depression. J Biol Chem 279, 12286-12292.

Hubschmann MV, Skladchikova G, Bock E, Berezin V (2005) Neural cell adhesion molecule function is regulated by metalloproteinase-mediated ectodomain release. J Neurosci Res 80:826–837

Huh KH, Fuhrer C (2002) Clustering of nicotinic acetylcholine receptors: from the neuromuscular junction to interneuronal synapses. Mol Neurobiol 25, 79-112.

Innocenti M, Zippel R, Brambilla R, Sturani E (1999) CDC25Mm/Ras-GRF1 regulates both Ras and Rac signaling pathways. FEBS Lett 460:357–362.

Ivanov A, Pellegrino C, Rama S, Dumalska I, Salyha Y, Ben-Ari Y, Medina I (2006) Opposing role of synaptic and extrasynaptic NMDA receptors in regulation of the extracellular signal-regulated kinases (ERK) activity in cultured rat hippocampal neurons. J Physiol 572: 789-798.

Jahr CE, Stevens CF (1987) Glutamate activates multiple single channel conductances in hippocampal neuron. Nature 325:522-525.

Jahr CE, Stevens CF (1993) Calcium permeability on the N-methyl-D-aspartate receptor channel in hippocampal neurons in culture. Proc Natl Acad Sci USA 90:11573-11577.

Javitt DC (2006) Is the glycine site half saturated or half unsaturated? Effects of glutamatergic drugs in schizophrenia patients. Curr Opin Psychiatry 19, 151- 157.

Jorgensen OS (1995) Neural cell adhesion molecule (NCAM) as a quantitative marker in synaptic remodeling. Neurochem Res. 20(5):533-47.

Jorgensen OS, Bock E (1974) Brain specific synaptosomal membrane proteins demonstrated by crossed immunoelectrophoresis. J Neurochem 23, 879-880.

REFERENCE LIST

Kadmon G, Kowitz A, Altevogt P, Schachner M (1990a) Functional cooperation between the neural adhesion molecules L1 and N-CAM is carbohydrate dependent. J Cell Biol 110: 209-218.

Kadmon G, Kowitz A, Altevogt P, Schachner M (1990b) The neural cell adhesion molecule N-CAM enhances L1-dependent cell-cell interactions. J Cell Biol 110: 193-208.

Kalus I, Bormann U, Mzoughi M, Schachner M, Kleene R (2006) Proteolytic cleavage of the neural cell adhesion molecule by ADAM17/TACE is involved in neurite outgrowth. J Neurochem 98:78–88.

Kameyama K, Lee HK, Bear MF, Huganir RL (1998) Involvement of a postsynaptic protein kinase A substrate in the expression of homosynaptic long-term depression. Neuron 21(5): 1163-75.

Katagiri H, Tanaka K, Manabe T (2001) Requirement of appropriate glutamate concentrations in the synaptic cleft for hippocampal LTP induction. Eur J Neurosci 14, 547-553.

Kater SB, Rehder V (1995) The sensory-motor role of growth cone filopodia. Curr Opin Neurobiol. 5(1):68-74.

Kawakami R, Shinohara Y, Kato Y, Sugiyama H, Shigemoto R, Ito I. (2003) Asymmetrical allocation of NMDA receptor epsilon2 subunits in hippocampal circuitry. Science. 9;300(5621):990-4.

Kemp N, McQueen J, Faulkes S, Bashir ZI (2000) Different forms of LTD in the CA1 region of the hippocampus: role of age and stimulus protocol." Eur J Neurosci 12(1):360-6.

Kerr DS, Abraham WC (1995) Cooperative interactions among afferents govern the induction of homosynaptic long-term depression in the hippocampus. Proc Natl Acad Sci USA 92, 11637-11641.

Kim MJ, Dunah AW, Wang YT, Sheng M (2005) Differential roles of NR2A- and NR2B-containing NMDA receptors in Ras-ERK signaling and AMPA receptor trafficking. Neurol 46:745-760.

Kirkwood A, Rozas C, Kirkwood J, Perez F, Bear MF (1999) Modulation of long-term synaptic depression in visual cortex by acetylcholine and norepinephrine. J Neurosci 19(5): 1599-609.

Kiss JZ, Rougon G (1997) Cell biology of polysialic acid. Curr Opin Neurobiol 7: 640-646.

Kiss JZ, Troncoso E, Djebbara Z, Vutskits L, Muller D (2001) The role of neural cell adhesion molecules in plasticity and repair. Brain Res. Brain Res. Rev. 36, 175-184.

Kiss JZ, MullerD (2001) Contribution of the neural cell adhesion molecule to neuronal and synaptic plasticity. Rev. Neurosci. 12, 297-310.

REFERENCE LIST

Kiyono M, Satoh T, Kaziro Y (1999) G-protein β γ subunit-dependent Racguanine nucleotide exchange activity of Ras-GRF1/CDC25Mm. Proc Natl Acad Sci USA 96:4826–4831.

Kleckner NW, Dingledine R (1988) Requirement for glycine in activation of NMDA-receptors expressed in Xenopus oocytes. Science. 1988 Aug 12;241(4867):835-7.

Kleene R, Schachner M (2004) Glycans and neural cell interactions. Nat Rev Neurosci 5: 195-208.

Kohl BK, Dannhardt G (2001) The NMDA receptor complex: a promising target for novel antiepileptic strategies. Curr Med Chem 8, 1275-1289.

Kohr G (2006) NMDA receptor function: subunit composition versus spatial distribution. Cell Tissue Res 326, 439-446.

Kohr G, Jensen V, Koester HJ, Mihaljevic AL, Utvik JK, Kvello A, Ottersen OP, Seeburg PH, Sprengel R, Hvalby O (2003) Intracellular domains of NMDA receptor subtypes are determinants for longterm potentiation induction. J Neurosci 23, 10791-10799.

Konorski J (1948) Conditoned reflex and neuron organization. Cambridge, UK: Hefner.

Kullmann DM, Erdemli G, Asztely F (1996) LTP of AMPA and NMDA receptor-mediated signals: evidence for presynaptic expression and extrasynaptic glutamate spill-over. Neuron 17, 461-474.

Kurino M, Fukunada K, Ushio Y, Miyamoto E (1995) Activation of mitogen-activated protein kinase in cultured rat hippocampal neurons by stimulation of glutamate receptors. J Neurochem 65, 1282-1289.

Kurosawa N, Yoshida Y, Kojima N, Tsuji S (1997) Polysialic acid synthase (ST8Sia II/STX) mRNA expression in the developing mouse central nervous system. J Neurochem 69: 494-503.

Kuryatov A, Laube B, Betz H, Kuhse J (1994) Modulational analysis of the glycine-binding site of the NMDA receptor: structural similarity with bacterial amino acid-binding proteins. Neuron 12, 1291-1300.

Larson J, Wong D, Lynch G (1986) Patterned stimulation at the theta frequency is optimal for the induction of hippocampal long-term potentiation. Brain Res. 19;368(2):347-50.

Lee HK, Kameyama K, Hugarin RL, Bear MF (1998) NMDA induces long-term synaptic depression and dephosphorylation of the GluR1 subunit of AMPA receptors in hippocampus. Neuron. 21(5):1151-62.

Lee HK, Takamiya K, Han JS, Man H, Kim CH, Rumbaugh G, Yu S, Ding L, He C, Petralia RS, Wenthold RJ, Gallagher M, Huganir RL (2003) Phosphorylation of the AMPA receptor GluR1 subunit is required for synaptic plasticity and retention of spatial memory." Cell 112(5): 631-43.

REFERENCE LIST

Leshchyns'ka I, Sytnyk V, Morrow JS, Schachner M (2003) Neural cell adhesion molecule (NCAM) association with PKCbeta2 via betaI spectrin is implicated in NCAM-mediated neurite outgrowth. J Cell Biol 161: 625-639.

Lester RA, Clements JD, Westbrook GL, Jahr CE (1990) Channel kinetics determine the time course of NMDA receptor-mediated synaptic currents. Nature. 9;346 (6284):565-7.

Lewis CM, Levinson DF, Wise LH, DeLisi LE, Straub RE Hovatta I, Williams NM, Schwab SG, Pulver AE, Faraone SV, Brzustowicz LM, Kaufmann CA, Garver DL, Gurling HM, Lindholm E, Coon H, Moises HW, Byerley W, Shaw SH, Mesen A, Sherrington R, O'Neill FA, Walsh D, Kendler KS, Ekelund J, Paunio T, Lonnqvist J, Peltonen L, O'Donovan MC, Owen MJ, Wildenauer DB, Maier W, Nestadt G, Blouin JL, Antonarakis SE, Mowry BJ, Silverman JM, Crowe RR, Cloninger CR, Tsuang MT, Malaspina D, Harkavy-Friedman JM, Svrakic DM, Bassett AS, Holcomb J, Kalsi G, McQuillin A, Brynjolfson J, Sigmundsson T, Petursson H, Jazin E, Zoega T, Helgason T (2003) Genome scan meta-analysis of chizophrenia and bipolar disorder, part II: Schizophrenia. Am J Hum Genet 73:34–48.

Lewis DA, Hashimoto T, Volk DW (2005) Cortical inhibitory neurons and schizophrenia. Nat Rev Neurosci 6:312–324.

Li S, Tian X, Hartley DM, Feig LA (2006) Distinct roles for Ras-guanine nucleotide-releasing factor 1 (Ras-GRF1) and Ras-GRF2 in the induction of long-term potentiation and long-term depression. J Neurosci 26:1721-15729.

Liao D, Hessler NA, Malinow R (1995) Activation of postsynaptically silent synapses during pairing-induced LTP in CA1 region of hippocampal slice. Nature 375(6530): 400-4.

Lisman J (1994) The CaM kinase II hypothesis for the storage of synaptic memory. Trends Neurosci 17(10): 406-12.

Lisman J, Schulman H, Cline H (2002) The molecular basis of CaMKII function in synaptic and behavioural memory. Nat Rev Neurosci 3(3): 175-90.

Liu, J., Fukunaga, K., Yamamoto, H., Nishi, K., and Miyamoto, E. (1999). Differential roles of Ca(2+)/calmodulin-dependent protein kinase II and mitogen-activated protein kinase activation in hippocampal long-term potentiation. J Neurosci 19, 8292-8299.

Liu L, Wong TP, Pozza MF, Lingenhoehl K, Wang Y, Sheng M, Auberson YP, Wang YT (2004) Role of NMDA receptor subtypes in governing the direction of hippocampal synaptic plasticity. Science 304, 1021-1024.

Lois C, Garcia-Verdugo JM, Alvarez-Buylla A (1996) Chain migration of neuronal precursors. Science 271: 978-981.

Luo J, Wang Y, Yasuda RP, Dunah AW, Wolfe BB (1997) The majority of N-methyl-D-aspartate receptor complex in the adult rat cerebral cortex contain at least three different subunits (NR1/NR2A/NR2B). Mol Pharmacol 51, 79-86.

REFERENCE LIST

Luthi A, Laurent JP, Figurov A, Muller D, Schachner M (1994) Hippocampal long-term potentiation and neural cell adhesion molecules L1 and NCAM. Nature 372: 777-779.

Lynch G, Larson J, Kelso S, Barrionuevo G, Schottler F (1983). Intracellular injections of EGTA block induction of hippocampal long-term potentiation. Nature 305(5936): 719-21.

Lynch MA (2004) Long-term potentiation and memory. Physiol Rev 84(1): 87-136.

MacDermott AB, Mayer ML, Westbrook GL,Smith SJ, Barker JL (1986) NMDA-receptor activation increases cytoplasmic calcium concentration in cultured spinal cord neurones. Nature 321:519-22.

Malenka RC, Lancaster B, Zucker RS (1992) Temporal limits on the rise in postsynaptic calcium required for the induction of long-term potentiation. Neuron 9:121-128.

Malenka RC, Nicoll RA (1999) Long-term potentiation-a decade of progress? Science 285(5435): 1870-4.

Maness PF, Schachner M (2007) Neural recognition molecules of the immunoglobulin superfamily: signaling transducers of axon guidance and neuronal migration. Nat Neurosci 10:19–26.

Marenco S, Weinberger DR (2000) The neurodevelopmental hypothesis of schizophrenia: following trail of evidence from cradle to grave. Dev Psychopathol 12:501–527.

Massey PV, Johnson BE, Moult PR, Auberson YP, Brown MW, Molnar E, Collingridge GL, Bashir ZI (2004) Differential roles of NR2A and NR2B-containing NMDA receptors in cortical long-term potentiation and longterm depression. J Neurosci 24, 7821-7828.

Mayer ML, Westbrook GL, Guthrie PB (1984) Voltage-dependent block by Mg^{2+} of NMDA responses in spinal cord neurons. Nature 309:261-263.

McNaughton BL (1982) Long-term synaptic enhancement and short-term potentiation in rat fascia dentate act through different mechanisms. J Physiol 324:249-262.

Miller PD, Chung WW, Lagenaur CF, DeKosky ST (1993) Regional distribution of neural cell adhesion molecule (N-CAM) and L1 in human and rodent hippocampus. J. Comp Neurol. 327, 341-349.

Monyer H, Burnashev N, Laurie D, Sakmann B, Seeburg PH (1994) Developmental and regional expression in the rat brain and functional properties of four NMDA receptors. Neuron 12, 529-540.

Monyer H, Sprengel R, Schoepfer R, Herb A, Higuchi M, Lomeli H, Burnashev N, Sakmann B, Seeburg PH (1992) Heteromeric NMDA receptors: molecular and functional distinction of subtypes. Science 256, 1217-1221.

REFERENCE LIST

Moore CI, Browning MD, Rose GM (1993) Hippocampal plasticity induced my primed bursts, but not long-term potentiation, stimulation is impaired in area CA1 of aged Fischer 344 rats. Hippocampus 3:57-66.

Moore SE, Walsh FS (1986) Nerve dependent regulation of neural cell adhesion molecule expression in skeletal muscle. Neuroscience 18:499-505.

Morishita W, Lu W, Smith GB, Nicoll RA, Bear MF, Malenka RC (2007) Activation of NR2B-containing NMDA receptors is not required for NMDA receptor-dependent long-term depression. Neuropharmacology 52, 71-76.

Moriyoshi K, Masu M, Ishii T, Shigemoto R, Mizuno N, Nakanishi S (1991) Molecular cloning and characterization of the rat NMDA receptor. Nature 354, 31-37.

Muglia P, Macciardi F, Kennedy JL (1999) The neurodevelopmental hypothesis of Schizophrenia: genetic investigations. CNS Spectrum 4:78–90

Mulkeen D, Anwyl R, Rowan M (1988) The effects of external calcium on long-term potentiation in the rat hippocampal slice. Brain Res 447, 234-238.

Muller D, Djebbara-Hannas Z, Jourdain P, Vutskits L, Durbec P, Rougon G, Kiss JZ (2000) Brain-derived neurotrophic factor restores long-term potentiation in polysialic acid-neural cell adhesion molecule-deficient hippocampus. Proc Natl Acad Sci U S A 97: 4315-4320.

Muller D, Wang C, Skibo G, Toni N, Cremer H, Calaora V, Rougon G, Kiss JZ (1996) PSA-NCAM is required for activity-induced synaptic plasticity. Neuron 17: 413-422.

Mullkey RM, Endo S, Shenolikar S, Malenka RC (1994) Involvement of a calcineurin/inhibitor-1 phosphatase cascade in hippocampal long-term depression." Nature 369(6480):486-8.

Nakayama J, Angata K, Ong E, Katsuyama T, Fukuda M (1998) Polysialic acid, a unique glycan that is developmentally regulated by two polysialyltransferases, PST and STX, in the central nervous system: from biosynthesis to function. Pathol Int 48: 665-677.

Nelson RW, Bates PA, Rutishauser U (1995) Protein determinants for specific polysialylation of the neural cell adhesion molecule. J Biol Chem 270: 17171-17179.

Neugebauer KM, Tomaselli KJ, Lilien J and Reichardt LF(1988) N-cadherin, NCAM, and integrins promote retinal neurite outgrowth on astrocytes in vitro. J Cell Biol 107:1177-87.

Neves G, Cooke SF, Bliss TV (2008) Synaptic plasticity, memory and the hippocampus: a neural network approach to causality. Nat Rev Neurosci. 9(1):65-75.

Nguyen C, Mattei MG, Mattei JF, Santoni MJ, Goridis C and Jordan BR (1986) Localization of the human NCAM gene to band q23 of chromosome 11: the third gene coding for a cell interaction molecule mapped to the distal portion of the long arm of chromosome 11. J Cell Biol 102:711-5.

REFERENCE LIST

Niethammer P, Delling M, Sytnyk V, Dityatev A, Fukami K, Schachner M (2002) Cosignaling of NCAM via lipid rafts and the FGF receptor is required for neuritogenesis. J Cell Biol 157:521–532.

Nowak L, Bregestovski P, Herbet A, Prochiantz A (1984) Magnesium gates glutamate-activated channels in mouse central neurons. Nature 307:462-465.

O'Connell AW, Fox GB, Barry T, Murphy KJ, Fichera G, Foley AG, Kelly J, Regan CM (1997) Spatial learning activates neural cell adhesion molecule polysialylation in a corticohippocampal pathway within the medial temporal lobe. J Neurochem 68: 2538-2546.

Ong E, Nakayama J, Angata K, Reyes L, Katsuyama T, Arai Y, Fukuda M (1998) Developmental regulation of polysialic acid synthesis in mouse directed by two polysialyltransferases, PST and STX. Glycobiology 8: 415-424.

Ono K, Tomasiewicz H, Magnuson T, Rutishauser U (1994) N-CAM mutation inhibits tangential neuronal migration and is phenocopied by enzymatic removal of polysialic acid. Neuron 13:595– 609.

Passafaro MV, Piech, Sheng M (2001) Subunit-specific temporal and spatial patterns of AMPA receptor exocytosis in hippocampal neurons. Nat Neurosci 4(9): 917-26.

Persohn E, Pollerberg GE, Schachner M (1989) Immunoelectron-microscopic localization of the 180 kD component of the neural cell adhesion molecule N-CAM in postsynaptic membranes. J Comp Neurol 1;288:92-100.

Petralia RS, Sans N, Wang YX, Wenthold RJ (2005) Ontogeny of postsynaptic density proteins at glutamatergic synapses. Mol Cell Neurosci 29, 436-452.

Phillips GR, Krushel LA, Crossin KL (1997) Developmental expression of two rat sialyltransferases that modify the neural cell adhesion molecule, N-CAM. Brain Res Dev Brain Res 102: 143-155.

Pollerberg GE, Burridge K, Krebs KE, Goodman SR, Schachner M (1987) The 180-kD component of the neural cell adhesion molecule N-CAM is involved in a cell-cell contacts and cytoskeleton-membrane interactions. Cell Tissue Res 250: 227-236.

Polo-Parada L, Bose CM, Landmesser LT (2001) Alterations in transmission, vesicle dynamics, and transmitter release machinery at NCAM-deficient neuromuscular junctions. Neuron 32, 815-828.

Priestley T, Laughton P, Myers J, Le Bourdelles B, Kerby J, Whiting PJ (1995) Pharmacological properties of recombinant human N-methyl-Daspartate receptors comprising NR1a/NR2A and NR1a/NR2B subunit assemblies expressed in permanently transfected mouse fibroblast cells. Mol Pharmacol 48, 841-848.

Pyapali GK, Sik A, Penttoner M, Buzsaki G, Turner DA (1998) Dendritic properties of hippocampal CA1 pyramidal neurons in the rat: intracellular staining in vivo and in vitro. J Comp Neurol 391:335-352.

REFERENCE LIST

Rafuse, V.F., Polo-Parada, L. & Landmesser, L.T. (2000) Structural and functional alterations of neuromuscular junctions in NCAM-deficient mice. J Neurosci 20, 6529-6539.

Reynolds GP, Harte MK (2007) The neuronal pathology of schizophrenia: molecules and mechanisms. Biochem Soc Trans 35:433–436

Ronn LC, Bock E, Linnemann D, Jahnsen H (1995) NCAM-antibodies modulate induction of long-term potentiation in rat hippocampal CA1. Brain Res 677: 145-151.

Rosenzweig Es, Rao G, McNaughton BL, Barnes CA (1997) Role of temporal summation in age-related long-term potentiation-induction deficits. Hippocampus 7:549-558.

Rumbaugh S, Vicini S (1999) Distinct synaptic and extrasynaptic NMDA receptors in developing cerebellar granule neurons. J Neurosci 19, 10603-10610.

Rutishauser U (1996) Polysialic acid and the regulation of cell interactions. Curr Opin Cell Biol 8: 679-684.

Rutishauser U, Hoffman S, Edelma GM (1982) Binding properties of a cell adhesion molecule from neural tissue. Proc Natl Acad Sci U S A. 79(2):685-9.

Rutishauser U, Landmesser L (1996) Polysialic acid in the vertebrate nervous system: a promoter of plasticity in cell-cell interactions. Trends Neurosci 19: 422-427.

Rutishauser U (2008) Polysialic acid in the plasticity of the developing and adult vertebrate nervous system. Nat Rev Neurosci 9, 26-35.

Salmen B. Alterations of Ca2+ mediated signaling in Tenascin-C and NCAM deficient mice. PhD thesis Bochum 2002.

Sandi C, Merino JJ, Cordero MI, Kruyt ND, Murphy KJ, Regan CM (2003) Modulation of hippocampal NCAM polysialylation and spatial memory consolidation by fear conditioning. Biol Psychiatry 54: 599-607.

Scatton B (1993) The NMDA receptor complex. Fundam Clin Pharmacol. 7(8):389-400.

Schachner M (1994) Neural recognition molecules in disease and regeneration. Curr Opin Neurobiol 4: 726-734.

Schachner M, Martini R (1995) Glycans and the modulation of neural-recognition molecule function. Trends Neurosci 18: 183-191.

Schachner M (1997) Neural recognition molecules and synaptic plasticity. Curr Opin Cell Biol 9: 627-634.

Scheidegger EP, Lackie PM, Papay J, Roth J (1994) In vitro and in vivo growth of clonal sublines of human small cell lung carcinoma is modulated by polysialic acid of the neural cell adhesion molecule. Lab Invest 70: 95-106.

REFERENCE LIST

Scheidere CL, Dobrunz LE, McMahon LL (2004) Novel form of long-term synaptic depression in rat hippocampus induced by activation of alpha 1 adrenergic receptors. J Neurophysiol 91(2): 1071-7.

Schell MJ, Molliver ME, Snyder SH (1995) D-serine, an endogenous synaptic modulator: localization to astrocytes and glutamate-stimulated release. Proc Natl ACAd Sci USA. 25;92(9):3948-52.

Scholey AB, Rose SP, Zamani MR, Bock E, Schachner M (1993) A role for the neural cell adhesion molecule in a late, consolidating phase of glycoprotein synthesis six hours following passive avoidance training of the young chick. Neuroscience 55: 499-509.

Scoville WB, Milner B (1957) Loss of recent memory after bilateral hippocampal lesions. J Neurol Neurosurg Psychiatry 20(1):11-21.

Seeburg PH, Higuchi M, Sprengel R (1998) RNA editing of brain glutamate receptor channels: mechanism and physiology. Brain Res Brain Res Rev. 26 (2-3):217-29.

Seilheimer B, Schachner M(1988) Studies of adhesion molecules mediating interactions between cells of peripheral nervous system indicate a major role for L1 in mediating sensory neuron growth on Schwann cells in culture. J Cell Biol 107:341-51

Seki T, Arai Y (1993) Highly polysialylated neural cell adhesion molecule (NCAM-H) is expressed by newly generated granule cells in the dentate gyrus of the adult rat. J Neurosci 13: 2351-2358.

Senkov O, Sun M, Weinhold B, Gerardy-schahn R, Schachner M, Dityatev A (2006) Polysialylated neural cell adhesion molecule is involved in induction of long-term potentiation and memory acquisition and consolidation in a fear-conditioning paradigm. J Neurosci 26: 10888-109898.

Senkov O. Functional role of the polysialylated neural cell adhesion molecule in fear conditioning of mice (Mus musculus L., 1758). PhD thesis Hamburg 2007. http://www.sub.uni-hamburg.de/opus/volltexte/2007/3242/

Sheng M, Cummings J, Roldan LA, Jan YN, Jan LY (1994) Changing subunit composition of heteromeric NMDA receptors during development of rat cortex. Nature 368, 144-147.

Sherwin AL (1999) Neuroactive amino acids in focally epileptic human brain: a review. Neurochem Res 24, 1387-1395.

Shi SH (2001) Amersham Biosciences & Science Prize. AMPA receptor dynamics and synaptic plasticity. Science 294(5548): 1851-2.

Shi Y, Gaestel M (2002) In the cellular garden of forking paths: how p38 MAPKs signal for downstream assistance. Biol Chem 383, 1519-1536.

Shou C, Farnsworth CL, Neel BG, Feig LA (1992) Molecular cloning of cDNAs encoding a guanine nucleotide-releasing factor for Ras p21. Nature 358:351–354.

REFERENCE LIST

Sommer BK, Keinanen K, Verdoorn TA, Wisden W, Burnashev N, Herb A, Köhler M, Takagi T, Sakmann B, Seeburg PH (1990) Flip and flop: a cell-specific functional switch in glutamate-operated channels of the CNS. Science 249(4976): 1580-5.

Staubli U, Lynch G (1987) Stable hippocampal long-term potentiation elicited by 'theta' pattern stimulation. Brain Res 435(1-2): 227-34.

Stocca G, Vicini S (1998) Increased contribution of NR2A subunit to synaptic NMDA receptors in developing rat cortical neurons. J Phisiol 507 (Pt 1), 13-24.

Stoenica L, Senkov O, Gerardy-Schahn R, Weinhold B, Schachner M, Dityatev A (2006) In vivo synaptic plasticity in the dentate gyrus of mice deficient in the neural cell adhesion molecule NCAM or its polysialic acid. Eur J Neurosci 23, 2255-2264.

Stork O, Welzl H, Cremer H, Schachner M (1997) Increased intermale aggression and neuroendocrine response in mice deficient for the neural cell adhesion molecule (NCAM). Eur J Neurosci 9:1117–1125.

Stork O, Welzl H, Wolfer D, Schuster T, Mantei N, Stork S, Hoyer D, Lipp H, Obata K, Schachner M (2000) Recovery of emotional behaviour in neural cell adhesion molecule (NCAM) null mutant mice through transgenic expression of NCAM180. Eur J Neurosci 12:3291–3306

Stork O, Welzl H, Wotjak CT, Hoyer D, Delling M, Cremer H, Schachner M (1999) Anxiety and increased 5-HT1A receptor response in NCAM null mutant mice. J. Neurobiol. 40, 343–355.

Stummeyer K, Dickmanns A, Muhlenhoff M, Gerardy-Schahn R, Ficner R (2005) Crystal structure of the polysialic acid-degrading endosialidase of bacteriophage K1F. Nat Struct Mol Biol 12, 90-96.

Sugihara H, Moriyoshi K, Ishii T, Masu M, Nakanishi S (1992) Structures and properties of seven isoforms of the NMDA receptor generated by alternative splicing. Biochem Biophys Res Commun 185, 826-832.

Sullivan PF, Keefe RS, Lange LA, Lange EM, Stroup TS, Lieberman J, Maness PF (2007) NCAM1 and neurocognition in schizophrenia. Biol Psychiatry 61:902–910

Sweatt JD (2004) Mitogen-activated protein kinases in synaptic plasticity and memory. Curr Opin Neurobiol 14(3): 311-7.

Sytnyk V, Leshchyns'ka I, Delling M, Dityateva G, Dityatev A, Schachner M (2002) Neural cell adhesion molecule promotes accumulation of TGN organelles at sites of neuron-to-neuron contacts. J. Cell Biol. 159, 649-661.

Sytnyk V, Leshchyns'ka I, Nikonenko AG, Schachner M (2006) NCAM promotes assembly and activity-dependent remodeling of the postsynaptic signaling complex. J Cell Biol 174, 1071-1085.

Tang YG, Zucker RS (1997) Mitochondrial involvement in post-tetanic potentiation of synaptic transmission. Neuron 18:483-491.

REFERENCE LIST

Tao R, Li C, Zheng Y, Qin W, Zhang J, Li X, Xu Y, Shi YY, Feng G, He L (2007) Positive association between SIAT8B and schizophrenia in the Chinese Han population. Schizophr Res 90, 108-114.

Theodosis DT, Rougon G, Poulain DA (1991) Retention of embryonic features by an adult neuronal system capable of plasticity: polysialylated neural cell adhesion molecule in the hypothalamo-neurohypophysial system. Proc Natl Acad Sci U S A 88: 5494-5498.

Thiels E, Xie X, Yeckel MF, Barrionuevo G, Berger TW (1996) NMDA receptor-dependent LTD in different subfields of hippocampus in vivo and in vitro. Hippocampus 6(1): 43-51.

Thiery JP, Brackenbury R, Rutishauser U, Edelman GM (1977) Adhesion among neural cells of the chick embryo. Prog Clin Biol Res. 15:199-206.

Tombaugh GC, Rowe WB, Chow AR, Michael TH, Rose GM (2002) Theta-frequency synaptic potentiation in CA1 in vitro distinguishes cognitively impaired from unimpaired ader Fischer 344 rats. J Neurosci 22:9932-9940.

Tovar KR, Westbrook GL (1999) The incorporation of NMDA receptors with a distinct subunit composition at nascent hippocampal synapses in vitro. J Neurosci 19, 4180-4188.

Tsvetkov E, Shin RM, Bolshakov VY (2004) Glutamate uptake determines pathway specificity of long-term potentiation in the neural circuitry of fear conditioning. Neuron 41, 139-151.

Ueda Y, Doi T, Tokumaru J, Mitsuyama Y, Willmore LJ (2000) Kindling phenomena induced by the repeated short-term high potassium stimuli in the ventral hippocampus of rats: on-line monitoring of extracellular glutamate overflow. Exp Brain Res 135, 199-203.

van Dam EJ, Ruiter B, Kamal A, Ramal A, Ramakers GM, Gispen WH, de Graan PN (2002) N-methyl-D-aspartate-induced long-term depression is associated with a decrease in postsynaptic protein kinase C substrate phosphorylation in rat hippocampal slices. Neurosci Lett. 8;320(3):129-32.

Vawter MP, Usen N, Thatcher L, Ladenheim B, Zhang P, VanderPutten DM, Conant K, Herman MM, van Kammen DP, Sedvall G, Garver DL, Freed WJ (2001) Characterization of human cleaved N-CAM and association with schizophrenia. Exp Neurol 172:29–46.

Walsh FS, Doherty P (1997) Neural cell adhesion molecules of the immunoglobulin superfamily: role in axon growth and guidance. Annu Rev Cell Dev Biol 13: 425-456.

Wang Q, Walsh DM, Rowan MJ, Selkoe DJ, Anwyl R (2004) Block of long-term potentiation by naturally secreted and synthetic amyloid betapeptide in hippocampal slices is mediated via activation of the kinases c-Jun N-terminal kinase, cyclin-dependent kinase 5, and p38 mitogen-activated protein kinase as well as metabotropic glutamate receptor type 5. J Neurosci 24, 3370-3378.

REFERENCE LIST

Weinhold B, Seidenfaden R, Rockle I, Muhlenhoff M, Schertzinger F, Conzelmann S, Marth JD, Gerardy-Schahn R, Hildebrandt H (2005) Genetic ablation of polysialic acid causes severe neurodevelopmental defects rescued by ncam deletion. J Biol Chem. 30;280(52):42971-7.

Wigström H, Gustafsson B (1986). Postsynaptic control of hippocampal long-term potentiation. J Physiol (Paris) 81(4): 228-36.

Williams EJ, Mittal B, Walsh FS, Doherty P (1995) A Ca2+/calmodulin kinase inhibitor, KN-62, inhibits neurite outgrowth stimulated by CAMs and FGF. Mol Cell Neurosci 6: 69-79.

Wood GK, Tomasiewicz H, Rutishauser U, Magnuson T, Quirion R, Rochford J, Srivastava LK (1998) NCAM-180 knockout mice display increased lateral ventricle size and reduced prepulse inhibition of startle. Neuroreport 9, 461-466.

Wu L, Saggau P (1994) Presynaptic calcium is increased during normal synaptic transmission and paired-pulse facilitation, but not in long-term potentiation in area CA1 of hippocampus. J Neurosci 14:645-654.

Wuhrer M, Geyer H, von der OM, Gerardy-Schahn R, Schachner M, Geyer R (2003) Localization of defined carbohydrate epitopes in bovine polysialylated NCAM. Biochimie 85: 207-218.

Yamamoto N, Inui K, Matsuyama Y, Harada A, Hanamura K, Murakami F, Ruthazer ES, Rutishauser U, Seki T (2000) Inhibitory mechanism by polysialic acid for lamina-specific branch formation of thalamocortical axons. J Neurosci 20: 9145-9151.

Yasuda H, Barth Al, Stellwagen D, Malenka RC (2003). A developmental switch in the signaling cascades for LTP induction. Nat Neurosci 6(1): 15-6.

Zhao MG, Toyoda H, Lee YS, Wu LJ, Ko SW, Zhang XH, Jia Y, Shum F, Xu H, Li BM, Kaang BK, Zhuo M (2005) Roles of NMDA NR2B subtype receptor in prefrontal long-term potentiation and contextual fear memory. Neuron 47, 859-872.

Zhu JJ, Qin Y, Zhao M, Van Aelst L, Malinow R (2002) Ras and Rap control AMPA receptor trafficking during synaptic plasticity. Cell 110, 443-455.

Zucker RS, Regehr WG (2002) Short-term synaptic plasticity. Annu Rev Physiol 64:355-405.

X. Acknowledgements

The whole work was carried out at the Institute for Biosynthesis of Neuronal Structures of the Center for Molecular Neurobiology (ZMNH) at the University of Hamburg. I have been feeling so lucky to join this scientific group in February 2005 and to carry my Ph.D. study in harmonic and creative atmosphere. I would like to thank Prof. Melitta Schachner giving me opportunity to join her Institute, for providing facilities, guidance, fruitful discussions and for support during these years.

I would also like to thank Prof. Konrad Wiese for the external supervision of this study.

I am especially grateful to Dr. Alexander Dityatev for being the best supervisor I could ever imagine. Thanks for fantastic project - investigating the molecular mechanisms of memory formation, thanks for widening and deepening my perspective and understanding of science, for the unlimited patience, valuable discussions, fascinating ideas, support and motivation during these years.

I also would like to thank to the present and former colleagues in the laboratory for their help during this work. Especial thanks to Dr. Olena Bukalo who helped me a lot with the first steps in this project, for introducing me in the new methods and for helping me to overcome all kinds of problems. Thanks to Dr. Eka Lepsveridze for introducing me the new methods, for everyday help and helpful discussions. I would like to say thanks to all electrophysiology group members: Dr. Oleg Senkov, Tiberiu Stan, Giorgi Papashvili, Luminita Stoenica, Julia Langer for interesting seminars, helpful discussions, collaboration and friendship. My special thanks to Dr. Galina Dityateva who kindly supported me during this study, for the optimistic attitude to life and kind smile even during the tough periods.

I am thankful to all colleagues from ZMNH for their friendship collaboration and moral support. Many thanks to all members of our "Synaptic Plasticity" group: Dr. Fabio Morellini, Dr. Thomas Tilling, Mira Zenthöfer, Laetitia Fellini, for interesting seminars, helpful discussions and useful remarks during the seminars. Thanks to Vsevolod Bodrikov, Yana Chernyshova, Aksana Andreyeva, and Dmytro Puchkov for friendship and interesting scientific and not only discussions during tee breaks. Thanks to Achim Dahlmann for urgent providing all the chemicals I needed for my experiments, for genotyping of NCAM mice and Eva Kronberg for animal care. Thanks to Fritz Kuschera and Torsten Renz for help in fixing technical problems, for reparations and modifications of my setup. I would like to thank also the EDV service group for there professional work. Many thanks to all the friends in Hamburg and to all German people and Germany for hospitality and giving me an opportunity to do science of such quality.

ACKNOWLEDGEMENTS

I also would like to thank to Meifang Xiao, Dr. Sergei Grebenyuk and Dr. Olena Bukalo for their collaboration that resulted in several insights presented in this manuscript. Thanks to Oleg Senkov, Benedikt Salmen, Catrina Sims for their experiments supporting this study. Thanks to Harold Cremer for NCAM deficient mice. Thanks Dr. Yves Auberson for the antagonist of NR2A-NMDARs, NVPAAM077. Thanks to Rita Gerardy-Schahn for the enzyme EndoNF and anti-PSA antibodies. Thanks to Larry Feig for Ras-GRF1 deficient mice.

I would like to cordially thank all my lecturers from Tbilisi State University, especially from the Department of Animal and Human Physiology. My special thanks to Eka Mitaishvili and Margo Tavadze for being nice lectures of mine and for teaching general physiology. I am especially thankful to Dr. Zaqaria Nanobashvili at Departament of Neurophysiology Beritashvili institute of Georgian Academy of Sciences, for being my supervisor during my master study, for nice project and for inspiring me to the scientific work. Many thanks to the colleges at Neurophysiology department especially to Dr. Tamar Chachua and Dr. Irina Bilanishvili who helped me during my master study; teaching experimental skills and being friendly coworkers.

My warmest thanks to all my friends and relatives in Georgia, who always remembered, loved and believed in me. Many thanks to all my friends from Tbilisi State University, for the times spend together, for support and friendship during my study 1998-2004. Thanks to Shalva Barjadze, Eka Bakuradze, Tea Berulava and Rususdan Okujava for keeping in touch in spite of such a long distance, for friendship and support.

And, of course, I am grateful to my family, my parents and my brothers for giving me support during my study and for understanding me being thousands kilometer distance away from home during these 3.5 years.

Philip R. Lee
Ph.D Staff Scientist
National Institute of Health
35 Lincoln Drive
Bethesda 20892, MD USA
Phone +1 301 451 4538
Fax: +1 301 480 2707
E-mail plee@mail.nih.gov

Department Biology
University Hamburg
Martin Luther King-Platz 2
D-20146 Hamburg

5th May 2008

As an English native speaker hereby I confirm that the PhD thesis by Gaga Kochlamazashvili entitled as "Neural cell adhesion molecule-associated polysialic acid regulates synaptic plasticity by balancing the signaling through NR2A- and NR2B-containing NMDA receptors in the mouse (*Mus musculus* L., 1758)" is written in correct grammar and appropriate style.

Philip R Lee, Ph.D
Staff Scientist